ELECTROMAGNETIC MODELING BASED ON DIRECTIONAL TIME-DISTANCE ENERGY TRANSFER ANALOGIES

by

TIMOTHY MICHAEL MINTEER

A dissertation submitted in partial fulfillment of
the requirements for the degree of

DOCTOR OF PHILOSOPHY

WASHINGTON STATE UNIVERSITY
School of Electrical Engineering and Computer Science

MAY 2013

To the Faculty of Washington State University:

The members of the Committee appointed to examine the dissertation of TIMOTHY MICHAEL MINTEER find it satisfactory and recommend that it be accepted.

John B. Schneider, Ph.D., Chair

Robert G. Olsen, Ph.D.

Philip L. Marston, Ph.D.

ACKNOWLEDGMENTS

I would like to thank Dr. John B. Schneider, Associate Professor, School of Electrical Engineering and Computer Science, Washington State University, Pullman, WA for his review and support of this work. In addition, I would like to thank Dr. Robert G. Olsen, Associate Dean for Undergraduate Programs and Student Services, School of Electrical Engineering and Computer Science and Dr. Philip L. Marston, Professor of Physics, Department of Physics and Astronomy, both with Washington State University, Pullman, WA for their service as doctoral committee members and their review and feedback for this work. I would also like to thank Schweitzer Engineering Laboratories, Inc., Pullman, WA for their support in the continued education of their employees.

ELECTROMAGNETIC MODELING BASED ON DIRECTIONAL TIME-DISTANCE ENERGY TRANSFER ANALOGIES

Abstract

by Timothy Michael Minteer, Ph.D.
Washington State University
May 2013

Chair: John B. Schneider

A new electromagnetic model is established based on an average rate of directional time-distance energy transfers. A directional time-distance energy transfer is analogous to an energy carrier mediator (boson) exchange. Electromagnetic force is modeled as mean valued, continual emission and absorption of energy carrier mediators.

For an isolated spherically symmetric static charge distribution, Maxwell's stress equation is recast using a variant of Stokes' Theorem. The recast stress equation eliminates the stress normal to the electric field and establishes a stress only aligned with the electric field. The remaining stress is identified as an external omnidirectional Poincaré stress, inwardly directed towards the charge distribution. The Poincaré stress is modeled as a mean valued, continual exchange of bosons between the charge distribution and the distant matter of the universe.

For two separated spherically symmetric static charge distributions, Maxwell's stress equation is recast using a variant of Stokes' Theorem. The recast stress equation develops a line stress that only exists on the straight path between the two charge distributions. The line stress is identified as a Coulomb stress modeled as a mean valued, continual exchange

of photons back and forth between two like-charge distributions.

For an isolated differential current element, Maxwell's stress equation is recast using a variant of Stokes' Theorem. The recast stress equation establishes a pinch stress that is normal to the magnetic field and is directed inward toward the differential current element. Similar to the Poincaré stress, the pinch stress is omnidirectional and is modeled as a mean valued, continual exchange of bosons between the current element and the distant matter of the universe.

For two separated static differential current elements, a Neumann stress is established by analyzing the historical current force formulas known to be compatible with Maxwell's equations for closed circuits. The term Neumann stress is assigned to the line stress that only exists at each point on the straight path between two separated, differential current elements. Similar to the Coulomb stress, the Neumann stress is modeled as a mean valued, continual exchange of photons back and forth between two differential current elements in opposite directions.

TABLE OF CONTENTS

LIST OF TABLES

LIST OF FIGURES

Dedication

To my wonderful granddaughters:

Araena Joy

Auburn Jeannine

Cleopatra Amira

Zola Isabel

CHAPTER 1. INTRODUCTION

Electromagnetic modeling is an important aspect of advancing the understanding and application of electromagnetic phenomena. From Faraday's lines of force [1] and Maxwell's ethereal stress [2] (pertaining to electric and magnetic fields) to Feynman's diagrams [3] of photon-electron interaction in quantum electrodynamics (QED), models provide a conceptual insight into the physics of electromagnetism.

The new electromagnetic model of this dissertation may provide fresh or different insight into some electromagnetic systems. It provides an alternate conceptualization of the path of electromagnetic forces. In addition, the new model may inspire new inventions or develop a new area of expertise in the realm of electromagnetic energy transfer technologies.

In general, a given model may be an approximate (1st order, 2nd order, etc.) or an exact representation of some physical law or phenomena. The model itself need not have any physical relevance. However, it should have results that are comparable to analytic solutions or empirical test data. For example, a good electromagnetic model should be in agreement with Maxwell's equations.

The new electromagnetic model of this dissertation is based on an analogy of an average rate of directional time-distance energy transfers. A directional time-distance energy transfer is analogous to a photon or boson exchange (i.e., energy carrier mediator exchange). When the directional time-distance energy transfer analogy is related to the

interaction of charges or currents, the energy carrier mediator may be considered a photon. When the directional time-distance energy transfer analogy is related to a solid structure containing/supporting a charge or current distribution, the energy carrier mediator may be considered more generally as a boson (i.e., may consists of photons and/or other bosons).

This dissertation presents an electromagnetic model/analogy and makes no claim that the model should be taken physically literal. However, the laws of physics do apply to this model and the analogies presented.

The underlying principles of directional time-distance energy transfer are:

1. Energy transfer occurs in discrete quanta of energy being emitted from one particle of matter at a given point in time and successively absorbed by a different particle of matter at some later point in time.

2. Energy transfer occurs in a straight line (invariable in free space), directionally from the location of the emitting particle (at the emission time) to the location of the absorbing particle (at the absorption time).

3. Energy transfer occurs at the speed of light, thus relating the time difference between energy emission and absorption to the distance between the locations of the emission and absorption events.

A directional time-distance energy transfer may be viewed as an energy carrier mediator (boson) exchange. Therefore, the acronym QET (quantum energy transfer) is used throughout this dissertation for a directional time-distance energy transfer. Averaging a sequence of QETs for a given period of time and a given region of space (i.e., mean energy

quanta, mean transfer repetition rate, mean spatial straight path location) yields a mean QET flux density (W/m^2).

The rudimentary premise of directional time-distance energy transfer is that forces of nature (including electromagnetic forces) are a result of an average rate of QETs (boson interactions) between particles of matter. When energy is emitted from a particle there is an impulse force to the particle in the direction opposite to the transfer path (i.e., recoil impulse). Similarly, when energy is absorbed by a particle there is an impulse force to the particle in the direction of the transfer path (i.e., impact impulse). The average rate of recoil impulses (from energy emissions) and the impact impulses (from energy absorptions) produce a pressure or push force.

Although this dissertation conceptualizes directional time-distance energy transfers in general, it accentuates energy transfers relating to electromagnetics. Particularly, the new electromagnetic model is based on QETs into and out of molecular regions (elements or compounds) that are electrically charged (positively or negatively) and/or have electrical current passing through them. Details of energy transfer contained within molecular regions are outside the scope of this dissertation. Energy transfers into and out of molecular regions are viewed as interacting with the molecules as a whole and the details of energy transfers to/from specific sub-atomic particles of matter are also outside the scope of this dissertation.

The subsequent chapters of this dissertation are summarized as follows:

Chapter 2. Directional time-distance energy transfer (QET): defines directional time-distance energy transfer or QET (quantum energy transfer) in general.

Chapter 3. Background of force between masses, charges, and currents: contains various historical aspects related to the force between masses, charges, and currents and/or the exchange of energy between them.

Chapter 4. Mass, force, and QET: briefly touches on the quantum energy transfers interacting with mass associated with gravity and inertia.

Chapter 5. A QET model for the Poincaré stress of an isolated, spherically symmetric static charge distribution: establishes the Poincaré stress by recasting Maxwell's stress equation for an isolated, spherically symmetric charge distribution. The recast stress equation identifies a Poincaré stress as the only stress external to the charge distribution. The Poincaré stress is aligned with the electric field, is omnidirectional, and is directed inward toward the charge distribution.

Chapter 6. A QET model for the Coulomb and Poincaré stresses of two separated, spherically symmetric static charge distributions: establishes the Coulomb stress by recasting Maxwell's stress equation for two separated, spherically symmetric static charge distributions. The term Coulomb stress is assigned to the line stress that only exists at each point on the straight path between two separated, spherically symmetric charge distributions.

Chapter 7. A QET model for the pinch stress of a differential current element at the origin: establishes the pinch stress by recasting Maxwell's stress equation for an isolated, differential current element. The pinch stress is normal to the magnetic field and is directed inward toward the differential current

element.

Chapter 8. A QET model for the Neumann and pinch stresses of two separated, static differential current elements: establishes the Neumann stress by analyzing the historical current force formulas known to be compatible with Maxwell's equations for closed circuits. The term Neumann stress is assigned to the line stress that only exists at each point on the straight path between two separated, differential current elements.

Chapter 9. Coulomb stress for two separated, spherically symmetric charge distributions both moving with the same constant velocity: analyzes the Coulomb stress between two charge distributions moving with the same velocity by applying the Lorentz transformation.

Chapter 10. Summary of Poincaré, Coulomb, Neumann, and pinch stresses.

Appendix A. Derivation of Γ_e, the constant of quantum energy transfer rate to mass (W/kg).

Appendix B. Derivation of Maxwell's stress equation for electrostatics in free space.

Appendix C. Derivation of a variant of Stokes' Theorem.

Appendix D. Vector identities.

Appendix E. Derivation of Maxwell's stress equation for magnetostatics in free space.

Appendix F. Determination of constraints for the general force equation between two differential current elements.

Appendix G. QET and Electrodynamics: terse description of an electrodynamic model

based on QET.

Appendix H. QET and the Cosmos: describes a cosmos model that is compatible with the QET model of this dissertation. In addition, briefly describes the QET interaction between molecular regions.

CHAPTER 2. DIRECTIONAL TIME-DISTANCE ENERGY TRANSFER (QET)

This chapter defines directional time-distance energy transfer or QET (quantum energy transfer) in general. The definition is for a single QET. However, the new electromagnetic model of this dissertation is based on an average rate of QETs as described in subsequent chapters. Application of QET includes gravitational and electromagnetic interactions between molecular regions.

For a given quantum energy emission from a first particle of matter there is a corresponding quantum energy absorption by a second particle of matter at a directional time-distance. The directional distance is established by the distance vector, $\vec{\mathbf{d}}_{21}$, from the first particle's location at the emission time to the second particle's location at the absorption time.

The time between the quantum energy emission and corresponding absorption events is related to the distance between the event locations:

$$t_2 - t_1 = \frac{\left|\vec{\mathbf{d}}_{21}\right|}{c}, \tag{2.1}$$

where c is the speed of light in free space.

An illustration of a QET is shown in Figure 2.1. The two particles P_1 and P_2 are moving along separate paths as indicated by the dashed lines of Figure 2.1 (in the direction of the arrows shown at the tips of the dashed lines). At time t_1, a quanta of energy is emitted

from particle P_1 (at the location indicated by the solid black dot). At a later time t_2, the corresponding quanta of energy is absorbed by particle P_2 (at the location indicated by the gray dot).

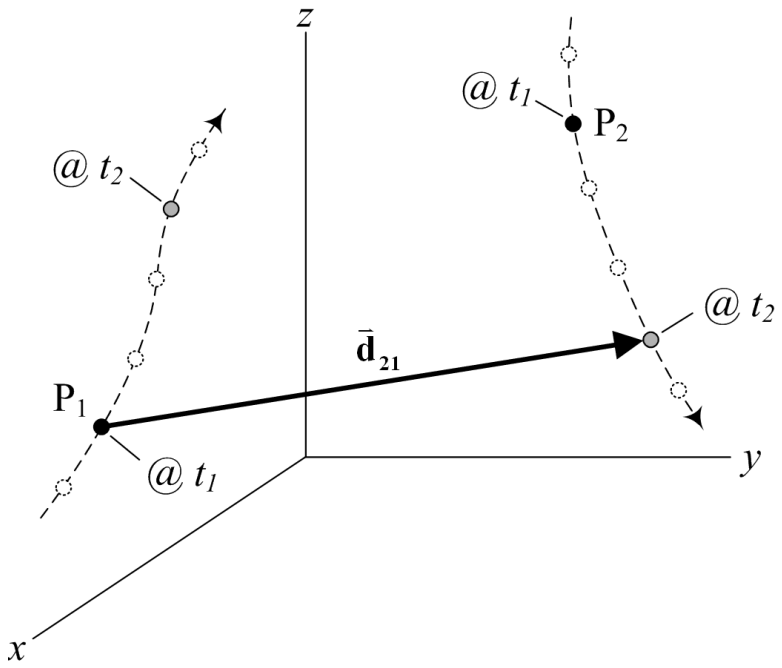

Figure 2.1: Quantum energy transfer (QET) illustration.

An example of QET is the straight path of a photon being emitted from one atom and being absorbed by a different atom at some later point in time. QETs have the following characteristics:

1. QETs only occur between particles of matter.

2. A quanta energy is only absorbed by a particle if at some prior time the corresponding quanta energy was emitted from another particle.

3. Similarly, a quanta energy is only emitted from a particle if at some later time the

corresponding quanta energy will be absorbed by another particle.

4. The transfer of quantum energy occurs in a straight line, at the speed of light (as observed in any inertial reference frame). The distances between quantum energy emission and corresponding absorption event locations range from sub-atomic minuteness to the furthest expanse of the universe.

5. There are no collisions or interference between QETs in free space. Therefore, there may be a plethora of QETs ostensibly passing through a given location in space void of matter at a particular point in time.

6. Based on the assumption that molecular regions consist of many moving particles of matter and a large percentage of free space (at any particular point in time), QETs may statistically pass through molecular regions located between the emission and absorption points.

7. When quantum energy is emitted, there is a recoil impulse to the corresponding particle of matter in the opposing direction of the QET.

8. When quantum energy is absorbed, there is an impact impulse to the corresponding particle of matter in the direction of the QET.

Items 3 and 7 imply that a present impulse is related to a future event. The implications of this are touched upon in Chapter 3. The impulses from quantum energy emission and absorption events contribute to push or pressure forces which constitute the forces of

nature (i.e., no pull or tension forces occur from directional time-distance energy transfers). A variation on Newton's third law summarizes QET:

For every action impulse (quantum energy emission) there is an equal and opposite reaction impulse (quantum energy absorption) at a directional time-distance.

The magnitude of the nth QET, U_n (J), and the unit vector in the direction of the nth QET, $\hat{\mathbf{a}}_n$, are related to the impulse action, $\vec{\mathbf{I}}_{en}$ (N•s), or reaction, $\vec{\mathbf{I}}_{an}$, on the particles of matter respectively emitting or absorbing the quantum energy. The impulse on the emitting particle of matter at emission time, t_{en}, for the nth QET is:

$$\vec{\mathbf{I}}_{en}\left(t_{en}\right) = -\frac{U_n}{c}\hat{\mathbf{a}}_n. \tag{2.2}$$

Similarly, the impulse on the absorbing particle of matter at absorption time, t_{an}, for the nth QET is:

$$\vec{\mathbf{I}}_{an}\left(t_{an}\right) = \frac{U_n}{c}\hat{\mathbf{a}}_n = -\vec{\mathbf{I}}_{en}\left(t_{en}\right), \tag{2.3}$$

where t_{an} and t_{en} are associated in accordance with (2.1).

An example of an impulse/force as a result of QET is the radiation pressure from light being absorbed or emitted from an object.

It should be noted that the net impulse on a first particle of matter traveling at a velocity $\vec{\mathbf{v}}_{1n}$ at the time of emitting quantum energy U_n in the direction of $\hat{\mathbf{a}}_n$ is related to the change in momentum of the equivalent mass of the quantum energy:

$$\vec{\mathbf{I}}_{en(\text{net})} = \frac{U_n}{c^2}\vec{\mathbf{v}}_{1n} - \frac{U_n}{c}\hat{\mathbf{a}}_n. \tag{2.4}$$

Likewise, the net impulse on a second particle of matter traveling at a velocity $\vec{\mathbf{v}}_{2n}$ at the time of absorbing quantum energy U_n in the direction of $\hat{\mathbf{a}}_n$ is related to the change in

momentum of the equivalent mass of the quantum energy:

$$\vec{\mathbf{I}}_{an(\text{net})} = \frac{U_n}{c}\hat{\mathbf{a}}_n - \frac{U_n}{c^2}\vec{\mathbf{v}}_{2n}. \tag{2.5}$$

CHAPTER 3. BACKGROUND OF FORCE BETWEEN MASSES, CHARGES, AND CURRENTS

This chapter contains various aspects related to the force between masses, charges, and currents and/or the exchange of energy between them. The following paragraphs may seem disjointed with each other and somewhat terse. The goal of this section is to identify the many pieces (in some way relevant to the directional time-distance energy transfer of this dissertation) in an efficient manner without getting bogged down in the details of each piece. The various references provide a starting place when further understanding is desired.

Action/reaction forces from interactions between matter (gravitation), static charges (electrostatics), and stationary currents (magnetostatics) have been propounded to occur in straight lines between each corresponding mass, charge, or current element. These forces were once viewed as action at a distance. Since time is not involved (i.e., the system is static/stationary), these forces were also conceived as instantaneous.

Isaac Newton's universal law of gravitation establishes the force between each particle of matter [4]. The differential element of force on a first differential mass element interacting with a second differential mass element separated by the distance d_{21} (with unit directional vector, $\hat{\mathbf{a}}_{21}$, from the first to the second differential mass element) is:

$$d^2\vec{\mathbf{F}}_1 = G\frac{(\rho_1 dV_1)\,(\rho_2 dV_2)}{d_{21}^2}\hat{\mathbf{a}}_{21}, \tag{3.1}$$

where G is the gravitational constant 6.674×10^{11} N•m^2/kg^2, ρ is the mass density, and dV is the differential volume of the mass element.

Coulomb's Law was formulated by Charles-Augustin de Coulomb for the electrostatic interaction between charged particles [5]. The differential element of force on a first differential charge element interacting with a second differential charge element is:

$$d^2\vec{\mathbf{F}}_1 = -\frac{1}{4\pi\varepsilon_o}\frac{(\rho_1 dV_1)(\rho_2 dV_2)}{d_{21}^2}\hat{\mathbf{a}}_{21}, \tag{3.2}$$

where ρ is the charge density. As a side note, Coulomb also developed a similar force relationship between magnetized materials (i.e., permanent magnets and ferromagnets), inversely proportional to the square of the distance [6].

Twenty years after Alessandro Volta invented the electric pile or battery [7], Hans Christian Oersted discovered[1] that a magnetic needle tended to turn at right angles to a wire shorting out the terminals of a battery [8]. Oersted published the assertion that there is always a magnetic circulation around an electric current in a conductor [9]. Within months of Oersted's announcement, André-Marie Ampère delivered[2] a series of lectures on electrical current and magnetism [10]. Two years later Ampère published his fundamental law relating electrical current and the magnetic field (i.e., Ampère's Law[3]) [11].

André-Marie Ampère proposed a formula for the interaction between two station-

---

[1] July, 1820

[2] September, 1820

[3] 1822

ary current elements, the resulting force acts along the straight line between the current elements [12]. Accordingly, the differential force element on a first differential current element interacting with a second differential current element is [13]:

$$d^2\vec{\mathbf{F}}_1 = \frac{\mu_o}{4\pi}\frac{2\left(\vec{\mathbf{J}}_1 dV_1\right)\cdot\left(\vec{\mathbf{J}}_2 dV_2\right) - 3\left[\left(\vec{\mathbf{J}}_1 dV_1\right)\cdot\hat{\mathbf{a}}_{21}\right]\left[\left(\vec{\mathbf{J}}_2 dV_2\right)\cdot\hat{\mathbf{a}}_{21}\right]}{d_{21}^2}\hat{\mathbf{a}}_{21}, \tag{3.3}$$

where dV is the differential volume of the current element.

Franz Ernst Neumann also developed a formula for a force acting along the straight line between two stationary current elements [14, 15]. For Neumann, the differential element of force on a first differential current element interacting with a second differential current element is:

$$d^2\vec{\mathbf{F}}_1 = \frac{\mu_o}{4\pi}\frac{\left(\vec{\mathbf{J}}_1 dV_1\right)\cdot\left(\vec{\mathbf{J}}_2 dV_2\right)}{d_{21}^2}\hat{\mathbf{a}}_{21}. \tag{3.4}$$

As a side note, Neumann developed an expression for the mutual inductance of two closed current circuits containing a similar expression as (3.4) [16, 17].

The differential force element in all four equations (3.1), (3.2), (3.3), and (3.4) act in the direction (attraction) or opposite direction (repulsion) of the unit directional vector, $\hat{\mathbf{a}}_{21}$, from the first to the second corresponding differential element. Similarly, successive directional time-distance energy transfers (the basis for this dissertation) between two molecular charge or current elements also constitute repulsion directionally away from the straight line between the two molecular elements.

Historically, electromagnetic concepts and models have aided in the progression and application of electromagnetic field theory. Michael Faraday envisioned electric lines of force [18], magnetic lines of force (observed with iron filings or a magnetic needle) [19],

and even gravitational lines of force [20]. James Maxwell describes Faraday's physical lines of force and the state of stress in the medium (i.e., tension in the direction of the lines of force and pressure normal to this direction) as a kind of action at a distance resulting from "the tension of ropes and the pressure of rod" [21].

Based on the Biot-Savart Law [22], Hermann Günther Grassmann proposed a formula for the interaction between two stationary current elements [23]. Grassmann concluded that Ampère's formula (3.3) generated unlikely results and the principle from which it is derived must come under suspicion. With Ampère's formula, there is no force between two parallel current sources when the angle between them is 35.3°. For angles greater than 35.3° there is attraction. However, for angles less than 35.3° there is repulsion. Unlike Ampère's formula of (3.3), the resulting force for Grassmann's formula is not necessarily acting along the straight line between the current elements, but always acts perpendicular to the current elements. Accordingly, the differential force element on a first differential current element interacting with a second differential current element is [24]:

$$\begin{aligned} d^2\vec{\mathbf{F}}_1 &= -\frac{\mu_o}{4\pi}\frac{\left(\vec{\mathbf{J}}_1 dV_1\right)\times\left[\left(\vec{\mathbf{J}}_2 dV_2\right)\times\hat{\mathbf{a}}_{21}\right]}{d_{21}^2} \\ &= \frac{\mu_o}{4\pi}\frac{\left(\vec{\mathbf{J}}_1 dV_1\right)\cdot\left(\vec{\mathbf{J}}_2 dV_2\right)\hat{\mathbf{a}}_{21}-\left[\left(\vec{\mathbf{J}}_1 dV_1\right)\cdot\hat{\mathbf{a}}_{21}\right]\left(\vec{\mathbf{J}}_2 dV_2\right)}{d_{21}^2}. \end{aligned} \tag{3.5}$$

A peculiarity of Grassmann's formula is that forces on two differential current elements are not always equal and opposite (i.e., in violation of Newton's third law). Although (3.3) and (3.5) generally give different differential force element values, the net force on a differential current element, exerted by another closed circuit (e.g., current density in a wire loop) resulting from integrating an assemblage of differential current elements around

the closed circuit, are equivalent [25]. Historically, there are an infinite number of formulas identified that are equivalent to (3.3) and (3.5) for the net force on a stationary differential current element exerted by the differential elements in a stationary closed circuit (see derivations by Whittaker [26], O'Rahilly [27], Stefan [28], and Moon and Spencer [29]):

$$d^2\vec{\mathbf{F}}_1 = -\frac{\mu_o}{4\pi d_{21}^2}\left\{\begin{array}{l} 3\,(1-k_1)\left[\left(\vec{\mathbf{J}}_1 dV_1\right)\cdot\hat{\mathbf{a}}_{21}\right]\left[\left(\vec{\mathbf{J}}_2 dV_2\right)\cdot\hat{\mathbf{a}}_{21}\right]\hat{\mathbf{a}}_{21} \\ +\,(k_1-2)\left(\vec{\mathbf{J}}_1 dV_1\right)\cdot\left(\vec{\mathbf{J}}_2 dV_2\right)\hat{\mathbf{a}}_{21} \\ +\,k_1\left[\left(\vec{\mathbf{J}}_1 dV_1\right)\cdot\hat{\mathbf{a}}_{21}\right]\left(\vec{\mathbf{J}}_2 dV_2\right)+k_2\left[\left(\vec{\mathbf{J}}_2 dV_2\right)\cdot\hat{\mathbf{a}}_{21}\right]\left(\vec{\mathbf{J}}_1 dV_1\right) \end{array}\right\}, \quad (3.6)$$

where k_1 and k_2 are arbitrary constants.

In order for $d^2\vec{\mathbf{F}}_2 = -d^2\vec{\mathbf{F}}_1$ (i.e., Newton's third law to be maintained), the two constants are constrained as: $k_1 = k_2$. Ampère's formula (3.3) is obtained by choosing the two constants of (3.6) as: $k_1 = k_2 = 0$. Grassmann's formula (3.5) is obtained by choosing: $k_1 = 1$ and $k_2 = 0$ and hence Newton's third law is not maintained.

Moon and Spencer derived an additional formula set for the force between differential current elements by removing Ampère's original constraint that a current element can't have a tangential force component (when interacting with a closed circuit), while maintaining Ampère's constraint that current element forces only act along the straight line between them [12]. Accordingly, the differential force element on a first differential current element interacting with a second differential current element is [29]:

$$d^2\vec{\mathbf{F}}_1=-\frac{\mu_o}{4\pi d_{21}^2}\left\{\begin{array}{l} 3(1-k_1)\left[\left(\vec{\mathbf{J}}_1 dV_1\right)\cdot\hat{\mathbf{a}}_{21}\right]\left[\left(\vec{\mathbf{J}}_2 dV_2\right)\cdot\hat{\mathbf{a}}_{21}\right] \\ +(k_1-2)\left(\vec{\mathbf{J}}_1 dV_1\right)\cdot\left(\vec{\mathbf{J}}_2 dV_2\right) \\ +k_3\left[\left(\vec{\mathbf{J}}_1 dV_1\right)\times\left(\vec{\mathbf{J}}_2 dV_2\right)\right]\cdot\hat{\mathbf{a}}_{21} \end{array}\right\}\hat{\mathbf{a}}_{21}, \quad (3.7)$$

where k_1 and k_3 are arbitrary constants. Ampère's formula (3.3) is obtained by choosing the two constants of (3.7) as: $k_1 = k_3 = 0$. Neumann's formula (3.4) is obtained by choosing the two constants of (3.7) as: $k_1 = 1$ and $k_3 = 0$.

Equations (3.6) and (3.7) (and thus (3.3), (3.4) and (3.5)) generally give different differential force element values and even a different net force on a differential current element, exerted by another closed circuit. However, all five equations give the same equal and opposite force on one stationary closed circuit exerted by another stationary closed circuit.

Hendrik Antoon Lorentz established a force equation for a charge in the presence of an electric and magnetic field [30]. Lorentz's force equation is also applicable to differential current elements as well as differential charge elements (assuming a differential current element is equivalent to a differential charge element moving at a directional velocity $\vec{\mathbf{v}}$, $\vec{\mathbf{J}}dV = (\rho dV)\,\vec{\mathbf{v}}$). The corresponding differential element of force on a differential volume within a subsystem of charge and current densities (denoted by subscript 1) resulting from the electric field and magnetic flux density generated by the total system of charge and current densities is [31]:

$$d\vec{\mathbf{F}}_1 = (\rho_1 dV_1)\,\vec{\mathbf{E}} + \left(\vec{\mathbf{J}}_1 dV_1\right) \times \vec{\mathbf{B}}. \tag{3.8}$$

To utilize (3.8), all charge and current densities in the total system must be known or determined. If the system contains any conductors (stationary or moving), dielectrics, ferromagnetic materials, time varying sources, etc., ascertaining these charge and current densities/distributions and the electric filed and magnetic flux density involves the complete solution of Maxwell's equations external and internal to the various materials.

As a side note, (3.8) may also be applied using the electric field and magnetic flux density excluding the partial fields calculated from the subsystem of charge and current densities (i.e., $\vec{\mathbf{E}} - \vec{\mathbf{E}}_1$ and $\vec{\mathbf{B}} - \vec{\mathbf{B}}_1$: the partial fields calculated from the rest of the charge and current densities not contained in the subsystem). This approach gives the same results for the total force on the subsystem under the assumption there is no subsystem net self-force (i.e., no net force as a result of the partial electric and magnetic flux density fields from the charge and current densities of the subsystem).

Another approach for determining the force on a charge and/or current density is to use Maxwell's stress equation for electromagnetic fields [2]. Maxwell envisioned stress in the ether/medium caused by the existence of electric and magnetic fields. The differential force element on a differential volume of charge and/or current density resulting from the electric and magnetic fields and flux densities generated by the total system of charge and current densities is [32]:

$$d\vec{\mathbf{F}} = \left[\vec{\mathbf{E}}\left(\nabla \cdot \vec{\mathbf{D}}\right) + \left(\nabla \times \vec{\mathbf{E}}\right) \times \vec{\mathbf{D}} + \left(\nabla \times \vec{\mathbf{H}}\right) \times \vec{\mathbf{B}} - \frac{\partial}{\partial t}\left(\vec{\mathbf{D}} \times \vec{\mathbf{B}}\right)\right] dV. \quad (3.9)$$

Although (3.9) appears more complicated than (3.8), when applied to a region/volume of space the first three terms can typically be converted from volume to surface integrals [32]. The differential surface element of force may provide insight into the directional time-distance energy transfer flux density (the basis for this dissertation) passing through a given surface. The last term in (3.9) is proportional to the partial time derivative of the Poynting vector $\vec{\mathbf{S}}$. The Poynting vector was developed by John Henry Poynting and is

defined as [33]:

$$\vec{\mathbf{S}} = \vec{\mathbf{E}} \times \vec{\mathbf{H}}. \tag{3.10}$$

The Poynting vector specifies the magnitude and direction of the net electromagnetic energy flux density at a given location in the electromagnetic field. The average of all electromagnetic directional time-distance energy transfers (with transfer path through a given location) corresponds to the Poynting vector. Oliver Heaviside proposed the existence of additional, "circuital" energy flux(es) whose divergence is zero [34]. Continuous directional time-distance energy transfers between two like charged, static objects is an example of electromagnetic energy flux having zero divergence (i.e., energy flux having no net energy transfer are not part of the Poynting vector).

For quantum electrodynamics (QED), Richard Phillips Feynman describes photons interacting with electrons based on probabilities [3]. In particle physics (including QED), the mediator (boson) is the energy carrier. The photon is the mediator for QED and the graviton for quantum gravitation. The photon and graviton both have zero mass, travel at the speed of light and don't interfere with other zero mass mediators [35].

Directional time-distance energy transfer or QET (the basis for this dissertation) is similar to the mediator/boson transfer in particle physics. However, in QED, the photon can cause both repulsion (recoil and impact impulses from particle transfer) as well as attraction (analogous to the throwing and then tugging of a rope) [36]. Directional time-distance energy transfers only produce a pressure or push (repulsion) force (i.e., tension or pull forces do not exist). Therefore, attraction needs to be explained by some other mechanism.

Oliver Heaviside pictured gravitation as the result of "the pressure of radiation produced by galactic energy-tubes." These energy-tubes are a result of the "many millions of galaxies" and are "a consequence of the radiant energy-mass relationships existing in this cosmic system." H. J. Josephs further describes Heaviside's concept of gravitation [37]:

> "... he imagined that all space was filled with energy-tubes, moving in straight lines according to Newton's first law, and in all directions with the speed of light. A single planet alone in space would be subject to a rain of these galactic energy-tubes from all directions at once and so would remain still. But two planets in space would screen each other from the galactic rays coming in particular directions. Consequently the galactic energy-density in the space between the two planets would be reduced and so they would be urged towards each other."

Heaviside's energy-tubes may be viewed as describing the graviton in quantum gravity/particle physics. Georges-Louis Le Sage originally devised a kinetic theory of gravitation [38], having a similar pushing effect as Heaviside's energy-tubes. Feynman discarded this pushing/kinetic theory of gravity because of the drag it predicts would be experienced by moving bodies (i.e., the gravitation model can't be a rain of energy-tubes) [39, 40]. However, the QET model of this dissertation (i.e., an influx and out-flux of QETs proportional to a mass) doesn't exhibit this drag issue for moving bodies.

Ernst Mach suggested a connection with the masses of the universe contributing to inertial motions [41]. Mach's principle has been coined to relate the inertia force (on accelerating local masses) as a result of the fixed, distant matter of the universe. In other

words, the force that presses a person against the door of an automobile navigating a sharp corner is caused by the entire matter of the universe [42]. The concept of an object alone in free space having inertia properties is not compatible with Mach's principle. In terms of this dissertation, the inertia of a local mass is the result of directional time-distance energy transfers with surrounding distant matter of the universe.

In a similar manner, an underlying premise of this dissertation is that local charge and current densities not only interact with each other but also with the distant matter of the universe. If there is a repulsion between two objects (having like charges or opposite current flow), it is a result of a greater average of directional time-distance energy transfers (QETs) back and forth between the two objects compared to the QETs in the opposite direction between the objects and the rest of the universe. Likewise, if there is an "attraction" between two objects (having opposite charges or parallel current flow), it is a result of a lesser average of QETs back and forth between the two objects compared to the QETs in the opposite direction between the objects and the rest of the universe. In both the repulsion and attraction cases, the objects are always pushed (apart or together, respectively) as a result of the summation of impulses from the QETs emitted (recoil impulse) and absorbed (impact impulse) by the object.

For electrodynamics, (3.2) must be modified to incorporate the results of moving charge densities. Wilhelm Eduard Weber proposed a formula for the interaction between two moving charges (as a function of their relative position, velocity, and acceleration), the resulting force acting along the straight line between the two charges [43]. Accordingly, the differential force element on a first differential charge element interacting with a second

differential charge element is [44]:

$$d^2\vec{\mathbf{F}}_1 = -\frac{1}{4\pi\varepsilon_o}\frac{(\rho_1 dV_1)(\rho_2 dV_2)}{d_{21}^2}\left[1-\frac{1}{2c^2}\left(\frac{\partial d_{21}}{\partial t}\right)^2+\frac{1}{c^2}\frac{\partial^2 d_{21}}{\partial t^2}\right]\hat{\mathbf{a}}_{21}. \tag{3.11}$$

Applying (3.11) to differential current elements (assuming neutral conductors) yields Ampère's formula of (3.3). Since (3.11) contains an acceleration term, Ampère's formula of (3.3) is also valid for time-varying currents (in neutral conductors) as well as curved conductors [45].

Walter Ritz proposed a general formula for the interaction between two moving charges (based on circuital currents), where the resulting force is not necessarily acting along the straight line between the charge elements [46]. The corresponding differential force element on a first differential charge element interacting with a second differential charge element is [47]:

$$\begin{aligned} d^2\vec{\mathbf{F}}_1 = -\frac{1}{4\pi\varepsilon_o}\frac{(\rho_1 dV_1)(\rho_2 dV_2)}{d_{21}^2}\Bigg\{\Bigg[1+\frac{3-\lambda}{4c^2}v_{21}^2-\frac{3(1-\lambda)}{4c^2}\left(\frac{\partial d_{21}}{\partial t}\right)^2+\frac{\vec{\mathbf{d}}_{21}\cdot\vec{\mathbf{a}}_2}{2c^2}\Bigg]\hat{\mathbf{a}}_{21} \\ +\frac{1+\lambda}{2c^2}\left(\frac{\partial d_{21}}{\partial t}\right)\vec{\mathbf{v}}_{21}-\frac{d_{21}}{2c^2}\vec{\mathbf{a}}_2\Bigg\}, \end{aligned} \tag{3.12}$$

where $\vec{\mathbf{v}}_{21}$ is the relative velocity of the second differential charge element with respect to the first, $\vec{\mathbf{a}}_2$ is the acceleration of the second differential charge element, and λ is an arbitrary constant. The terms containing λ integrate to zero for the force on a first closed current circuit (e.g., current density in a wire loop) interacting with a second differential current element. Equation (3.12) applied to differential current elements (assuming neutral conductors) yields a differential force element that is not necessarily acting along the straight line between the current elements, but is equal and opposite to the force on the second differential current element [48].

Georg Friedrich Bernhard Riemann suggested that electrodynamic effects are explained by the action from a charged mass propagating to other charged masses at the speed of light. He formulated a retarded electric scalar potential [49]. Ludvig Valentin Lorenz also suggested a formula for the retarded electric scalar potential and retarded magnetic vector potential [50]. The retarded electric scalar potential, ϕ_{ret}, and retarded magnetic vector potential, $\vec{\mathbf{A}}_{\text{ret}}$, (Coulomb gauge) are used to determine the electric field and magnetic flux density satisfying Maxwell's equations [51]:

$$\phi_{\text{ret}} = \frac{1}{4\pi\varepsilon_{\text{o}}} \iiint \frac{[\rho]_{\text{ret}}}{r} dV', \tag{3.13}$$

$$\vec{\mathbf{A}}_{\text{ret}} = \frac{\mu_{\text{o}}}{4\pi} \iiint \frac{\left[\vec{\mathbf{J}}\right]_{\text{ret}}}{r} dV', \tag{3.14}$$

$$\begin{aligned} \vec{\mathbf{E}} =& -\nabla\phi_{\text{ret}} - \frac{\partial \vec{\mathbf{A}}_{\text{ret}}}{\partial t} \\ =& \frac{1}{4\pi\varepsilon_{\text{o}}} \iiint \left\{ \frac{[\rho]_{\text{ret}}}{r^2} + \frac{1}{rc}\left[\frac{\partial\rho}{\partial t'}\right]_{\text{ret}} \right\} \hat{\mathbf{a}}_r dV' - \frac{\mu_{\text{o}}}{4\pi} \iiint \frac{1}{r}\left[\frac{\partial \vec{\mathbf{J}}}{\partial t'}\right]_{\text{ret}} dV', \end{aligned} \tag{3.15}$$

$$\begin{aligned} \vec{\mathbf{B}} =& \nabla \times \vec{\mathbf{A}}_{\text{ret}} \\ =& \frac{\mu_{\text{o}}}{4\pi} \iiint \left\{ \frac{\left[\vec{\mathbf{J}}\right]_{\text{ret}}}{r^2} + \frac{1}{rc}\left[\frac{\partial \vec{\mathbf{J}}}{\partial t'}\right]_{\text{ret}} \right\} \times \hat{\mathbf{a}}_r dV', \end{aligned} \tag{3.16}$$

where r is the distance from the source point (at an earlier time) to the field (observation) point (at the present time), $\hat{\mathbf{a}}_r$ is the unit vector directed toward the field point, and the retardation symbol, $[]_{\text{ret}}$, indicates evaluation at an earlier (retarded) time, $t' = t - r/c$.

The electric field and magnetic flux density calculated using the retarded integrals of (3.15) and (3.16) for a system of charge and current densities (excluding the partial fields from the first subsystem of charge and current densities, if desired) can be applied to Lorentz's force equation (3.8) to determine the differential force element within a first subsystem of charge and current densities. Combining (3.8), (3.15), and (3.16) produces a differential element of force that may be viewed as retarded action at a distance.

An electric field and magnetic flux density calculated using advanced integrals (i.e., advanced electric scalar and magnetic vector potentials) are also a solution to Maxwell's equation. John Archibald Wheeler and Richard Feynman proposed an electromagnetic interaction that involved half retarded and half advanced Lienard-Wiechert potential solutions [52]. Their approach was based on Hugo Martin Tetrode's notion that energy can't be radiated unless there is an absorber receiving the energy [53].

The background information in this chapter provides a supporting framework for directional time-distance energy transfers or QETs (quantum energy transfers) as highlighted below:

1. Similar to QED, QET occurs in discrete quanta of energy being emitted from one particle of matter at a given point in time and successively absorbed by a different particle at a later point in time.

2. Unlike QED, QETs only produce a pressure or push (repulsion) force (i.e, tension or pull forces do not exist).

3. Similar to Tetrode's absorber concept, QETs occur only as a pair; one particle of

matter is the emitter and another particle of matter is the absorber.

4. Similar to QED, there is no collisions/interference between QETs.

5. Retarded and advanced potential differential elements are correlated with QETs; they both ‘propagate’ at the speed of light in a straight path between past/future locations.

6. Retarded potentials are correlated with quantum energy absorption (i.e., a particle of matter absorbs energy from an emitter in the past).

7. Advanced potentials are correlated with quantum energy emission (i.e., a particle of matter emits energy to an absorber in the future).

8. Although QET is a causal transaction (i.e., quantum energy is emitted at one point in time and absorbed at some later point in time), the recoil impulse from quantum energy emission based on the future absorber location is non-causal.

9. The impulse forces from QETs are correlated with the differential force elements of (3.1), (3.2), and (3.3) or (3.4) for statics; the resulting force is towards or away from the directional vector between two differential elements of mass, charge, or current densities.

10. Similar to Heaviside’s energy-tubes concept of gravity, QETs occur between the masses of the universe and local masses; two local masses screen each other from these QETs causing the local masses to be pushed together.

11. Unlike Le Sage’s kinetic theory of gravitation, QETs to/from an object are proportional to the mass of the object itself (i.e., not a function of an abundance of tiny

corpuscles moving at high speeds in all directions interacting with a mass density).

12. Similar to Mach's principle, inertia is a result of QETs between a local mass and the masses of the universe.

13. Unlike Mach's principle, a local mass has a finite average rate of QETs and therefore can't interact with the entire masses of the universe; although there is a given probably of interaction with every mass element of the universe.

14. If there is an electric or magnetic repulsion between two objects (having like charges or opposite current flow), it is a result of a greater average of QETs back and forth between the two objects compared to the QETs in the opposite direction between the objects and the rest of the universe.

15. Likewise, if there is an "attraction" between two objects (having opposite charges or parallel current flow), it is a result of a lesser average of QETs back and forth between the two objects compared to the QETs in the opposite direction between the objects and the rest of the universe.

16. The force on moving differential charge and current elements is correlated with the retarded potentials (i.e., absorbed energy transfers from emitters in the past) and advanced potentials (i.e., emitted energy transfers to absorbers in the future) and therefore should also be a function of the velocities and accelerations of the differential elements; the resulting force not necessarily being in line with the distance vector between the two differential elements.

17. The average of all QETs occurring (i.e., transferring) through a given location is deduced to be the Poynting vector.

18. There are additional energy fluxes (not part of the Poynting vector) accounting for the QETs related to the electric and magnetic interactions.

CHAPTER 4. MASS, FORCE, AND QET

Although the primary emphasis of this dissertation deals with electromagnetic directional time-distance energy transfer (QET), it is useful to briefly touch on the QETs interacting with mass associated with gravity and inertia. However, this chapter doesn't go into any details of gravity or inertia. This chapter provides a formula for calculating the force on a given system of particles of matter given knowledge of the QETs emitted from and absorbed by the system in a given amount of time.

A system of particles of matter (e.g., sub-atomic particles, atoms, molecules, objects, planets, solar systems ...) has a corresponding mass, m (kg). If a) the mass of a system remains constant, b) the momentum of the system is conserved, and c) there is no net flow of thermal and electromagnetic energy into or out of the system, then:

1. The mean rate of quantum energy absorptions, $\bar{P}_a$ (W), corresponding to QETs directionally into the system, is proportional to the mass, m, of the system.

2. The mean rate of quantum energy emissions, $\bar{P}_e$ (W), corresponding to QETs directionally out of the system is also proportional to the mass, m, of the system.

3. The mean rate of quantum energy absorptions into the system is equivalent to the mean rate of quantum energy emissions out of the system: $\bar{P}_a = \bar{P}_e$. In other words, there is no net gain or loss of the system's energy.

4. The mean force and torque on the system (resulting from the QETs into and out of

the system) is null.

Assume that between the times t_o and $t_o + \Delta t$ there are N quantum energy absorptions (with magnitudes U_{an}) directionally into the system (with corresponding directional unit vectors $\hat{\mathbf{a}}_{an}$). Additionally, assume that between the same times there are K quantum energy emissions (with magnitudes U_{ek}) directionally out of the system (with corresponding directional unit vectors $\hat{\mathbf{a}}_{ek}$).

The mean rate of quantum energy absorptions directionally into the system, $\bar{P}_a$ is:

$$\bar{P}_a = \frac{1}{\Delta t}\sum_{n=1}^{N} U_{an} = \Gamma m, \tag{4.1}$$

where Γ is the constant of QET rate to mass (W/kg), applicable in the limit for sufficiently large Δt. The constant of mean quantum energy absorption/emission rate to mass Γ is proposed to be equivalent to Γ_e derived in Appendix A as:

$$\Gamma = \Gamma_e = \frac{8\pi\varepsilon_o m_e c^5}{e^2} = 1.913 \times 10^{40} \quad (\text{W/kg})\,. \tag{4.2}$$

The mean rate of quantum energy emissions directionally out of the system, $\bar{P}_e$ is:

$$\bar{P}_e = \frac{1}{\Delta t}\sum_{k=1}^{K} U_{ek} = \Gamma m = \bar{P}_a. \tag{4.3}$$

The net force on the system as a result of quantum energy absorption directionally into the system, $\vec{\mathbf{F}}_a$ is:

$$\vec{\mathbf{F}}_a = \frac{1}{c\Delta t}\sum_{n=1}^{N} U_{an}\hat{\mathbf{a}}_{an} \quad (\text{N})\,. \tag{4.4}$$

The net force on the system as a result of quantum energy emissions directionally out of the system, $\vec{\mathbf{F}}_e$ is:

$$\vec{\mathbf{F}}_e = \frac{1}{c\Delta t}\sum_{k=1}^{K} U_{ek}\hat{\mathbf{a}}_{ek} = -\vec{\mathbf{F}}_a. \tag{4.5}$$

The net forces $\vec{\mathbf{F}}_a$ and $\vec{\mathbf{F}}_e$ may be non-zero. However, the total net force from QETs into and out of the system (i.e., the summation of the two forces) is null. Therefore, the net forces $\vec{\mathbf{F}}_a$ and $\vec{\mathbf{F}}_e$ are equal and opposite (in the limit for sufficiently large Δt). The net system torques from QETs into and out of the system may be non-zero, and also are equal and opposite (i.e., the total net system torque is null).

The basic model/concept of gravity is (as described in Chapter 3): QETs occur between the masses of the universe and local masses; two local masses screen each other from these QETs causing the local masses to be pushed together.

The basic model/concept of inertia is related to the net forces $\vec{\mathbf{F}}_a$ and $\vec{\mathbf{F}}_e$ on a system. When a system is at rest (as observed in an inertial reference frame), both net forces $\vec{\mathbf{F}}_a$ and $\vec{\mathbf{F}}_e$ are zero. However, if the system is moving with a given velocity, $\vec{\mathbf{F}}_a$ will be non-zero, having a direction opposite the velocity (i.e., greater net impact force on the front side of system). In addition, $\vec{\mathbf{F}}_e$ will be non-zero, having the same direction as the velocity (i.e., greater net recoil force on the back side of the system). $\vec{\mathbf{F}}_a$ and $\vec{\mathbf{F}}_e$ are equal and opposite, so the net force will be zero. If the system is accelerated, $\vec{\mathbf{F}}_a$ and $\vec{\mathbf{F}}_e$ are no longer equal and opposite, giving rise to a net force (i.e., the force of inertia).

CHAPTER 5. A QET MODEL FOR THE POINCARÉ STRESS OF AN ISOLATED, SPHERICALLY SYMMETRIC STATIC CHARGE DISTRIBUTION

The goal of this and the subsequent chapter is to establish a QET (boson interaction) model that provides a visualization of the stresses internal and external to static charge distributions [54]. The internal and external charge distribution stresses are derived from the recasting of Maxwell's stress equation. Therefore, the electrostatic QET model of this dissertation is mathematically consistent with Maxwell's stress equation.

The QET model for electrostatics may provide fresh or different insight into electrostatic systems. The model provides an alternate conceptualization of the path of electrostatic forces and the location of stored electrostatic potential energy. In addition, the QET model provides an illustrative link between classical electrostatics and the quantum realm.

Maxwell's stress equation for electrostatics identifies a tensile stress in the direction of the electric field and a pressure normal to this direction. The principle aim of this chapter is to determine how Maxwell's stress equation (applied to a closed surface external for an isolated, spherically symmetric static charge distribution) can be recast to eliminate the stress normal to the electric field while maintaining a radial stress aligned with the field [55]. The motivation to pursue this endeavor is to establish a mathematical basis for an external omnidirectional pressure, inwardly directed that may be attributed to the Poincaré

stress [56, 57] maintaining the equilibrium of the charge distribution.

For electrostatics, the electromagnetic momentum density [58] is null. Therefore, from the conservation of momentum, the electrostatic force $\vec{\mathbf{f}}$ per unit volume at any given location is:

$$\vec{\mathbf{f}} = \nabla \cdot \overleftrightarrow{\mathbf{T}}, \tag{5.1}$$

where $\overleftrightarrow{\mathbf{T}}$ is the Maxwell stress tensor [59]. For electrostatics in free space, terms of the Maxwell stress tensor are:

$$T_{ij} = \varepsilon_{\mathrm{o}} E_i E_j - \frac{\varepsilon_{\mathrm{o}}}{2} \delta_{ij} E^2, \tag{5.2}$$

where ε_{o} is the permittivity of free space, δ_{ij} is the Kronecker delta (i.e., 1 if the indices are the same, 0 otherwise), and E_i or E_j is the x, y, or z component of the electric field. Maxwell's stress equation for electrostatics in free space can be obtained by applying the divergence theorem to the total force for a given volume using (5.1) (see also an alternate derivation in [60] and Appendix B):

$$\begin{aligned} \vec{\mathbf{F}} &= \iiint \vec{\mathbf{f}} \, dV = \iiint \left(\nabla \cdot \overleftrightarrow{\mathbf{T}} \right) dV = \oiint \overleftrightarrow{\mathbf{T}} \cdot d\vec{\mathbf{S}} \\ &= \varepsilon_{\mathrm{o}} \oiint \vec{\mathbf{E}} \left(\vec{\mathbf{E}} \cdot d\vec{\mathbf{S}} \right) - \frac{\varepsilon_{\mathrm{o}}}{2} \oiint E^2 d\vec{\mathbf{S}}. \end{aligned} \tag{5.3}$$

An interesting outcome of Maxwell's stress equation is that the force on a charge distribution may be attributed to the electric field in the free space around the charge distribution, rather than to the charge distribution itself [61]. Maxwell's stress equation may be applied to any surface that either encloses all charge distributions or separates one charge distribution (with any enclosed surface shape) from a second charge distribution [62].

The simplest example of a spherically symmetric charge distribution is a hollow shell having a uniform surface charge distribution. Maxwell's stress equation at the shell surface depicts the outward electrostatic pressure on the shell surface corresponding to the repulsive Coulomb force between all shell charge distribution elements. The Poincaré stress is traditionally viewed as an internal pulling, mechanical stress of the shell's physical structure balancing the outward electrostatic pressure. The Maxwell stress (per unit area) at concentric spherical surfaces (with radius r) away from the spherical shell falls off as $1/r^4$.

In contrast, for this simple spherical shell charge distribution, the QET model of this chapter depicts the Poincaré stress as an inwardly directed, omnidirectional pressure. The pressure is a result of a mean valued, continual QETs between the charge distribution and the distant matter of the universe. The Poincaré stress (per unit area) at concentric spherical surfaces away from the spherical shell falls off as $1/r^2$ compared to $1/r^4$ for the Maxwell stress.

This chapter establishes the external Poincaré stress that is mathematically compatible with Maxwell's stress equation. Unlike Maxwell's stress, the Poincaré stress has no stress component normal to the electric field, but only has a stress component aligned with the straight 'path' of the QET (i.e., aligned with the electric field external to the spherical shell).

The electrostatic potential energy of the spherical shell is traditionally computed by integration of the square of the electric field over the volume of space from the shell's surface to infinity (i.e., the electric field inside the hollow shell is null) [63]. Therefore, the electrostatic potential energy is classically viewed as being stored in the electric field. Al-

ternatively, the electrostatic potential energy may be computed by integration of the product of the electric potential and the charge density at the charge distribution shell [64]. In this case, the electrostatic potential energy may be viewed as being stored in the charge distribution itself.

In contrast, for this simple spherical shell charge distribution, the QET model of Chapter 6 identifies the electrostatic potential energy as trapped energy inside the hollow shell. The trapped energy is a result of a mean valued, continual exchange of photons between all shell charge distribution elements. Chapter 6 also develops an internal line stress between two separated, spherically symmetric static charge distributions. The line stress is shown to be mathematically consistent with Maxwell's stress equation. The spherical shell charge distribution may be constructed from the superposition of many dumbbell components [57] (the two separated charge distributions making up a dumbbell component).

The spherical shell charge distribution example highlights the primary differences between the traditional approach and the QET model for electrostatics. The traditional approach defines the Poincaré stress as internal to the structure and establishes that the electrostatic potential energy is stored in the electric field external to the shell (or alternately in the charge distribution itself). In contrast, the QET model defines the Poincaré stress as an external stress and establishes the electrostatic potential energy as trapped energy inside the hollow shell.

For an isolated, spherically symmetric static charge distribution, Maxwell's stress equation applied to any closed surface (containing all or none of the charge distribution) yields a total force that is null. This is easily shown for any concentric spherical surface

outside of the charge distribution due to symmetry. The purpose of recasting Maxwell's stress equation for a spherically symmetric static charge distribution is not to produce an alternate method of obtaining the same null result. Instead, the purpose of recasting is to ascertain a stress with a component only in the radial direction.

Maxwell's stress equation designates a differential element of stress at a specific location on a given surface. As shown in Section 5.1, Maxwell's stress equation for the spherically symmetric charge distribution may be recast in an infinite number of ways, all producing the null result for the total force on any closed surface (containing all or none of the charge distribution). However, there are two outcomes of importance. First, Maxwell's stress equation may be recast such that in addition to the total force on a closed surface being null, every differential element of stress on the surface is null as well. Second, Maxwell's stress equation may be recast such that every differential element of stress only has a component in the radial direction. The first is an interesting result while the second supports the QET electrostatic model of this dissertation.

Section 5.1 methodically steps through the details of recasting Maxwell's stress equation for a conic closed surface in free space away from an isolated spherically symmetric static charge distribution at the origin. A variant of Stokes' Theorem (derived in Appendix C) is used in this recasting process. The end result is a recast stress equation for a closed surface that depicts an inward surface tension only in the radial direction, parallel to the electric field for a spherically symmetric charge distribution.

Section 5.1 is purposely arduous in the recasting process which may appear to take the longest route to obtain the desired results. However, the application of the variant of

Stokes' Theorem is uncommon and justifies such rigor. The end result is the recasting of the differential element of Maxwell's stress equation from a stress with a component normal to the electric field and a component in the radial direction that falls off as $1/r^4$ to a Poincaré stress with a differential element only in the radial direction that falls off as $1/r^2$.

Section 5.2 generalizes the results of Section 5.1 for an arbitrary spherically symmetric charge distribution location and arbitrary closed surface. Again, the recasting of Maxwell's stress equation is realized by applying a variant of Stokes' Theorem. However, the recasting process itself is more concise.

Section 5.3 expounds on the Poincaré stress identified in the recast stress equation. Modeled as energy carrier mediator interactions with the distant matter of the universe, this stress is shown to conform with Mach's principle.

5.1 Recasting of Maxwell's Stress Equation in Free Space, Away from an Isolated Spherically Symmetric Static Charge Distribution at the Origin

In classical electrostatics, the electric field external to a spherically symmetric charge distribution (centered at the origin), with total charge, q, is [65]:

$$\vec{\mathbf{E}} = \frac{q}{4\pi\varepsilon_o r^2}\hat{\mathbf{a}}_r, \tag{5.4}$$

where r is the distance from the origin and $\hat{\mathbf{a}}_r$ is the radial unit vector of the electric field location.

Maxwell's stress equation (5.3) may be used to determine the force on each surface of the conic closed surface shown in Figure 5.1. The surfaces at $r = a$ and $r = b$ are spherical

surfaces (i.e., only a radial component normal to the surface) and the side surface only has an azimuthal component normal to the surface. The angle α specifies the tilt of the side surface S_{side} with respect to the z axis.

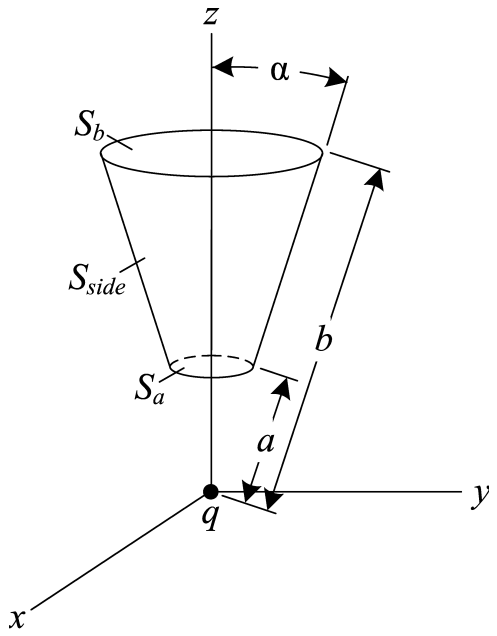

Figure 5.1: Conic closed surface symmetric about the z axis with spherical surfaces at $r = a$ and $r = b$.

The force from Maxwell's stress equation for surface S_a is:

$$\vec{\mathbf{F}}_a = \varepsilon_o \iint_{S_a} \vec{\mathbf{E}} \left(\vec{\mathbf{E}} \cdot d\vec{\mathbf{S}} \right) - \frac{\varepsilon_o}{2} \iint_{S_a} E^2 d\vec{\mathbf{S}} = \varepsilon_o \iint_{S_a} E^2 d\vec{\mathbf{S}} - \frac{\varepsilon_o}{2} \iint_{S_a} E^2 d\vec{\mathbf{S}} = \frac{\varepsilon_o}{2} \iint_{S_a} E^2 d\vec{\mathbf{S}}, \tag{5.5}$$

and the force in the z direction for surface S_a is:

$$F_{a_z} = -\frac{\varepsilon_o}{2} \int_0^{2\pi} \int_0^{\alpha} \left(\frac{q}{4\pi\varepsilon_o a^2} \right)^2 a^2 \sin\theta \cos\theta d\theta d\phi = -\frac{q^2 \sin^2 \alpha}{32\pi\varepsilon_o a^2}. \tag{5.6}$$

The force from Maxwell's stress equation for surface S_b is:

$$\vec{\mathbf{F}}_b = \frac{\varepsilon_o}{2} \iint_{S_b} E^2 d\vec{\mathbf{S}}, \tag{5.7}$$

and the force in the z direction for surface S_b is:

$$F_{b_z} = \frac{\varepsilon_o}{2} \int_0^{2\pi} \int_0^{\alpha} \left(\frac{q}{4\pi\varepsilon_o b^2} \right)^2 b^2 \sin\theta \cos\theta d\theta d\phi = \frac{q^2 \sin^2 \alpha}{32\pi\varepsilon_o b^2}. \tag{5.8}$$

The force from Maxwell's stress equation for surface S_{side} is:

$$\vec{\mathbf{F}}_{side} = \varepsilon_o \iint_{S_{side}} \vec{\mathbf{E}} \left(\vec{\mathbf{E}} \cdot d\vec{\mathbf{S}} \right) - \frac{\varepsilon_o}{2} \iint_{S_{side}} E^2 d\vec{\mathbf{S}} = 0 - \frac{\varepsilon_o}{2} \iint_{S_{side}} E^2 d\vec{\mathbf{S}} = -\frac{\varepsilon_o}{2} \iint_{S_{side}} E^2 d\vec{\mathbf{S}}, \tag{5.9}$$

and the force in the z direction for surface S_{side} is:

$$F_{side_z} = \frac{\varepsilon_o}{2} \int_0^{2\pi} \int_a^b \left(\frac{q}{4\pi\varepsilon_o r^2} \right)^2 r \sin\alpha \sin\alpha \, dr \, d\phi = \frac{q^2 \sin^2 \alpha}{32\pi\varepsilon_o} \left(\frac{1}{a^2} - \frac{1}{b^2} \right). \tag{5.10}$$

For any closed surface containing free space, the net force from Maxwell's stress equation is null. This is true for the sum of the three surface forces of (5.6), (5.8), and (5.10):

$$F_{total_z} = F_{a_z} + F_{b_z} + F_{side_z} = 0. \tag{5.11}$$

The three forces on each surface of the conic closed surface of Figure 5.1 give some general insight into Maxwell's stress equation. James Maxwell related Michael Faraday's physical lines of force (electric lines of force in this case) [1] to a state of stress in the medium (i.e., tension in the direction of the lines of force and pressure normal to this direction) [21]. Surfaces S_a and S_b are in the direction of the electric lines of force and the surface S_{side} is normal to this direction.

The primary goal of this section is to determine if Maxwell's stress equation for the conic closed surface of Figure 5.1 can be recast to eliminate the stress normal to the electric lines of force while maintaining a radial stress (for an isolated spherically symmetric static

distribution). To accomplish this goal, the following variant of Stokes' Theorem is used (see derivation in Appendix C):

$$\oint \vec{\mathbf{C}} \times d\vec{\boldsymbol{\ell}} = \iint \left[\left(\nabla \cdot \vec{\mathbf{C}} \right) d\vec{\mathbf{S}} - \nabla_{\mathrm{C}} \left(\vec{\mathbf{C}} \cdot d\vec{\mathbf{S}} \right) \right], \tag{5.12}$$

where the C subscript of the del operator indicates that partial derivatives are only applied to the vector field $\vec{\mathbf{C}}$ (see (C.5)).

The variant of Stokes' Theorem is used to convert the Maxwell's stress equation force contribution on the side surface of the cone to forces on the ring edges at $r = a$ and $r = b$. Figure 5.2(a) shows a closed contour bounding the surface S_{side}: traversing clockwise around the top ring edge at $r = b$, down the side surface, continuing counter-clockwise around the bottom ring edge at $r = a$, and returning up the side surface. Figure 5.2(b) shows that the net result of the closed contour of (a) is two separate ring edges, one at $r = a$ and the other at $r = b$.

The objective is to determine a $\vec{\mathbf{C}}$ such that the variant of Stokes' Theorem applied to the closed contour of Figure 5.2(a) results in a force on surface S_{side} equivalent to the Maxwell's stress equation force for this surface. A first step to achieve this objective is to systematically establish how the variant of Stokes' Theorem applied to S_{side} operates on a $\vec{\mathbf{C}}$ of the general form:

$$\vec{\mathbf{C}}_n = \frac{k_n}{r^n} \hat{\mathbf{a}}_r, \tag{5.13}$$

where k_n is an arbitrary constant and n is a positive integer.

The divergence of $\vec{\mathbf{C}}_n$ is:

$$\nabla \cdot \vec{\mathbf{C}}_n = k_n \left[\frac{\partial}{\partial x} \frac{x}{r^{n+1}} + \frac{\partial}{\partial y} \frac{y}{r^{n+1}} + \frac{\partial}{\partial z} \frac{z}{r^{n+1}} \right] = \frac{k_n \left(2 - n\right)}{r^{n+1}}, \tag{5.14}$$

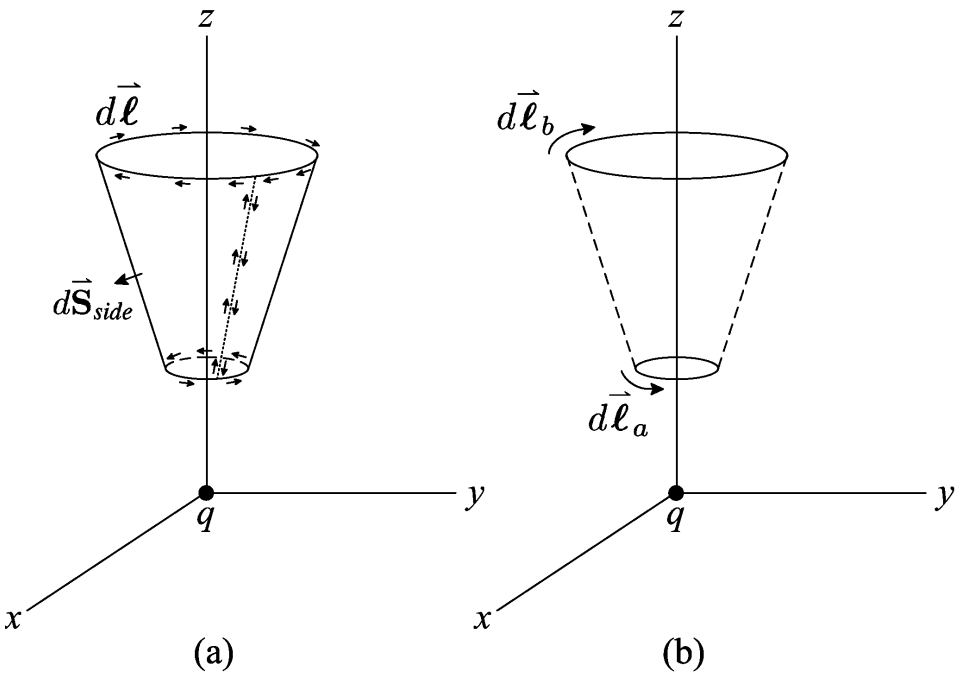

Figure 5.2: Force on (a) closed contour bounding the surface S_{side} is equivalent to (b) two ring edges at $r = a$ and $r = b$.

and the gradient of the vector [66] $\vec{\mathbf{C}}_n$ is:

$$\begin{aligned}\nabla\vec{\mathbf{C}}_n &= k_n\begin{bmatrix}\frac{\partial}{\partial x}\frac{x}{r^{n+1}} & \frac{\partial}{\partial x}\frac{y}{r^{n+1}} & \frac{\partial}{\partial x}\frac{z}{r^{n+1}}\\ \frac{\partial}{\partial y}\frac{x}{r^{n+1}} & \frac{\partial}{\partial y}\frac{y}{r^{n+1}} & \frac{\partial}{\partial y}\frac{z}{r^{n+1}}\\ \frac{\partial}{\partial z}\frac{x}{r^{n+1}} & \frac{\partial}{\partial z}\frac{y}{r^{n+1}} & \frac{\partial}{\partial z}\frac{z}{r^{n+1}}\end{bmatrix}\\ &= -\frac{k_n(n+1)}{r^{n+3}}\begin{bmatrix}x^2-\frac{r^2}{n+1} & xy & xz\\ xy & y^2-\frac{r^2}{n+1} & yz\\ xz & yz & z^2-\frac{r^2}{n+1}\end{bmatrix}.\end{aligned} \tag{5.15}$$

The differential surface element for S_{side} is:

$$d\vec{\mathbf{S}}_{side} = dS_{side}\hat{\mathbf{a}}_\theta = dS_{side}\begin{bmatrix} \dfrac{xz}{r\sqrt{x^2+y^2}} \\ \dfrac{yz}{r\sqrt{x^2+y^2}} \\ -\dfrac{\sqrt{x^2+y^2}}{r} \end{bmatrix}, \tag{5.16}$$

and:

$$\nabla_{\mathrm{C}_n}\left(\vec{\mathbf{C}}_n \cdot d\vec{\mathbf{S}}_{side}\right) = \left(\nabla\vec{\mathbf{C}}_n\right)\cdot d\vec{\mathbf{S}}_{side} = \frac{k_n}{r^{n+1}}d\vec{\mathbf{S}}_{side}. \tag{5.17}$$

Combining (5.14), (5.17), and the integrand in the right side of (5.12) for the surface S_{side} yields:

$$\begin{aligned}\left(\nabla\cdot\vec{\mathbf{C}}_n\right)d\vec{\mathbf{S}}_{side} - \nabla_{\mathrm{C}_n}\left(\vec{\mathbf{C}}_n\cdot d\vec{\mathbf{S}}_{side}\right) &= \frac{k_n\,(2-n)}{r^{n+1}}d\vec{\mathbf{S}}_{side} - \frac{k_n}{r^{n+1}}d\vec{\mathbf{S}}_{side} \\ &= \frac{k_n\,(1-n)}{r^{n+1}}d\vec{\mathbf{S}}_{side}.\end{aligned} \tag{5.18}$$

From the general results of (5.18), Maxwell's stress equation for surface S_{side} (5.9) can be converted to contour ring forces at $r = a$ and $r = b$ using a $\vec{\mathbf{C}}$ of the form given in (5.13) by selecting $n = 3$ and k_3 such that:

$$\vec{\mathbf{C}} = \frac{k_3}{r^3}\hat{\mathbf{a}}_r = \frac{\varepsilon_\mathrm{o}}{4}\left(\frac{q}{4\pi\varepsilon_\mathrm{o}}\right)^2\frac{1}{r^3}\hat{\mathbf{a}}_r = \frac{\varepsilon_\mathrm{o} r E^2}{4}\hat{\mathbf{a}}_r. \tag{5.19}$$

The two contour ring forces at $r = a$ and $r = b$ can subsequently be converted to surface forces at S_a and S_b using the variant of Stokes' Theorem (5.12). In general, for a $\vec{\mathbf{C}}$ of the form given in (5.13) and the gradient of the vector $\vec{\mathbf{C}}_n$ given in (5.15) applied to a spherical outward surface:

$$d\vec{\mathbf{S}}_r = dS_r\hat{\mathbf{a}}_r = \frac{dS_r}{r}\begin{bmatrix} x \\ y \\ z \end{bmatrix} \tag{5.20}$$

(i.e., only a radial component normal to the surface such as S_b in Figure 5.1), yields:

$$\nabla_{\mathrm{C}_n}\left(\vec{\mathbf{C}}_n \cdot d\vec{\mathbf{S}}_r\right) = \left(\nabla\vec{\mathbf{C}}_n\right) \cdot d\vec{\mathbf{S}}_r = -\frac{nk_n}{r^{n+1}} d\vec{\mathbf{S}}_r. \tag{5.21}$$

Combining (5.14), (5.21), and the integrand in the right side of (5.12) for a spherical surface S_r yields:

$$\left(\nabla\cdot\vec{\mathbf{C}}_n\right)d\vec{\mathbf{S}}_r - \nabla_{\mathrm{C}_n}\left(\vec{\mathbf{C}}_n\cdot d\vec{\mathbf{S}}_r\right) = \frac{k_n\,(2-n)}{r^{n+1}} d\vec{\mathbf{S}}_r - -\frac{nk_n}{r^{n+1}} d\vec{\mathbf{S}}_r = \frac{2k_n}{r^{n+1}} d\vec{\mathbf{S}}_r. \tag{5.22}$$

Converting the contour ring force at $r = a$ with the $\vec{\mathbf{C}}$ of (5.19) and the contour direction $d\vec{\boldsymbol{\ell}}_a$ of Figure 5.2(b) and combining it with the Maxwell's stress equation for surface S_a of (5.5) yields null not only for the force on surface S_a but also for each differential element of the surface force integrand:

$$\vec{\mathbf{F}}_a = -\iint_{S_a} \frac{\varepsilon_{\mathrm{o}} E^2}{2} d\vec{\mathbf{S}} + \frac{\varepsilon_{\mathrm{o}}}{2} \iint_{S_a} E^2 d\vec{\mathbf{S}} = 0. \tag{5.23}$$

Similarly, converting the contour ring force at $r = b$ with the $\vec{\mathbf{C}}$ of (5.19) and the contour direction $d\vec{\boldsymbol{\ell}}_b$ of Figure 5.2(b) and combining it with the Maxwell's stress equation for surface S_b of (5.7) yields null:

$$\vec{\mathbf{F}}_b = -\iint_{S_b} \frac{\varepsilon_{\mathrm{o}} E^2}{2} d\vec{\mathbf{S}} + \frac{\varepsilon_{\mathrm{o}}}{2} \iint_{S_b} E^2 d\vec{\mathbf{S}} = 0. \tag{5.24}$$

It is interesting to note that using the variant of Stokes' Theorem to convert the Maxwell's stress equation force on the side surface of the cone S_{side} to ring forces on the cone ends and then subsequently using the variant of Stokes' Theorem to convert these ring forces to forces on the end surfaces S_a and S_b cancels out the Maxwell's stress equation force on these end surfaces. It is also interesting to note by inspection of (5.18) and (5.22)

that a $\vec{\mathbf{C}}$ of the form given in (5.13) with $n = 1$ may be added to (5.19) and still provide a valid conversion of Maxwell's stress equation for surface S_{side} to ring forces at $r = a$ and $r = b$:

$$\vec{\mathbf{C}}_{recast} = \frac{\varepsilon_o r E^2}{4}\hat{\mathbf{a}}_r + \frac{k}{8\pi r}\hat{\mathbf{a}}_r, \tag{5.25}$$

where k may be an arbitrary constant.

Converting the contour ring force at $r = a$ with the recasting $\vec{\mathbf{C}}$ of (5.25) and the contour direction $d\vec{\boldsymbol{\ell}}_a$ of Figure 5.2(b) and combining it with the Maxwell's stress equation for surface S_a of (5.5) yields:

$$\vec{\mathbf{F}}_a = -\iint\limits_{S_a}\left(\frac{\varepsilon_o E^2}{2} + \frac{k}{4\pi a^2}\right)d\vec{\mathbf{S}} + \frac{\varepsilon_o}{2}\iint\limits_{S_a} E^2 d\vec{\mathbf{S}} = -\iint\limits_{S_a}\frac{k}{4\pi a^2}d\vec{\mathbf{S}}. \tag{5.26}$$

Similarly, converting the contour ring force at $r = b$ with the recasting $\vec{\mathbf{C}}$ of (5.25) and the contour direction $d\vec{\boldsymbol{\ell}}_b$ of Figure 5.2(b) and combining it with the Maxwell's stress equation for surface S_b of (5.7) yields:

$$\vec{\mathbf{F}}_b = -\iint\limits_{S_b}\left(\frac{\varepsilon_o E^2}{2} + \frac{k}{4\pi b^2}\right)d\vec{\mathbf{S}} + \frac{\varepsilon_o}{2}\iint\limits_{S_b} E^2 d\vec{\mathbf{S}} = -\iint\limits_{S_b}\frac{k}{4\pi b^2}d\vec{\mathbf{S}}. \tag{5.27}$$

The force on surface S_a and S_b given in (5.26) and (5.27) are equal and opposite and represent an inward surface tension where the units of the constant k are N/sr. The outcome of this section is the recasting of Maxwell's stress equation using the variant of Stokes' Theorem:

$$\vec{\mathbf{F}}_{recast} = -\oiint\frac{k}{4\pi r^2}\hat{\mathbf{a}}_r\left(\hat{\mathbf{a}}_r \cdot d\vec{\mathbf{S}}\right). \tag{5.28}$$

For a spherically symmetric charge distribution centered at the origin, (5.28) may be applied to any closed surface which either encloses all or none of the charge distribution

(with no charge distribution at any surface element). If the closed surface is a sphere (also centered at the origin) enclosing the entire charge distribution, then the recast stress equation suggest an omnidirectional inward pressure. Section 5.3 establishes that the constant k is proportional to the electrostatic potential energy of the charge distribution.

5.2 Recasting of Maxwell's Stress Equation in Free Space for an Isolated Spherically Symmetric Static Charge Distribution at an Arbitrary Location for an Arbitrary Surface

The purpose of this section is to generalize the results of the preceding section for an arbitrary charge distribution location and arbitrary surface. Figure 5.3 shows an arbitrary surface away from a spherically symmetric charge distribution at $\vec{\mathbf{r}}_1' = x_1'\hat{\mathbf{a}}_x + y_1'\hat{\mathbf{a}}_y + z_1'\hat{\mathbf{a}}_z$ with total charge q_1. The electric field at any observation point, $\vec{\mathbf{r}}$, is:

$$\vec{\mathbf{E}}_1 = \frac{q_1}{4\pi\varepsilon_o r_1^3}\vec{\mathbf{r}}_1, \tag{5.29}$$

where:

$$\vec{\mathbf{r}}_1 = \vec{\mathbf{r}} - \vec{\mathbf{r}}_1' = (x - x_1')\,\hat{\mathbf{a}}_x + (y - y_1')\,\hat{\mathbf{a}}_y + (z - z_1')\,\hat{\mathbf{a}}_z = \begin{bmatrix} x_1 \\ y_1 \\ z_1 \end{bmatrix} = \begin{bmatrix} x - x_1' \\ y - y_1' \\ z - z_1' \end{bmatrix}. \tag{5.30}$$

Maxwell's stress equation for an arbitrary surface S can be recast using the method similar to the previous section. For any arbitrary closed contour on the arbitrary closed surface (shown as the ring in Figure 5.3), the variant of Stokes' Theorem is used to convert equal and opposite closed contour integrals to two surface integral portions bounded by the respective closed contours.

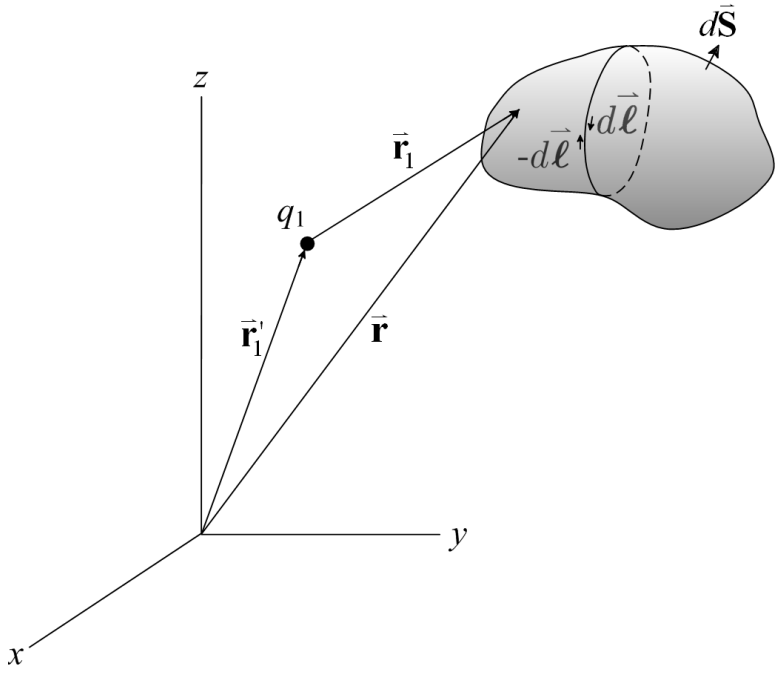

Figure 5.3: Arbitrary surface away from a spherically symmetric charge distribution with total charge q_1.

The following $\vec{\mathbf{C}}_1$ is chosen such that after converting to a surface force using (5.12) and combining with the Maxwell's stress equation of (5.3) (for the surface S) yields a component that is only radially aligned with respect to the spherical charge distribution location:

$$\begin{aligned}\vec{\mathbf{C}}_1 &= -\frac{\varepsilon_o}{4}\left(\frac{q_1}{4\pi\varepsilon_o}\right)^2 \frac{1}{r_1^3}\hat{\mathbf{a}}_{r_1} - \frac{k}{8\pi}\frac{1}{r_1}\hat{\mathbf{a}}_{r_1} \\ &= -\frac{\varepsilon_o}{4}\left(\frac{q_1}{4\pi\varepsilon_o}\right)^2 \frac{1}{r_1^4}\begin{bmatrix} x - x_1' \\ y - y_1' \\ z - z_1' \end{bmatrix} - \frac{k}{8\pi}\frac{1}{r_1^2}\begin{bmatrix} x - x_1' \\ y - y_1' \\ z - z_1' \end{bmatrix},\end{aligned} \tag{5.31}$$

where k is an arbitrary constant. The divergence of $\vec{\mathbf{C}}_1$ is:

$$\begin{aligned}\nabla\cdot\vec{\mathbf{C}}_1 =& -\frac{\varepsilon_o}{4}\left(\frac{q_1}{4\pi\varepsilon_o}\right)^2\left(\frac{\partial}{\partial_x}\frac{x-x_1'}{r_1^4}+\frac{\partial}{\partial_y}\frac{y-y_1'}{r_1^4}+\frac{\partial}{\partial_z}\frac{z-z_1'}{r_1^4}\right)\\ &-\frac{k}{8\pi}\left(\frac{\partial}{\partial_x}\frac{x-x_1'}{r_1^2}+\frac{\partial}{\partial_y}\frac{y-y_1'}{r_1^2}+\frac{\partial}{\partial_z}\frac{z-z_1'}{r_1^2}\right)\\ =&\frac{\varepsilon_o}{4}\left(\frac{q_1}{4\pi\varepsilon_o}\right)^2\frac{1}{r_1^4}-\frac{k}{8\pi}\frac{1}{r_1^2}=\frac{\varepsilon_o}{4}E_1^2-\frac{k}{8\pi r_1^2},\end{aligned} \tag{5.32}$$

and the gradient of the vector $\vec{\mathbf{C}}_1$ is:

$$\begin{aligned}\nabla\vec{\mathbf{C}}_1 =& -\frac{\varepsilon_o}{4}\left(\frac{q_1}{4\pi\varepsilon_o}\right)^2\begin{bmatrix}\frac{\partial}{\partial_x}\frac{x-x_1'}{r_1^4} & \frac{\partial}{\partial_x}\frac{y-y_1'}{r_1^4} & \frac{\partial}{\partial_x}\frac{z-z_1'}{r_1^4}\\ \frac{\partial}{\partial_y}\frac{x-x_1'}{r_1^4} & \frac{\partial}{\partial_y}\frac{y-y_1'}{r_1^4} & \frac{\partial}{\partial_y}\frac{z-z_1'}{r_1^4}\\ \frac{\partial}{\partial_z}\frac{x-x_1'}{r_1^4} & \frac{\partial}{\partial_z}\frac{y-y_1'}{r_1^4} & \frac{\partial}{\partial_z}\frac{z-z_1'}{r_1^4}\end{bmatrix}\\ &-\frac{k}{8\pi}\begin{bmatrix}\frac{\partial}{\partial_x}\frac{x-x_1'}{r_1^2} & \frac{\partial}{\partial_x}\frac{y-y_1'}{r_1^2} & \frac{\partial}{\partial_x}\frac{z-z_1'}{r_1^2}\\ \frac{\partial}{\partial_y}\frac{x-x_1'}{r_1^2} & \frac{\partial}{\partial_y}\frac{y-y_1'}{r_1^2} & \frac{\partial}{\partial_y}\frac{z-z_1'}{r_1^2}\\ \frac{\partial}{\partial_z}\frac{x-x_1'}{r_1^2} & \frac{\partial}{\partial_z}\frac{y-y_1'}{r_1^2} & \frac{\partial}{\partial_z}\frac{z-z_1'}{r_1^2}\end{bmatrix},\end{aligned} \tag{5.33}$$

and:

$$\begin{aligned}\nabla_{\mathrm{C}_1}\left(\vec{\mathbf{C}}_1\cdot d\vec{\mathbf{S}}\right) =& \left(\nabla\vec{\mathbf{C}}_1\right)\cdot d\vec{\mathbf{S}}\\ =&\varepsilon_o\vec{\mathbf{E}}_1\left(\vec{\mathbf{E}}_1\cdot d\vec{\mathbf{S}}\right)-\frac{\varepsilon_o}{4}E_1^2 d\vec{\mathbf{S}}-\frac{k}{8\pi r_1^2}d\vec{\mathbf{S}}+\frac{k}{4\pi r_1^2}\hat{\mathbf{a}}_{r_1}\left(\hat{\mathbf{a}}_{r_1}\cdot d\vec{\mathbf{S}}\right).\end{aligned} \tag{5.34}$$

Combining (5.32), (5.34), and the right side of (5.12) and adding this result to the

Maxwell's stress equation (5.3) for the surface S yields:

$$\begin{aligned}
\vec{\mathbf{F}}_{1_{recast}} &= \oiint \left[\begin{array}{l} \varepsilon_{\mathrm{o}} \vec{\mathbf{E}}_1 \left(\vec{\mathbf{E}}_1 \cdot d\vec{\mathbf{S}} \right) - \dfrac{\varepsilon_{\mathrm{o}}}{2} E_1^2 d\vec{\mathbf{S}} \\ + \left(\nabla \cdot \vec{\mathbf{C}}_1 \right) d\vec{\mathbf{S}} - \nabla_{\mathrm{C}_1} \left(\vec{\mathbf{C}}_1 \cdot d\vec{\mathbf{S}} \right) \end{array} \right] \\
&= \oiint \left[\begin{array}{l} \varepsilon_{\mathrm{o}} \vec{\mathbf{E}}_1 \left(\vec{\mathbf{E}}_1 \cdot d\vec{\mathbf{S}} \right) - \dfrac{\varepsilon_{\mathrm{o}}}{2} E_1^2 d\vec{\mathbf{S}} \\ + \left(\dfrac{\varepsilon_{\mathrm{o}}}{4} E_1^2 - \dfrac{k}{8\pi r_1^2} \right) d\vec{\mathbf{S}} \\ - \left(\begin{array}{l} \varepsilon_{\mathrm{o}} \vec{\mathbf{E}}_1 \left(\vec{\mathbf{E}}_1 \cdot d\vec{\mathbf{S}} \right) - \dfrac{\varepsilon_{\mathrm{o}}}{4} E_1^2 d\vec{\mathbf{S}} \\ - \dfrac{k}{8\pi r_1^2} d\vec{\mathbf{S}} + \dfrac{k}{4\pi r_1^2} \hat{\mathbf{a}}_{r_1} \left(\hat{\mathbf{a}}_{r_1} \cdot d\vec{\mathbf{S}} \right) \end{array} \right) \end{array} \right] \\
&= - \oiint \frac{k}{4\pi r_1^2} \hat{\mathbf{a}}_{r_1} \left(\hat{\mathbf{a}}_{r_1} \cdot d\vec{\mathbf{S}} \right).
\end{aligned} \tag{5.35}$$

Equation (5.35) represents the recasting of Maxwell's stress equation in free space for an arbitrary spherically symmetric static charge distribution location and an arbitrary surface (not containing any surface charge) using the variant of Stokes' Theorem. The recast stress equation depicts an inward surface tension only in the radial direction (relative to the charge distribution location) where the units of the constant k are N/sr.

5.3 Poincaré Stress and QET

Maxwell's stress equation applied to a closed surface external to an isolated, spherically symmetric static charge distribution has been recast using a variant of Stokes' Theorem. The recast stress equation (5.28) or (5.35) eliminates the stress normal to the electric field and manifests an inward surface tension only in the radial direction (relative to the charge distribution location).

The recasting may have the appearance of fabricating something from nothing. The argument being that for an arbitrary closed surface that either contains none or all of the charge distribution, there is nothing at the surface since Maxwell's stress equation has a net null result. However, Maxwell's stress equation may be used to determine the outward electrostatic pressure [61] (N/m^2) on a spherical shell with uniform charge distribution, total charge q, and radius a (see also an alternate derivation [67]):

$$\vec{\mathbf{p}}_a = \frac{\varepsilon_\mathrm{o}}{2} E^2 \hat{\mathbf{a}}_r = \frac{q^2}{32\pi^2 \varepsilon_\mathrm{o}\, a^4} \hat{\mathbf{a}}_r. \tag{5.36}$$

Similarly, the recast stress equation has some usefulness.

In general, the Poincaré stress is a non-electromagnetic, binding force that keeps a charge distribution stable [68, 69]. This binding force is typically viewed as being internal to the charge distribution (i.e., an inward pulling force equalizing the outward electrostatic pressure). However, the recast Maxwell's stress equation (5.28) identifies a stress that is external to the charge distribution, directed inward. Poincaré propounded at times that the equalizing stress was an external pressure [70].

An external Poincaré stress for a spherically symmetric charge distribution may be modeled as an omnidirectional average rate of QET influx (W/sr) in combination with an out-flux of an equal average rate of QETs. Since the average rate of influx and out-flux QETs are equal, there is no net gain or loss of energy in the charge distribution. The average rate of QET influx and out-flux depict a mean valued sequence of energy carrier mediators. For instance, the energy carrier mediators (bosons) may be gravitons or photons [71, 35]. The impact force of QET influx and the recoil force of QET out-flux [72] accounts for the inward pressure (N/sr).

Assume that the mean QET influx and out-flux is proportional to the electrostatic potential energy (or equivalent electrostatic mass) of the spherically symmetric charge distribution. For example, the electrostatic potential energy of a spherical shell with uniform charge distribution, total charge q and radius a is: $U_e = q^2/8\pi\varepsilon_o a$ [73]. Therefore, the constant k of (5.28) or (5.35) is proportional to the equivalent electrostatic mass $m = U_e/c^2$ of the charge distribution. Chapter 4 described a net rate of QET absorptions, $\bar{P}_a$, and emissions, $\bar{P}_e$, both proportional to the mass, m, of a system: $\bar{P}_a = \bar{P}_e = \Gamma m$. The constant of mean rate of QET absorptions/emissions to electrostatic mass Γ is proposed to be equivalent to Γ_e derived in Appendix A as:

$$\Gamma = \Gamma_e = \frac{8\pi\varepsilon_o m_e c^5}{e^2} = 1.913 \times 10^{40} \quad (\text{W/kg}) . \tag{5.37}$$

This derivation is based on Jules Henri Poincaré's conclusion that the electron is in equilibrium between the outward force of charge wanting to push it apart and an inward normal stress [74].

The Poincaré stress is the sum of the impact force density of quantum energy absorptions and recoil force density of quantum energy emissions. Therefore, for a spherically symmetric charge distribution with electrostatic potential energy, U_e, the Poincaré stress equation is (5.35) with $k = \left(\bar{P}_a + \bar{P}_e\right)/c = 2\Gamma U_e/c^3$:

$$\vec{\mathbf{F}}_{1_{Poincaré}} = -\oiint \frac{\Gamma U_e}{2\pi c^3 r_1^2} \hat{\mathbf{a}}_{r_1} \left(\hat{\mathbf{a}}_{r_1} \cdot d\vec{\mathbf{S}}\right) . \tag{5.38}$$

Jules Henri Poincaré also hinted of a relationship between the electrostatic equalizing stress and gravity [75]. Ernst Mach suggested a connection with the masses of the universe contributing to inertial motions [41]. Mach's principle has been coined to relate the inertia

force (on accelerating local masses) as a result of the fixed, distant matter of the universe [76, 77]. An isolated mass may have a large quantity of quantum energy bosons interacting with the distant matter of the universe [78].

Equation (5.38) may be interpreted in light of Mach's principle. An isolated, spherically symmetric static charge distribution has an average rate of QET influx and out-flux interacting with the distant matter of the universe, proportional to the equivalent electrostatic mass of the charge distribution. The recast stress equation depicts an inward omnidirectional pressure (i.e., Poincaré stress) for a spherical surface enclosing the charge distribution as a result of these QET interactions.

The mean rate of QET influx and out-flux resulting in the Poincaré stress may consist of a combination of photons and bosons. If the interaction is with the charge in the distribution, then the QETs may be considered photon exchanges. If the interaction is with the solid structure of the distribution itself, then the QETs may be considered bosons. The specifics of which are involved are not needed for this model. The important aspect for electrostatics is that the inwardly directed Poincaré stress is in equilibrium with the outward electrostatic force keeping the solid structure/charge distribution intact.

A rigid/solid structure plays an important role in electrostatics. The rigid structure contains the charges and is part of the mechanism for keeping the charge distribution in equilibrium (i.e., from flying apart). The Poincaré stress also plays an important part. For a spherically symmetric charge distribution, the underlying rigid structure has a radial tension trying to pull the structure apart. The Poincaré stress interacting with the rigid structure counteracts this tension in the structure keeping everything at equilibrium. If the

solid structure were not there, then the Poincaré stress interacting with the structure would also not be there and the charges in the charge distribution would start to accelerate away from each other.

The mean rate of QET influx and out-flux could be viewed as a continuum of omni-directional influx and out-flux of power exchange (W/sr) near (into and out of) the charge distribution. The concept of a continuum power exchange is not necessary and doesn't simplify the model. In fact, it complicates the exchanges/interactions with the distant matter of the universe. For a given charge distribution, there is a mean rate of energy exchange with the distant matter of the universe. However, the exchange is not always with the same distant matter every time. Instead, the exchange is with any distant matter and statistically varies with each QET.

5.4 Summary

Using a variant of Stokes' Theorem, Maxwell's stress equation for an isolated, spherically symmetric static charge distribution has been successfully recast. The recast stress equation identifies a non-electromagnetic Poincaré stress as the only stress external to the charge distribution. The Poincaré stress is aligned with the electric field, is omnidirectional, and is directed inward toward the charge distribution.

The Poincaré stress is modeled as an average rate of QET influx and an equivalent average rate of QET out-flux, the QETs exchanging bosons between the charge distribution and the distant matter of the universe. The inward pressure arises from the impact force of

energy influx and the recoil force of energy out-flux. The Poincaré stress is proportional to the equivalent mass of the electrostatic potential energy of the charge distribution.

For two or more spherically symmetric, separated static charge distributions, the recast stress equation of this chapter is insufficient. For a two charge distribution system, the total electric field $\vec{\mathbf{E}}$ is the superposition of the electric field from each separate charge distribution: $\vec{\mathbf{E}} = \vec{\mathbf{E}}_1 + \vec{\mathbf{E}}_2$. For this two charge system, Maxwell's stress equation (5.3) has additional cross terms from the expansion of electric field products that are further evaluated in the next chapter.

CHAPTER 6. A QET MODEL FOR THE COULOMB AND POINCARÉ STRESSES OF TWO SEPARATED, SPHERICALLY SYMMETRIC STATIC CHARGE DISTRIBUTIONS

The goal of this and the previous chapter is to establish a QET (boson interaction) model that provides a visualization of the stresses internal and external to static charge distributions. The internal and external charge distribution stresses are derived from the recasting of Maxwell's stress equation. Therefore, the electrostatic QET model of this dissertation is mathematically consistent with Maxwell's stress equation.

Chapter 5 established a Poincaré stress by recasting Maxwell's stress equation for an isolated, spherically symmetric static charge distribution using a variant of Stokes' Theorem. The Poincaré stress is aligned with the electric field, is omnidirectional, and is directed inward toward the charge distribution. The Poincaré stress is modeled as an average rate of QET influx and an equivalent average rate of QET out-flux, the QETs exchanging bosons between the charge distribution and the distant matter of the universe. The inward pressure arises from the impact force of QET influx and the recoil force of QET out-flux. The Poincaré stress is proportional to the equivalent mass of the electrostatic potential energy of the charge distribution.

The principle aim of this chapter is to determine how Maxwell's stress equation for two separated, spherically symmetric static charge distributions (applied to a closed surface enclosing one or both of the charge distributions) can be recast such that only a stress at a

single point aligned between the two charge distributions remains [79]. The motivation to pursue this endeavor is to establish a mathematical basis for a Coulomb stress[4] that only exists at each point on the straight path between the two charge distributions.

Two separated, spherically symmetric static charge distributions are a key building block for electrostatics. Two extremely small charge configurations (i.e., point charges) are often referred to as a dumbbell [80, 81]. Any arbitrary charge distribution may be assembled from a collection of interacting charge dumbbells. Therefore, dumbbell results may be generalized for a spherical shell or any other configuration of interest [57].

Maxwell's stress equation for electrostatics in free space is:

$$\vec{\mathbf{F}} = \varepsilon_o \oiint \vec{\mathbf{E}} \left(\vec{\mathbf{E}} \cdot d\vec{\mathbf{S}} \right) - \frac{\varepsilon_o}{2} \oiint E^2 d\vec{\mathbf{S}}, \tag{6.1}$$

where ε_o is the permittivity of free space.

For a two charge system, the total electric field $\vec{\mathbf{E}}$ is the superposition of the electric field from each separate charge distribution: $\vec{\mathbf{E}} = \vec{\mathbf{E}}_1 + \vec{\mathbf{E}}_2$ [57]. Therefore, Maxwell's stress equation for electrostatics in free space for a two charge system is:

$$\vec{\mathbf{F}} = \varepsilon_o \oiint \left(\vec{\mathbf{E}}_1 + \vec{\mathbf{E}}_2 \right) \left[\left(\vec{\mathbf{E}}_1 + \vec{\mathbf{E}}_2 \right) \cdot d\vec{\mathbf{S}} \right] - \frac{\varepsilon_o}{2} \oiint \left(\vec{\mathbf{E}}_1 + \vec{\mathbf{E}}_2 \right) \cdot \left(\vec{\mathbf{E}}_1 + \vec{\mathbf{E}}_2 \right) d\vec{\mathbf{S}}, \tag{6.2}$$

or:

$$\begin{aligned} \vec{\mathbf{F}} = & \varepsilon_o \oiint \vec{\mathbf{E}}_1 \left(\vec{\mathbf{E}}_1 \cdot d\vec{\mathbf{S}} \right) - \frac{\varepsilon_o}{2} \oiint E_1^2 d\vec{\mathbf{S}} + \varepsilon_o \oiint \vec{\mathbf{E}}_2 \left(\vec{\mathbf{E}}_2 \cdot d\vec{\mathbf{S}} \right) - \frac{\varepsilon_o}{2} \oiint E_2^2 d\vec{\mathbf{S}} \\ & + \varepsilon_o \oiint \vec{\mathbf{E}}_1 \left(\vec{\mathbf{E}}_2 \cdot d\vec{\mathbf{S}} \right) + \varepsilon_o \oiint \vec{\mathbf{E}}_2 \left(\vec{\mathbf{E}}_1 \cdot d\vec{\mathbf{S}} \right) - \varepsilon_o \oiint \left(\vec{\mathbf{E}}_1 \cdot \vec{\mathbf{E}}_2 \right) d\vec{\mathbf{S}}. \end{aligned} \tag{6.3}$$

---

[4]The term Coulomb stress is assigned to the line stress (developed in Section 6.1 from the recast stress equation) that only exists at each point on the straight path between two separated, spherically symmetric charge distributions.

Section 6.1 steps through the details of recasting Maxwell's stress equation for two separated, spherically symmetric charge distributions. The end result is a Coulomb stress only existing on the straight line between the centers of the two charge distributions.

Section 6.2 expounds on the Coulomb stress identified in the recast stress equation. For two like-charge distributions, the Coulomb stress is modeled as photon exchanges continually occurring between the two charge distributions. The amount of trapped energy associated with this continual photon exchange is shown to be equivalent to the electrostatic potential energy of the separated two like-charge distributions.

Section 6.3 describes how two like-charge distributions and two opposite charge distributions may be modeled with energy carrier mediators associated with the Coulomb stress and the Poincaré stress.

6.1 Recasting of Maxwell's Stress Equation in Free Space for Two Separated, Spherically Symmetric Static Charge Distributions

Consider two spherically symmetric static charge distributions in free space, the first centered at the origin ($r = 0$) with total charge q_1 and the second centered a distance d away on the z axis ($z = d$) with total charge q_2. The electric field $\vec{\mathbf{E}}_1$ for the first charge distribution is [65]:

$$\vec{\mathbf{E}}_1 = \frac{q_1}{4\pi\varepsilon_o r^2}\hat{\mathbf{a}}_r, \tag{6.4}$$

where r is the distance from the origin. The electric field $\vec{\mathbf{E}}_2$ for the second charge distribution is:

$$\vec{\mathbf{E}}_2 = \frac{q_2}{4\pi\varepsilon_\mathrm{o} r_2^2}\hat{\mathbf{a}}_{r_2}, \tag{6.5}$$

where r_2 is the distance from the second charge distribution and $\hat{\mathbf{a}}_{r_2}$ is the directional unit vector away from the second charge distribution.

For any arbitrary surface (no charge contained on the surface), the first four terms of (6.3) are nulled by applying the variant of Stokes' Theorem per the method of Section 5.2 and choosing:

$$\vec{\mathbf{C}}_{1\&2} = -\frac{\varepsilon_\mathrm{o} r E_1^2}{4}\hat{\mathbf{a}}_r - \frac{\varepsilon_\mathrm{o} r_2 E_2^2}{4}\hat{\mathbf{a}}_{r_2}. \tag{6.6}$$

The Poincaré stress related to the electrostatic potential energy of each individual charge distribution is being ignored for the evaluation of this section. Therefore, the Maxwell's Stress Equation for electrostatics in free space for this two charge system reduces to:

$$\vec{\mathbf{F}} = \varepsilon_\mathrm{o} \oiint \vec{\mathbf{E}}_1 \left(\vec{\mathbf{E}}_2 \cdot d\vec{\mathbf{S}}\right) + \varepsilon_\mathrm{o} \oiint \vec{\mathbf{E}}_2 \left(\vec{\mathbf{E}}_1 \cdot d\vec{\mathbf{S}}\right) - \varepsilon_\mathrm{o} \oiint \left(\vec{\mathbf{E}}_1 \cdot \vec{\mathbf{E}}_2\right) d\vec{\mathbf{S}}. \tag{6.7}$$

If a spherical surface is chosen centered at the origin, beyond the charge distribution for q_1, with radius $r < d$ as shown in Figure 6.1, then Maxwell's stress equation for electrostatics in free space for this surface reduces to ($\vec{\mathbf{E}}_1$ and $d\vec{\mathbf{S}}$ are always in the same direction):

$$\vec{\mathbf{F}} = \varepsilon_\mathrm{o} \oiint E_1 \vec{\mathbf{E}}_2 dS. \tag{6.8}$$

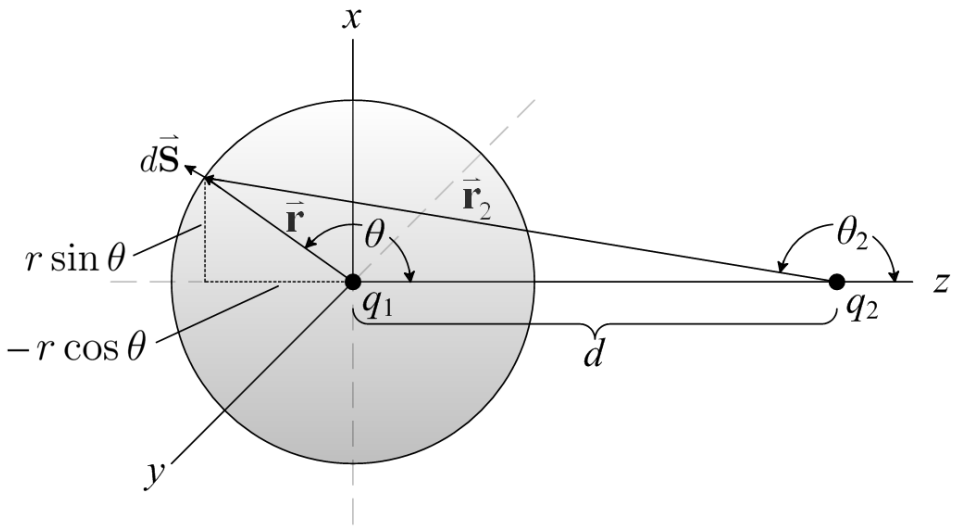

Figure 6.1: Spherical surface centered at the origin, beyond the charge distribution for q_1, with radius $r < d$.

Equation (6.8) is also valid for any radius $r \neq d$. Substituting (6.4) and (6.5) into (6.8) and expressing the result in cylindrical components ρ and z yields:

$$\begin{aligned}\vec{\mathbf{F}} &= \varepsilon_o \int_0^{\pi}\int_0^{2\pi} \left(\frac{q_1}{4\pi\varepsilon_o r^2}\right)\left(\frac{q_2}{4\pi\varepsilon_o r_2^2}\hat{\mathbf{a}}_{r_2}\right) r^2 \sin\theta \, d\phi \, d\theta \\ &= \frac{q_1 q_2}{16\pi^2\varepsilon_o}\int_0^{\pi}\int_0^{2\pi} \frac{\sin\theta_2 \hat{\mathbf{a}}_\rho + \cos\theta_2 \hat{\mathbf{a}}_z}{r_2^2} \sin\theta \, d\phi \, d\theta \\ &= \frac{q_1 q_2}{16\pi^2\varepsilon_o}\int_0^{\pi}\int_0^{2\pi} \frac{r\sin\theta \hat{\mathbf{a}}_\rho + (r\cos\theta - d)\,\hat{\mathbf{a}}_z}{(r^2+d^2-2rd\cos\theta)^{3/2}} \sin\theta d\phi d\theta,\end{aligned} \tag{6.9}$$

where: $\sin\theta_2 = (r\sin\theta)/r_2$, $\cos\theta_2 = (r\cos\theta - d)/r_2$, and $r_2 = \sqrt{r^2+d^2-2rd\cos\theta}$.

The net force from the ρ component is null because of cylindrical symmetry:

$$\vec{\mathbf{F}}_\rho = \frac{q_1 q_2}{16\pi^2\varepsilon_o}\int_0^{\pi}\int_0^{2\pi} \frac{r\sin^2\theta}{(r^2+d^2-2rd\cos\theta)^{3/2}} \hat{\mathbf{a}}_\rho \, d\phi \, d\theta = 0. \tag{6.10}$$

The force in the z direction is:

$$F_z = \frac{q_1 q_2}{16\pi^2\varepsilon_o}\int_0^{\pi}\int_0^{2\pi} \frac{\sin\theta\,(r\cos\theta - d)}{(r^2+d^2-2rd\cos\theta)^{3/2}} \, d\phi \, d\theta = -\frac{q_1 q_2\,[1-\mathrm{sgn}\,(r-d)]}{8\pi\varepsilon_o d^2}, \tag{6.11}$$

where sgn () is the sign (or signum) function [82]:

$$\text{sgn}\,(x) = \begin{cases} -1 & \text{for } x < 0 \\ 0 & \text{for } x = 0 \\ 1 & \text{for } x > 0 \end{cases}. \tag{6.12}$$

For $r < d$ (where the surface encloses all of q_1 and none of q_2), F_z is the Coulomb force [5]:

$$F_z = -\frac{q_1 q_2}{4\pi\varepsilon_o d^2}, \tag{6.13}$$

and for $r > d$ (where the surface encloses all of q_1 and q_2), $F_z = 0$.

The primary goal of this section is to determine if Maxwell's stress equation (6.9) for the spherical closed surface of Figure 6.1 can be recast using the variant of Stokes' Theorem (5.12) such that only a stress at a single point aligned between the two charge distributions remains.

The application of the variant of Stokes' Theorem requires a surface enclosed by a given contour. The contour of choice is the differential ring at a given angle θ as shown in Figure 6.2.

A brief overview of the utilization of differential rings is in order before proceeding. Maxwell's stress equation (6.9) can either be integrated in terms of differential surface elements dS:

$$\begin{aligned} \vec{\mathbf{F}} &= \frac{q_1 q_2}{16\pi^2\varepsilon_o r^2}\int_0^{\pi}\int_0^{2\pi} \frac{r\sin\theta\hat{\mathbf{a}}_\rho + (r\cos\theta - d)\hat{\mathbf{a}}_z}{(r^2 + d^2 - 2rd\cos\theta)^{3/2}} r^2\sin\theta d\phi d\theta \\ &= \int_0^{\pi}\int_0^{2\pi} \vec{\mathbf{F}}_S\, r^2\sin\theta d\phi d\theta = \oiint \vec{\mathbf{F}}_S\, dS, \end{aligned} \tag{6.14}$$

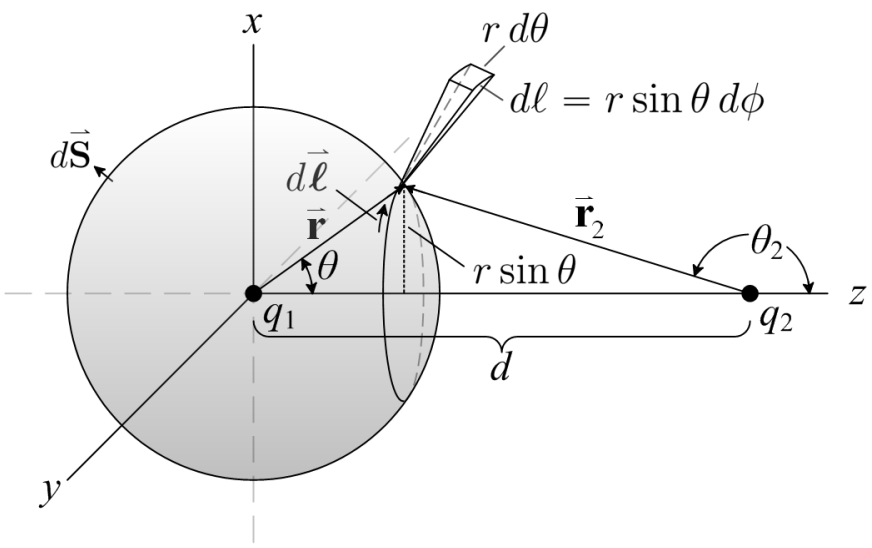

Figure 6.2: Spherical surface can be broken into differential rings.

or in terms of differential ring elements $d\ell$ with angular width $d\theta$:

$$\begin{aligned}\vec{\mathbf{F}} &= \frac{q_1 q_2}{16\pi^2 \varepsilon_o r}\int_0^{\pi}\int_0^{2\pi r\sin\theta} \frac{r\sin\theta\hat{\mathbf{a}}_\rho + (r\cos\theta - d)\,\hat{\mathbf{a}}_z}{\left(r^2+d^2-2rd\cos\theta\right)^{3/2}}\, d\ell d\theta \\ &= \int_0^{\pi}\int_0^{2\pi r\sin\theta} \vec{\mathbf{F}}_\ell \, d\ell d\theta = \oiint \vec{\mathbf{F}}_\ell \, d\ell d\theta.\end{aligned} \tag{6.15}$$

In general, the force for a given differential ring (at angle θ) can be converted to a force on the spherical surface portion bounded by the ring (according to the right hand rule) using the variant of Stokes' Theorem:

$$\begin{aligned}\oiint \delta(\theta'-\theta)\vec{\mathbf{F}}_\ell(\theta')d\ell d\theta' &= \oint \vec{\mathbf{F}}_\ell(\theta)\, d\ell = \oint \vec{\mathbf{C}} \times d\vec{\boldsymbol{\ell}} \\ &= \iint \left[\left(\nabla\cdot\vec{\mathbf{C}}\right)d\vec{\mathbf{S}} - \nabla_{\mathrm{C}}\left(\vec{\mathbf{C}}\cdot d\vec{\mathbf{S}}\right)\right] = \iint \vec{\mathbf{F}}_S\, dS,\end{aligned} \tag{6.16}$$

where $\delta()$ is the Dirac delta function [83]: $\delta(x) = 0$ for $x \neq 0$ and $\int_{-\infty}^{\infty}\delta(x) = 1$. $\vec{\mathbf{C}}$ is

chosen such that $\vec{\mathbf{C}} \times d\vec{\boldsymbol{\ell}} = \vec{\mathbf{F}}_\ell \, d\ell$:

$$\vec{\mathbf{C}} = \vec{\mathbf{F}}_\ell \times (-\hat{\mathbf{a}}_\phi) = -F_{\ell_z}\hat{\mathbf{a}}_\rho + F_{\ell_\rho}\hat{\mathbf{a}}_z = \begin{bmatrix} -F_{\ell_z}\cos\phi \\ -F_{\ell_z}\sin\phi \\ F_{\ell_\rho} \end{bmatrix}, \tag{6.17}$$

therefore: $\vec{\mathbf{C}} \times d\vec{\boldsymbol{\ell}} = \left(-F_{\ell_z}\hat{\mathbf{a}}_\rho + F_{\ell_\rho}\hat{\mathbf{a}}_z\right) \times (-\hat{\mathbf{a}}_\phi)\, d\ell = \vec{\mathbf{F}}_\ell \, d\ell$.

Applying the $\vec{\mathbf{C}}$ of (6.17) using the partial derivatives for $\vec{\mathbf{C}}$ in Table 6.1 to the integrand $\left(\nabla\cdot\vec{\mathbf{C}}\right)d\vec{\mathbf{S}} - \nabla_{\mathrm{C}}\left(\vec{\mathbf{C}}\cdot d\vec{\mathbf{S}}\right)$ of (6.16) yields:

$$\begin{aligned}
\left(\nabla\cdot\vec{\mathbf{C}}\right)d\vec{\mathbf{S}} - \nabla_{\mathrm{C}}\left(\vec{\mathbf{C}}\cdot d\vec{\mathbf{S}}\right) &= \left[\frac{\partial C_x}{\partial x} + \frac{\partial C_y}{\partial y} + \frac{\partial C_z}{\partial z}\right]d\vec{\mathbf{S}} - \begin{bmatrix} \frac{\partial C_x}{\partial x} & \frac{\partial C_y}{\partial x} & \frac{\partial C_z}{\partial x} \\ \frac{\partial C_x}{\partial y} & \frac{\partial C_y}{\partial y} & \frac{\partial C_z}{\partial y} \\ \frac{\partial C_x}{\partial z} & \frac{\partial C_y}{\partial z} & \frac{\partial C_z}{\partial z} \end{bmatrix}\cdot d\vec{\mathbf{S}} \\
&= \begin{bmatrix} \left(-\frac{F_{\ell_z}}{r} - \cos\theta\frac{\partial F_{\ell_\rho}}{\partial\rho} + \sin\theta\frac{\partial F_{\ell_\rho}}{\partial z}\right)\hat{\mathbf{a}}_\rho \\ +\left(-\frac{F_{\ell_z}\cot\theta}{r} - \cos\theta\frac{\partial F_{\ell_z}}{\partial\rho} + \sin\theta\frac{\partial F_{\ell_z}}{\partial z}\right)\hat{\mathbf{a}}_z \end{bmatrix} dS \\
&= -\frac{1}{r}\left[\left(F_{\ell_z} + \frac{\partial F_{\ell_\rho}}{\partial\theta}\right)\hat{\mathbf{a}}_\rho + \left(F_{\ell_z}\cot\theta + \frac{\partial F_{\ell_z}}{\partial\theta}\right)\hat{\mathbf{a}}_z\right] dS \\
&= -\frac{1}{r}\left[\left(F_{\ell_z} + \frac{\partial F_{\ell_\rho}}{\partial\theta}\right)\hat{\mathbf{a}}_\rho + \frac{1}{\sin\theta}\frac{\partial}{\partial\theta}\left(\sin\theta F_{\ell_z}\right)\hat{\mathbf{a}}_z\right] dS,
\end{aligned} \tag{6.18}$$

where: $\frac{\partial f}{\partial\rho} = \frac{\partial f}{\partial\theta}\frac{\partial\theta}{\partial\rho} = \frac{\cos\theta}{r}\frac{\partial f}{\partial\theta}$, $\frac{\partial f}{\partial z} = \frac{\partial f}{\partial\theta}\frac{\partial\theta}{\partial z} = -\frac{\sin\theta}{r}\frac{\partial f}{\partial\theta}$, and $d\vec{\mathbf{S}} = dS\,\hat{\mathbf{a}}_r = dS\begin{bmatrix}\sin\theta\cos\phi \\ \sin\theta\sin\phi \\ \cos\theta\end{bmatrix}$.

It is interesting to note that the z component of the resulting surface force density is only a function of the z component of the original ring force density. The outcome of (6.18) is the conversion of a ring force density $\vec{\mathbf{F}}_\ell$ using the variant of Stoke's Theorem to a surface force density $\vec{\mathbf{F}}_S$ as follows:

$$F_{S_z} = -\frac{1}{r\sin\theta}\frac{\partial}{\partial\theta}\left(\sin\theta F_{\ell_z}\right), \tag{6.19}$$

and

$$F_{S_\rho} = -\frac{1}{r}\left(F_{\ell_z} + \frac{\partial F_{\ell_\rho}}{\partial \theta}\right). \tag{6.20}$$

f	$\frac{\partial f}{\partial x}$	$\frac{\partial f}{\partial y}$	$\frac{\partial f}{\partial z}$
$\sin\phi$	$-\frac{\sin\phi\cos\phi}{r\sin\theta}$	$\frac{\cos^2\phi}{r\sin\theta}$	0
$\cos\phi$	$\frac{\sin^2\phi}{r\sin\theta}$	$-\frac{\sin\phi\cos\phi}{r\sin\theta}$	0
f	$\cos\phi\frac{\partial f}{\partial \rho}$	$\sin\phi\frac{\partial f}{\partial \rho}$	$\frac{\partial f}{\partial z}$
C_x	$-\cos^2\phi\frac{\partial F_{\ell_z}}{\partial \rho} - F_{\ell_z}\frac{\sin^2\phi}{r\sin\theta}$	$-\sin\phi\cos\phi\frac{\partial F_{\ell_z}}{\partial \rho} + F_{\ell_z}\frac{\sin\phi\cos\phi}{r\sin\theta}$	$-\cos\phi\frac{\partial F_{\ell_z}}{\partial z}$
C_y	$-\sin\phi\cos\phi\frac{\partial F_{\ell_z}}{\partial \rho} + F_{\ell_z}\frac{\sin\phi\cos\phi}{r\sin\theta}$	$-\sin^2\phi\frac{\partial F_{\ell_z}}{\partial \rho} - F_{\ell_z}\frac{\cos^2\phi}{r\sin\theta}$	$-\sin\phi\frac{\partial F_{\ell_z}}{\partial z}$
C_z	$\cos\phi\frac{\partial F_{\ell_\rho}}{\partial \rho}$	$\sin\phi\frac{\partial F_{\ell_\rho}}{\partial \rho}$	$\frac{\partial F_{\ell_\rho}}{\partial z}$

Table 6.1: Useful partial derivatives for $\vec{\mathbf{C}} = \begin{bmatrix} -F_{\ell_z}\cos\phi \\ -F_{\ell_z}\sin\phi \\ F_{\ell_\rho} \end{bmatrix}$.

And finally, a ring force density $\vec{\mathbf{F}}_\ell$ is derived such that when $\vec{\mathbf{C}} = \vec{\mathbf{F}}_\ell \times (-\hat{\mathbf{a}}_\phi)$ is applied using the variant of Stokes' Theorem, the resulting surface force density $\vec{\mathbf{F}}_S$ is equivalent to the reduced Maxwell's stress equation surface force of (6.14). By definition of $d\vec{\boldsymbol{\ell}}$ and $d\vec{\mathbf{S}}$ in Figure 6.2, the ring force density is on a differential ring at the azimuthal angle θ and the corresponding surface force density is in the direction with greater azimuthal angle than the ring's angle θ.

Solving (6.19) for F_{ℓ_z} and substituting F_{S_z} from (6.14) yields:

$$\begin{aligned} F_{\ell_z} &= -\frac{1}{\sin\theta}\left(\int r\sin\theta F_{S_z}\,d\theta + K_z\right) \\ &= -\frac{1}{\sin\theta}\int\frac{q_1q_2\sin\theta\,(r\cos\theta - d)}{16\pi^2\varepsilon_{\mathrm{o}}r(r^2+d^2-2rd\cos\theta)^{3/2}}\,d\theta - \frac{K_z}{\sin\theta} \\ &= \frac{q_1q_2\,(r-d\cos\theta)}{16\pi^2\varepsilon_{\mathrm{o}}rd^2\sin\theta(r^2+d^2-2rd\cos\theta)^{1/2}} - \frac{K_z}{\sin\theta}. \end{aligned} \tag{6.21}$$

The integration constant K_z is obtained by setting the net force in the z direction on the differential ring equal to the net force on the surface bounded by the ring. The net force in the z direction on the differential ring is:

$$F_z = \int_0^{2\pi} F_{\ell_z} r\sin\theta\,d\phi = \frac{q_1q_2\,(r-d\cos\theta)}{8\pi\varepsilon_{\mathrm{o}}d^2(r^2+d^2-2rd\cos\theta)^{1/2}} - 2\pi rK_z, \tag{6.22}$$

and the net force in the z direction on the surface bounded by the ring is:

$$\begin{aligned} F_z &= \int_\theta^\pi\int_0^{2\pi} F_{S_z} r^2\sin\theta'\,d\phi\,d\theta' = \frac{q_1q_2}{8\pi\varepsilon_{\mathrm{o}}}\int_\theta^\pi\frac{\sin\theta'\,(r\cos\theta'-d)}{(r^2+d^2-2rd\cos\theta')^{3/2}}\,d\theta' \\ &= \frac{q_1q_2\,(r-d\cos\theta)}{8\pi\varepsilon_{\mathrm{o}}d^2(r^2+d^2-2rd\cos\theta)^{1/2}} - \frac{q_1q_2}{8\pi\varepsilon_{\mathrm{o}}d^2}. \end{aligned} \tag{6.23}$$

Combining (6.22) and (6.23) and solving for K_z yields:

$$K_z = \frac{q_1q_2}{16\pi^2\varepsilon_{\mathrm{o}}rd^2}, \tag{6.24}$$

and therefore:

$$F_{\ell_z} = \frac{q_1q_2\,(r-d\cos\theta)}{16\pi^2\varepsilon_{\mathrm{o}}rd^2\sin\theta(r^2+d^2-2rd\cos\theta)^{1/2}} - \frac{q_1q_2}{16\pi^2\varepsilon_{\mathrm{o}}rd^2\sin\theta}. \tag{6.25}$$

The significance of (6.25) is that it identifies the z component of a differential ring force at any angle θ that is equivalent to the z component of the Maxwell's stress equation force on the surface bounded by the ring. In other words, the result is the conversion of the z component of the Maxwell's stress equation surface force to a ring force enclosing the

surface. The remaining step is to solve for the ρ component. Solving (6.20) for F_{ℓ_ρ} and substituting F_{S_ρ} from (6.14) and F_{ℓ_z} from (6.25) yields:

$$\begin{aligned}
F_{\ell_\rho} =& -\int \left(rF_{S_\rho} + F_{\ell_z}\right) d\theta + K_\rho \\
=& -\int \frac{q_1 q_2 \sin\theta}{16\pi^2\varepsilon_o (r^2+d^2-2rd\cos\theta)^{3/2}} d\theta \\
& -\int \frac{q_1 q_2 \left(r-d\cos\theta\right)}{16\pi^2\varepsilon_o rd^2 \sin\theta (r^2+d^2-2rd\cos\theta)^{1/2}} d\theta \\
& +\int \frac{q_1 q_2}{16\pi^2\varepsilon_o rd^2\sin\theta} d\theta + K_\rho \\
=& \frac{q_1 q_2}{16\pi^2\varepsilon_o rd(r^2+d^2-2rd\cos\theta)^{1/2}} \\
& -\frac{q_1 q_2}{16\pi^2\varepsilon_o rd}\left[\begin{array}{l} \tanh^{-1}\left[\dfrac{\left(r^2+d^2-2rd\cos\theta\right)^{1/2}}{d-r}\right] \\ +\tanh^{-1}\left[\dfrac{\left(r^2+d^2-2rd\cos\theta\right)^{1/2}}{d+r}\right] \end{array}\right] \\
& +\frac{q_1 q_2}{16\pi^2\varepsilon_o rd^2} \ln\left[\frac{\sin\theta}{\cos\theta+1}\right] + K_\rho.
\end{aligned} \tag{6.26}$$

The constant of integration K_ρ is shown later to be inconsequential. Equations (6.25) and (6.26) are now used to recast Maxwell's stress equation by selecting the differential ring location $\theta = 0$. This angle selection allows the force on the entire spherical surface to be converted to a force on a single differential ring at $\theta = 0$. For a spherical surface with $r < d$, the force in the z direction on this differential ring is found by integration of (6.25) around the ring. The force on this differential ring is equal to the Coulomb force:

$$\begin{aligned}
F_z =& \int_0^{2\pi} F_{\ell_z} r\sin\theta\, d\phi \Big|_{\theta=0} = 2\pi r\sin\theta F_{\ell_z}\Big|_{\theta=0} \\
=& \frac{q_1 q_2 \left(r-d\cos\theta\right)}{8\pi\varepsilon_o d^2 (r^2+d^2-2rd\cos\theta)^{1/2}}\Bigg|_{\theta=0} - \frac{q_1 q_2}{8\pi\varepsilon_o d^2} = -\frac{q_1 q_2}{4\pi\varepsilon_o d^2}.
\end{aligned} \tag{6.27}$$

The force in the ρ direction for any angle ϕ is found by evaluating $F_{\ell_\rho} r\sin\theta$ at $\theta = 0$. The constant of integration K_ρ of (6.26) multiplied by $r\sin\theta$ and evaluated at $\theta = 0$ is null.

Applying l'Hospital's rule [84], the force in the ρ direction for any angle ϕ is null (i.e., there is no hoop stress [85]):

$$F_\rho(\phi) = F_{\ell_\rho} r \sin\theta \Big|_{\theta=0} = \lim_{\theta\to 0} \frac{rF_{\ell_\rho}}{\dfrac{1}{\sin\theta}} = \lim_{\theta\to 0} \frac{r\dfrac{\partial F_{\ell_\rho}}{\partial\theta}}{\dfrac{\partial}{\partial\theta}\dfrac{1}{\sin\theta}} = \lim_{\theta\to 0} \frac{-r\left(rF_{S_\rho} + F_{\ell_z}\right)}{-\dfrac{\cos\theta}{\sin^2\theta}} = 0. \tag{6.28}$$

The ramification of recasting Maxwell's stress equation for the spherical surface to a stress at a single point (i.e., differential ring at $\theta = 0$) is significant. The recasting may be done for all spherical surfaces with radii ranging from just outside the charge distribution centered at the origin up to the charge distribution centered at $z = d$. The outcome is a constant line stress directionally aligned between the two charge distributions. The magnitude of the line stress is equivalent to the two charge distribution Coulomb force.

6.2 Coulomb Stress and QET

The term Coulomb stress is assigned to the line stress developed in the previous section from the recast stress equation. The Coulomb stress only exists at each point on the line between the two separated, spherically symmetric charge distributions. In general, a Coulomb stress equation may be defined for an arbitrary surface and arbitrary locations for two separated, spherically symmetric charge distributions:

$$\vec{\mathbf{F}}_{Coulomb} = \frac{q_1 q_2}{4\pi\varepsilon_o d^2} \oiint \delta^2(1+\hat{\mathbf{a}}_{r_1}\cdot\hat{\mathbf{a}}_{r_2})\,\mathrm{sgn}\,(\hat{\mathbf{a}}_{r_2}\cdot\hat{\mathbf{a}}_n)\hat{\mathbf{a}}_{r_1} dS, \tag{6.29}$$

where q_1 and q_2 are the total charges of the two charge distributions, d is the distance between the centers of the two charge distributions, $\delta^2()$ is the two dimensional or surface Dirac delta function [86], $\hat{\mathbf{a}}_{r_1}$ and $\hat{\mathbf{a}}_{r_2}$ are the directional unit vectors away from the first

and second charge distributions respectively, sgn () is the function defined in (6.12), and $\hat{\mathbf{a}}_n$ is the directional unit vector outward normal from the surface S.

The essence of (6.29) is a differential surface force element (equivalent to the Coulomb force) for every non-tangential intersection of the arbitrary surface S with the straight line between the two charge distributions. Equation (6.29) may have the appearance of merely stating the point to point, action-at-a-distance [87, 88] property of Coulomb's Law [89, 90]. However, the recasting process of the previous section shows that the Coulomb stress equation is mathematically compatible with Maxwell's stress equation.

For a two charge system (each charge spherically symmetric), Maxwell's stress equation (6.3) and the Coulomb stress equation (6.29) give the same result. If the arbitrary surface encloses only one of the charge distributions, then the result is the Coulomb force acting on the enclosed charge distribution. If the arbitrary surface encloses either none or both charge distributions, then the result is null.

If both charge distributions are of like charges, then the Coulomb stress may be modeled as an average rate of QETs (i.e., photons) exchanging back and forth between the two charge distributions. The line stress is modeled as the straight path of the photons. The impact force (of photons absorbed by the charge distribution) and recoil force (of photons emitted from the charge distribution) constitute the Coulomb force on the charge distributions.

The energy of a photon $U_{photon} = h\nu$ is quantized, where h is Planck's constant and ν is the photon frequency [71, 58]. Assume the photons exchanging back and forth between the two charge distributions have a mean [91, 92] energy $\bar{U}_{photon}$ (J) and a mean time rep-

etition of photon exchanges $\bar{t}_{rep}$ (s). Therefore, the mean rate of energy absorbed $\bar{P}_a$ (W) and emitted $\bar{P}_e$ (W) to and from each charge distribution is:

$$\bar{P}_a = \bar{P}_e = \frac{\bar{U}_{photon}}{\bar{t}_{rep}}. \tag{6.30}$$

The repulsive Coulomb force on each charge distribution is inferred to be the sum of the impact force from the mean energy absorbed and the recoil force from the mean energy emitted [72, 93]:

$$F = \frac{q_1 q_2}{4\pi\varepsilon_o d^2} = \frac{\bar{P}_a + \bar{P}_e}{c}, \tag{6.31}$$

where c is the speed of light in free space [94, 95].

The photon exchanges back and forth between the two charge distributions may be regarded as trapped energy along the path between them (i.e., the Coulomb stress). The amount of time between photon emission from one of the charge distributions and absorption to the other is $t_{12} = d/c$. Therefore, the amount of trapped energy is:

$$U_{trapped} = \left(\bar{P}_a + \bar{P}_e\right) t_{12} = \left(\bar{P}_a + \bar{P}_e\right) \frac{d}{c} = \frac{q_1 q_2}{4\pi\varepsilon_o d}. \tag{6.32}$$

It is interesting to note that the trapped energy of (6.32) is equivalent to the electrostatic potential energy for a two liked-charge system [96, 97] (q_1 and q_2) separated by a distance d.

6.3 Poincaré Stress, Coulomb Stress and QET

The Poincaré stress related to the electrostatic potential energy of each individual charge distribution was ignored for the evaluation of Section 6.1. For an isolated, spheri-

cally symmetric charge distribution, the Poincaré stress is aligned with the electric field, is omnidirectional, and is directed inward toward the charge distribution.

The inward pressure arises from the impact force of QET influx and the recoil force of QET out-flux. The QET influx and out-flux has been modeled as energy carrier mediators (bosons) interacting between the charge distribution and the distant matter of the universe. The Poincaré stress is proportional to the equivalent mass of the electrostatic potential energy of the individual charge distribution.

For two like-charge distributions (i.e., both positive or both negative) there is a Poincaré stress associated with each individual charge distribution. In addition, there is a Coulomb stress from QETs (i.e., photon exchanges) back and forth between the two charge distributions causing the charge distributions to be pushed apart. The mean QET flux density corresponding to the Coulomb stress between the two charge distributions may be determined by using superposition and (6.29). Each differential element of charge from the first charge distribution has photon exchanges back and forth with each differential element of charge from the second.

The concentration of mean QET flux density (i.e., energy flux density magnitude) is modeled/depicted in Figure 6.3(a). The darker gray regions represent a higher concentration of QETs, while the lighter gray regions denote a lower concentration. The mean QET flux density associated with the Poincaré stress for each individual charge density falls off as the inverse square of the distance from the charge distribution. The mean QET flux density associated with the Coulomb stress depicts the trapped energy from the photon exchanges back and forth between the two charge distributions.

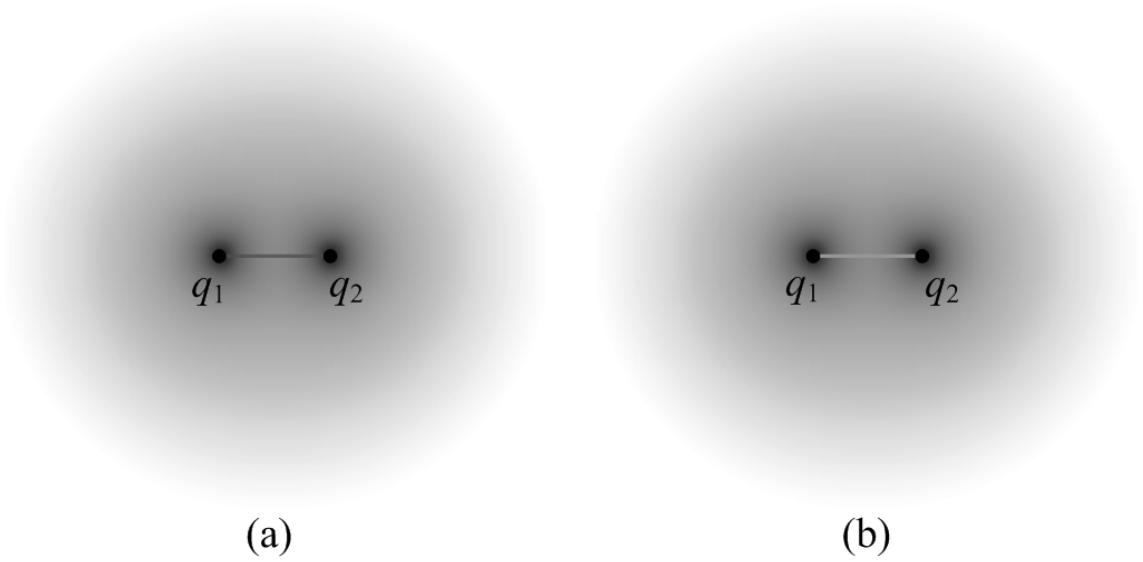

Figure 6.3: Illustration of Poincaré and Coulomb stress for two charge distributions: (a) like charges, (b) opposite charges.

In addition to the Poincaré stress associated with the two individual charge distributions, for a static condition there is an additional Poincaré stress maintaining the two charge distributions at equilibrium. The net effect of this additional Poincaré stress is a force that counteracts the Coulomb force associated with the photon exchange back and forth between the two charge distributions.

This additional Poincaré stress (proportional to the electrostatic potential energy of the two separated charge distributions) may be from QETs interacting with the charges in the distributions (i.e., photons) or from QETs interacting with the solid/rigid structure separating the two charge distributions (i.e., bosons). The specifics of which are involved are not needed for the electrostatic model. If the solid structure were not there, then the associated Poincaré stress (from QETs interacting with the solid structure) would also not

be there and the two charge distributions would start to accelerate away from each other.

At a large distance away from the charge distributions (compared to the distance between the two charge distributions), this additional Poincaré stress is assumed to be omnidirectional inward proportional to the electrostatic potential energy of the two charge distributions: $q_1 q_2/(4\pi\varepsilon_o d)$.

Two opposite charge distributions may be modeled in a similar, but slightly different manner. The two individual charge distributions have a Poincaré stress associated with them, omnidirectionally inward, proportional to the electrostatic mass of each charge distribution.

However, there is a missing amount of QETs back and forth between the two charge distributions associated with the Coulomb stress, causing the charge distributions to be pushed together. The concentration of mean QET flux density (i.e., energy flux density magnitude) is depicted in Figure 6.3(b).

The electrostatic model of this dissertation identifies a missing amount of QETs between the two opposite charged distributions. This missing amount of QETs is analogous to the screening of two local masses from QET interactions with the distant matter of the universe (identified in Chapter 4), causing two local masses to be pushed together.

The "screening" between two opposite charged distributions results in a lack of QET interactions between them. The Poincaré stress associated with each of the two charge distribution consists of QET interactions with the distant matter of the universe. Specifically of importance here is the QET portion of the Poincaré stress interacting with the charges in the distributions (i.e., the photons, but not the bosons interacting with the solid structure).

A logical conclusion is there are two "types" of photons for the QETs interacting with the positive and negative charge components of each distribution and the distant matter. The photons associated with the Poincaré stress for a positive charge distribution don't interact with a negative charge distribution (and vice versa). However, the details of the "types" of photons and breakdown of photons and bosons involved in the Poincaré stress are not necessary for the electrostatic model of this dissertation. The important aspect for the opposite charged distributions is that the net Poincaré stress develops a "screening" or missing amount of QETs transferring back and forth between the two charge distributions corresponding to the Coulomb stress.

The missing energy between the charge distributions is equivalent to the negative valued electrostatic potential energy $U_{missing} = q_1 q_2/(4\pi\varepsilon_o d)$ of the two opposite charge distributions. As a result of a decrease in the electrostatic mass for the opposite charge distributions, there is a reduction in the overall Poincaré stress thus maintaining the two charge distributions in equilibrium (i.e., a net force equal and opposite to the Coulomb force).

At a large distance away from the charge distributions (compared to the distance between the two charge distributions), the reduction in the Poincaré stress is assumed to be omnidirectional inward proportional to the electrostatic potential energy (negative) of the two opposite charge distributions.

6.4 Summary

Using a variant of Stokes' Theorem, Maxwell's stress equation for two separated, spherically symmetric static charge distributions has been successfully recast. The recast stress equation identifies a Coulomb stress that only exists at each point on the line between the two charge distributions. The resulting Coulomb stress equation is mathematically consistent with Maxwell's stress equation.

For two like-charge distributions, the Coulomb stress has been modeled as a mean rate of QETs absorbed and emitted by each charge distribution consisting of a continual exchange of photons back and forth between the charge distributions.

The impact force from the absorbed QETs and the recoil force from the emitted QETs constitute the Coulomb force pushing the charge distributions apart from each other. The amount of trapped energy in the exchange of photons between the two charge distributions has been shown to be the electrostatic potential energy of the two charge distribution system.

A model of the QETs associated with the Poincaré stress and Coulomb stress has been illustrated for the two charge system. For each individual charge distribution, there is a Poincaré stress, omnidirectionally inward and proportional to the electrostatic potential energy of the corresponding charge distribution.

If the two charges are like charged, then there is an additional Coulomb stress between the two charges and an additional Poincaré stress equalizing the Coulomb stress. If the two charges have opposite charges, then the Coulomb stress is a reduction in QETs be-

tween the two charges along with a reduced Poincaré stress equalizing the Coulomb stress.

The Coulomb stress accounts for the electrostatic potential energy of the two charge system (not including the individual charge distributions themselves) and is equivalent to the trapped energy (for like-charge distributions) or the missing energy (for opposite charge distributions) between the two charge distributions.

The two separated charge distribution dumbbell model of this chapter may be used to construct a hollow shell having a uniform surface charge distribution. For the hollow shell, the QET model depicts the Poincaré stress as an inwardly directed, omnidirectional pressure. The pressure is a result of a mean valued, continual exchange of bosons (i.e., QETs) between the charge distribution and the distant matter of the universe proportional to the electrostatic potential energy (or equivalent electrostatic mass) of the charge distribution. The electrostatic potential energy of the hollow shell with uniform surface charge distribution is modeled as trapped energy inside the hollow shell. The trapped energy is a result of a mean valued, continual exchange of photons (i.e., QETs) between all shell charge distribution elements.

The spherical shell charge distribution example highlights the primary differences between the traditional approach and the QET model of this dissertation. The traditional approach defines the Poincaré stress as internal to the structure and establishes that the electrostatic potential energy is stored in the electric field external to the shell (or alternately in the charge distribution itself). In contrast, the QET model defines the Poincaré stress as an external stress and establishes the electrostatic potential energy as trapped energy (i.e., QETs) inside the hollow shell.

CHAPTER 7. A QET MODEL FOR THE PINCH STRESS OF A DIFFERENTIAL CURRENT ELEMENT AT THE ORIGIN

The goal of this and the subsequent chapter is to establish a QET (boson interaction) model that provides a visualization of the stresses internal and external to constant current carrying solids [98, 99]. The internal and external magnetostatic stresses are derived from Maxwell's stress equation and historical current force formulas known to be compatible with Maxwell's equations for closed circuits. Therefore, the magnetostatic QET model of this dissertation is mathematically consistent with Maxwell's equations.

Maxwell's stress equation for magnetostatics identifies a tensile stress in the direction of the magnetic field and a pressure normal to this direction. The principle aim of this chapter is to determine how Maxwell's stress equation (applied to an external closed surface from a static current distribution) can be recast to eliminate the stress aligned with the magnetic field. In addition, the recast stress equation eliminates most of the stress normal to the magnetic field, leaving only an inward surface stress in the radial direction referenced to the location of the current distribution elements. This pressure, inwardly directed may be attributed to the pinch stress [100] associated with a static current distribution.

For magnetostatics, the electromagnetic momentum density [58] is null. Therefore, from the conservation of momentum, the magnetostatic force $\vec{\mathbf{f}}$ per unit volume at any given location is:

$$\vec{\mathbf{f}} = \nabla \cdot \overleftrightarrow{\mathbf{T}}, \tag{7.1}$$

where $\overleftrightarrow{\mathbf{T}}$ is the Maxwell stress tensor [59]. For magnetostatic in free space, terms of the Maxwell stress tensor are:

$$T_{ij} = \frac{1}{\mu_{\mathrm{o}}} B_i B_j - \frac{1}{2\mu_{\mathrm{o}}} \delta_{ij} B^2, \tag{7.2}$$

where μ_{o} is the permeability of free space . Maxwell's stress equation for magnetostatics in free space can be obtained by applying the divergence theorem to the total force for a given volume using (7.1) (see Appendix E for an alternate derivation):

$$\begin{aligned} \vec{\mathbf{F}} &= \iiint \vec{\mathbf{f}}\, dV = \iiint \left(\nabla \cdot \overleftrightarrow{\mathbf{T}} \right) dV = \oiint \overleftrightarrow{\mathbf{T}} \cdot d\vec{\mathbf{S}} \\ &= \mu_{\mathrm{o}} \oiint \vec{\mathbf{H}} \left(\vec{\mathbf{H}} \cdot d\vec{\mathbf{S}} \right) - \frac{\mu_{\mathrm{o}}}{2} \oiint H^2 d\vec{\mathbf{S}}. \end{aligned} \tag{7.3}$$

Section 7.1 evaluates Maxwell's stress equation in free space, away from a differential current element at the origin. For a conic enclosed surface, the total force from Maxwell's stress equation is not null. This nonzero result supports the reality that Maxwell's stress equation for magnetostatics based on the Biot-Savart Law and Lorentz's force equation is only applicable when at least one of the current carrying circuits is closed.

Section 7.2 steps through the details of recasting Maxwell's stress equation for a cylindrical wedge-shape closed surface away from an infinite line current. The end result is a recast stress equation for a closed surface that depicts an inward surface tension only in the polar direction towards the line current.

Section 7.3 recasts Maxwell's stress equation for a spherical closed surface away from a differential current element at the origin. The end result is a recast stress equation for a spherical surface that depicts an inward surface tension only in the radial direction towards the differential current element.

Section 7.4 expounds on the pinch stress identified in the recast stress equations. Modeled as energy carrier mediator interactions with the distant matter of the universe, this stress is shown to conform with Mach's principle.

7.1 Evaluating Maxwell's Stress Equation in Free Space, Away from a Differential Current Element at the Origin ($r = 0$) with Total Current, JdV, in the Positive z Direction

In classical magnetostatics, the magnetic field external to a differential current element at the origin $(r = 0)$ with total current JdV in the positive z direction is (based on the Biot-Savart Law [22]):

$$\vec{\mathbf{H}} = \frac{JdV}{4\pi r^3}\hat{\mathbf{a}}_z \times \vec{\mathbf{r}} = \frac{JdV\sin\theta}{4\pi r^2}\hat{\mathbf{a}}_\phi, \tag{7.4}$$

where r is the distance from the origin.

Maxwell's stress equation (7.3) may be used to determine the force on each surface of the conic closed surface shown in Figure 7.1. The surfaces at $r = a$ and $r = b$ are spherical surfaces (i.e., only a radial component normal to the surface) and the side surface only has an azimuthal component normal to the surface. The angle α specifies the tilt of the side surface S_{side} with respect to the z axis.

The force from Maxwell's stress equation for surface S_a is:

$$\vec{\mathbf{F}}_a = \mu_o \iint_{S_a} \vec{\mathbf{H}}\left(\vec{\mathbf{H}}\cdot d\vec{\mathbf{S}}\right) - \frac{\mu_o}{2}\iint_{S_a} H^2 d\vec{\mathbf{S}} = 0 - \frac{\mu_o}{2}\iint_{S_a} H^2 d\vec{\mathbf{S}} = -\frac{\mu_o}{2}\iint_{S_a} H^2 d\vec{\mathbf{S}}, \tag{7.5}$$

and the force in the z direction for surface S_a is:

$$F_{a_z} = \frac{\mu_o}{2}\int_0^{2\pi}\int_0^{\alpha}\left(\frac{JdV\sin\theta}{4\pi a^2}\right)^2 a^2\sin\theta\cos\theta d\theta d\phi = \frac{\mu_o\left(JdV\right)^2\sin^4\alpha}{64\pi a^2}. \tag{7.6}$$

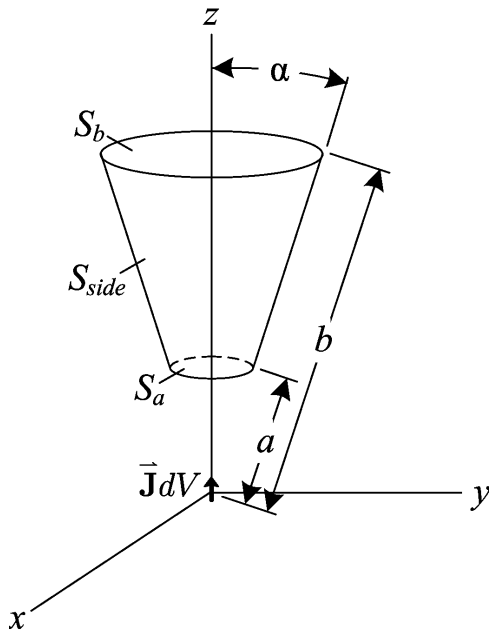

Figure 7.1: Conic closed surface symmetric about the z axis with spherical surfaces at $r = a$ and $r = b$.

The force from Maxwell's stress equation for surface S_b is:

$$\vec{\mathbf{F}}_b = -\frac{\mu_o}{2}\iint_{S_a} H^2 d\vec{\mathbf{S}}, \tag{7.7}$$

and the force in the z direction for surface S_b is:

$$F_{b_z} = -\frac{\mu_o}{2}\int_0^{2\pi}\int_0^{\alpha}\left(\frac{JdV\sin\theta}{4\pi b^2}\right)^2 b^2\sin\theta\cos\theta d\theta d\phi = -\frac{\mu_o\left(JdV\right)^2\sin^4\alpha}{64\pi b^2}. \tag{7.8}$$

The force from Maxwell's stress equation for surface S_{side} is:

$$\vec{\mathbf{F}}_{side} = \mu_o\iint_{S_{side}}\vec{\mathbf{H}}\left(\vec{\mathbf{H}}\cdot d\vec{\mathbf{S}}\right) - \frac{\mu_o}{2}\iint_{S_{side}} H^2 d\vec{\mathbf{S}} = 0 - \frac{\mu_o}{2}\iint_{S_{side}} H^2 d\vec{\mathbf{S}} = -\frac{\mu_o}{2}\iint_{S_{side}} H^2 d\vec{\mathbf{S}}, \tag{7.9}$$

and the force in the z direction for surface S_{side} is:

$$\begin{aligned} F_{side_z} =& \frac{\mu_o}{2} \int_0^{2\pi} \int_a^b \left(\frac{JdV \sin\alpha}{4\pi r^2} \right)^2 r \sin\alpha \sin\alpha \, dr \, d\phi \\ =& \frac{\mu_o \left(JdV\right)^2 \sin^4\alpha}{32\pi} \left(\frac{1}{a^2} - \frac{1}{b^2} \right). \end{aligned} \tag{7.10}$$

As shown in Section 5.1, for classical electrostatics the total force from Maxwell's stress equation on a conic surface outside a differential charge element at the origin is null. However, this is not true for the differential current element. The sum of the three surface forces of equations (7.6), (7.8), and (7.10) is not null. This nonzero result supports the reality that Maxwell's stress equation for magnetostatics based on the Biot-Savart Law and Lorentz's force equation "has meaning only as one element of a sum over a continuous set ... of a current loop or circuit" [101].

A variation of Maxwell's stress equation for magnetostatics based on one of the possible differential force elements of (3.7) is the most likely candidate for a meaningful stress equation involving a single differential current element. If such a variation of Maxwell's stress equation exists, it is presumed to yield a null force for any arbitrary enclosed surface where the single differential current element is not on the surface.

7.2 Recasting of Maxwell's Stress Equation in Free Space, Away from a Cylindrically Symmetric Infinite Line Current on the z Axis ($\rho = 0$) with Current, I, in the Positive z Direction

Maxwell's stress equation for magnetostatics is only applicable for closed circuits. The simplest 'closed circuit' to evaluate is the infinite line current. For an infinite cylindrically symmetric line current on the z axis with total current I in the positive z direction,

the magnetic field external to the line current is:

$$\vec{\mathbf{H}} = \frac{I}{2\pi\rho}\hat{\mathbf{a}}_\phi, \tag{7.11}$$

where ρ is the distance from the z axis.

Maxwell's stress equation (7.3) may be used to determine the force on each surface of the wedge closed surface shown in Figure 7.2. The surfaces at $\rho = a$ and $\rho = b$ are cylindrical surfaces (i.e., only a radial component normal to the surface), the side surfaces only have a polar component normal to the surface, and the top/bottom surfaces only have a z component normal to the surface. The angle α specifies the angle of the side surfaces S_{side} with respect to the y axis and w is the height of the wedge.

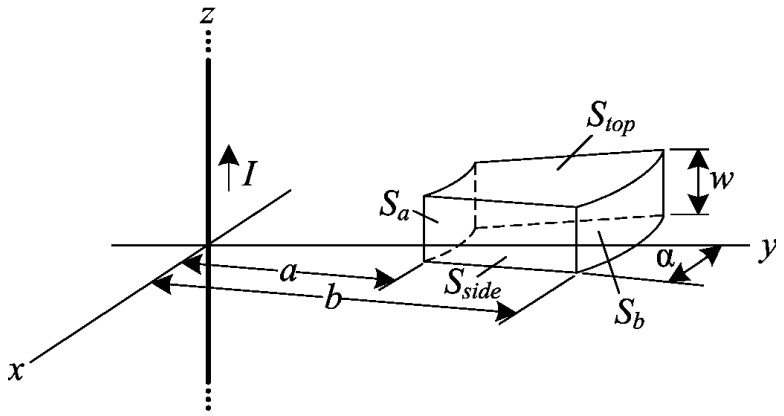

Figure 7.2: Wedge closed surface symmetric about the *y* axis with cylindrical surfaces at $\rho = a$ and $\rho = b$.

The force from Maxwell's stress equation for surface S_a is:

$$\vec{\mathbf{F}}_a = \mu_o \iint_{S_a} \vec{\mathbf{H}}\left(\vec{\mathbf{H}} \cdot d\vec{\mathbf{S}}\right) - \frac{\mu_o}{2}\iint_{S_a} H^2 d\vec{\mathbf{S}} = 0 - \frac{\mu_o}{2}\iint_{S_a} H^2 d\vec{\mathbf{S}} = -\frac{\mu_o}{2}\iint_{S_a} H^2 d\vec{\mathbf{S}}, \tag{7.12}$$

and the force in the y direction for surface S_a is:

$$F_{a_y} = \frac{\mu_o}{2} \int_0^w \int_{-\alpha}^{\alpha} \left(\frac{I}{2\pi a} \right)^2 a \cos\phi d\phi dz = \frac{\mu_o I^2 w \sin\alpha}{4\pi^2 a}. \tag{7.13}$$

The force from Maxwell's stress equation for surface S_b is:

$$\vec{\mathbf{F}}_b = -\frac{\mu_o}{2} \iint_{S_b} H^2 d\vec{\mathbf{S}}, \tag{7.14}$$

and the force in the y direction for surface S_b is:

$$F_{b_y} = -\frac{\mu_o}{2} \int_0^w \int_{-\alpha}^{\alpha} \left(\frac{I}{2\pi b} \right)^2 b \cos\phi d\phi dz = -\frac{\mu_o I^2 w \sin\alpha}{4\pi^2 b}. \tag{7.15}$$

The force from Maxwell's stress equation for the top S_{top} and bottom S_{bottom} surfaces are:

$$\begin{aligned} \vec{\mathbf{F}}_{top/bottom} =& \mu_o \iint_{S_{top/bottom}} \vec{\mathbf{H}} \left(\vec{\mathbf{H}} \cdot d\vec{\mathbf{S}} \right) - \frac{\mu_o}{2} \iint_{S_{top/bottom}} H^2 d\vec{\mathbf{S}} = 0 - \frac{\mu_o}{2} \iint_{S_{top/bottom}} H^2 d\vec{\mathbf{S}} \\ =& -\frac{\mu_o}{2} \iint_{S_{top/bottom}} H^2 d\vec{\mathbf{S}}, \end{aligned} \tag{7.16}$$

and there is no force contribution in the y direction for these two surfaces.

The force from Maxwell's stress equation for surface S_{side} is:

$$\begin{aligned} \vec{\mathbf{F}}_{side} =& \mu_o \iint_{S_{side}} \vec{\mathbf{H}} \left(\vec{\mathbf{H}} \cdot d\vec{\mathbf{S}} \right) - \frac{\mu_o}{2} \iint_{S_{side}} H^2 d\vec{\mathbf{S}} = \mu_o \iint_{S_{side}} H^2 d\vec{\mathbf{S}} - \frac{\mu_o}{2} \iint_{S_{side}} H^2 d\vec{\mathbf{S}} \\ =& \frac{\mu_o}{2} \iint_{S_{side}} H^2 d\vec{\mathbf{S}}, \end{aligned} \tag{7.17}$$

and the force in the y direction from both side surfaces S_{side} is:

$$F_{sides_y} = -2\frac{\mu_o}{2} \int_0^w \int_a^b \left(\frac{I}{2\pi\rho} \right)^2 \sin\alpha \, d\rho \, dz = -\frac{\mu_o I^2 w \sin\alpha}{4\pi^2} \left(\frac{1}{a} - \frac{1}{b} \right). \tag{7.18}$$

For any closed surface containing free space, the net force from Maxwell's stress equation for magnetostatics (resulting from a closed circuit) is null. This is true for the sum of the three surface forces of equations (7.13), (7.15), and (7.18):

$$F_{total_y} = F_{a_y} + F_{b_y} + F_{sides_y} = 0. \tag{7.19}$$

The six forces on each surface of the wedge closed surface of Figure 7.2 give some general insight into Maxwell's stress equation. James Maxwell related Michael Faraday's physical lines of force (magnetic lines of force in this case) [1] to a state of stress in the medium (i.e., tension in the direction of the lines of force and pressure normal to this direction) [21]. Surfaces S_{side} (front and back) are in the direction of the magnetic lines of force and the surfaces S_a, S_b, S_{top}, and S_{bottom} are normal to this direction.

The primary goal of this section is to determine if Maxwell's stress equation for the wedge closed surface of Figure 7.2 can be recast to eliminate the stress parallel to the magnetic lines of force while maintaining a radial stress (for an infinite line current). To accomplish this goal, the variant of Stokes' Theorem (5.12) is used. Similar to section 5.1, a first step to achieve this objective is to systematically establish how the variant of Stokes' Theorem applied to the various wedge surfaces operates on a $\vec{\mathbf{C}}$ of the general form:

$$\vec{\mathbf{C}}_n = \frac{k_n}{\rho^n}\hat{\mathbf{a}}_\rho, \tag{7.20}$$

where k_n is an arbitrary constant.

The divergence of $\vec{\mathbf{C}}_n$ is:

$$\nabla \cdot \vec{\mathbf{C}}_n = k_n\left[\frac{\partial}{\partial x}\frac{x}{\rho^{n+1}} + \frac{\partial}{\partial y}\frac{y}{\rho^{n+1}} + \frac{\partial}{\partial z}0\right] = \frac{k_n\,(1-n)}{\rho^{n+1}}, \tag{7.21}$$

and the gradient of the vector $\vec{\mathbf{C}}_n$ is:

$$\begin{aligned}\nabla\vec{\mathbf{C}}_n &= k_n\begin{bmatrix}\frac{\partial}{\partial x}\frac{x}{\rho^{n+1}} & \frac{\partial}{\partial x}\frac{y}{\rho^{n+1}} & \frac{\partial}{\partial x}0\\ \frac{\partial}{\partial y}\frac{x}{\rho^{n+1}} & \frac{\partial}{\partial y}\frac{y}{\rho^{n+1}} & \frac{\partial}{\partial y}0\\ \frac{\partial}{\partial z}\frac{x}{\rho^{n+1}} & \frac{\partial}{\partial z}\frac{y}{\rho^{n+1}} & \frac{\partial}{\partial z}0\end{bmatrix}\\ &= -\frac{k_n}{\rho^{n+3}}\begin{bmatrix} nx^2 - y^2 & (n+1)\,xy & 0\\ (n+1)\,xy & -x^2+ny^2 & 0\\ 0 & 0 & 0\end{bmatrix}.\end{aligned} \tag{7.22}$$

The differential surface element for the cylindrical surface S_b is:

$$d\vec{\mathbf{S}}_b = dS_b\hat{\mathbf{a}}_\rho = dS_b\begin{bmatrix}\frac{x}{\sqrt{x^2+y^2}}\\ \frac{y}{\sqrt{x^2+y^2}}\\ 0\end{bmatrix}, \tag{7.23}$$

and:

$$\nabla_{\mathbf{C}_n}\left(\vec{\mathbf{C}}_n\cdot d\vec{\mathbf{S}}_b\right) = \left(\nabla\vec{\mathbf{C}}_n\right)\cdot d\vec{\mathbf{S}}_b = -\frac{k_n n}{\rho^{n+1}}d\vec{\mathbf{S}}_b. \tag{7.24}$$

Combining (7.21), (7.24), and the integrand in the right side of (5.12) for the surface S_b yields:

$$\left(\nabla\cdot\vec{\mathbf{C}}_n\right)d\vec{\mathbf{S}}_b - \nabla_{\mathbf{C}_n}\left(\vec{\mathbf{C}}_n\cdot d\vec{\mathbf{S}}_b\right) = \frac{k_n\,(1-n)}{\rho^{n+1}}d\vec{\mathbf{S}}_b - -\frac{k_n n}{\rho^{n+1}}d\vec{\mathbf{S}}_b = \frac{k_n}{\rho^{n+1}}d\vec{\mathbf{S}}_b. \tag{7.25}$$

The differential surface element for the back side surface S_{side} is:

$$d\vec{\mathbf{S}}_{side} = dS_{side}\hat{\mathbf{a}}_\phi = dS_{side}\begin{bmatrix}-\frac{y}{\sqrt{x^2+y^2}}\\ \frac{x}{\sqrt{x^2+y^2}}\\ 0\end{bmatrix}, \tag{7.26}$$

and:

$$\nabla_{\mathbf{C}_n}\left(\vec{\mathbf{C}}_n\cdot d\vec{\mathbf{S}}_{side}\right) = \left(\nabla\vec{\mathbf{C}}_n\right)\cdot d\vec{\mathbf{S}}_{side} = \frac{k_n}{\rho^{n+1}}d\vec{\mathbf{S}}_{side}. \tag{7.27}$$

Combining (7.21), (7.27), and the integrand in the right side of (5.12) for the surface S_{side} yields:

$$\left(\nabla\cdot\vec{\mathbf{C}}_n\right)d\vec{\mathbf{S}}_{side}-\nabla_{\mathrm{C}_n}\left(\vec{\mathbf{C}}_n\cdot d\vec{\mathbf{S}}_{side}\right)=\frac{k_n\,(1-n)}{\rho^{n+1}}d\vec{\mathbf{S}}_{side}-\frac{k_n}{\rho^{n+1}}d\vec{\mathbf{S}}_{side}=-\frac{k_n n}{\rho^{n+1}}d\vec{\mathbf{S}}_{side}. \tag{7.28}$$

The differential surface element for the top surface S_{top} is:

$$d\vec{\mathbf{S}}_{top}=dS_{top}\hat{\mathbf{a}}_z=dS_{top}\begin{bmatrix}0\\0\\1\end{bmatrix}, \tag{7.29}$$

and:

$$\nabla_{\mathrm{C}_n}\left(\vec{\mathbf{C}}_n\cdot d\vec{\mathbf{S}}_{top}\right)=\left(\nabla\vec{\mathbf{C}}_n\right)\cdot d\vec{\mathbf{S}}_{top}=0. \tag{7.30}$$

Combining (7.21), (7.30), and the integrand in the right side of (5.12) for the surface S_{top} yields:

$$\left(\nabla\cdot\vec{\mathbf{C}}_n\right)d\vec{\mathbf{S}}_{top}-\nabla_{\mathrm{C}_n}\left(\vec{\mathbf{C}}_n\cdot d\vec{\mathbf{S}}_{top}\right)=\frac{k_n\,(1-n)}{\rho^{n+1}}d\vec{\mathbf{S}}_{top}-0=\frac{k_n\,(1-n)}{\rho^{n+1}}d\vec{\mathbf{S}}_{top}. \tag{7.31}$$

By inspecting the general results of (7.25), (7.28), and (7.31) and applying the method of Section 5.2, the following $\vec{\mathbf{C}}$ is chosen to recast Maxwell's stress equation for the infinite line current:

$$\vec{\mathbf{C}}=\frac{\mu_{\mathrm{o}}I^2}{8\pi^2\rho}\hat{\mathbf{a}}_\rho-\frac{k}{2\pi}\hat{\mathbf{a}}_\rho. \tag{7.32}$$

Therefore, applying the $\vec{\mathbf{C}}$ of (7.32) the recast stress equation for the infinite line current becomes:

$$\vec{\mathbf{F}}_{recast}=-\oiint\frac{k}{2\pi\rho}\hat{\mathbf{a}}_\rho\left(\hat{\mathbf{a}}_\rho\cdot d\vec{\mathbf{S}}\right)-\oiint\left(\frac{\mu_{\mathrm{o}}I^2}{8\pi^2\rho^2}+\frac{k}{2\pi\rho}\right)\hat{\mathbf{a}}_z\left(\hat{\mathbf{a}}_z\cdot d\vec{\mathbf{S}}\right). \tag{7.33}$$

The component in the z direction for the recast stress equation of (7.33) is an artifact of the infinite line current 'closed circuit'. Otherwise, the recast stress equation of (7.33) is similar to the recast stress equation of (5.28) for the spherically symmetric charge distribution.

7.3 Recasting of Maxwell's Stress Equation in Free Space, Away from a Differential Current Element at the Origin ($r = 0$) with Total Current, JdV, in the Positive z Direction for a Spherical Surface with Center at the Origin

For a spherical surface S with radius r and center at the origin, the Maxwell's stress equation is ($\vec{\mathbf{H}} \cdot d\vec{\mathbf{S}} = 0$):

$$\vec{\mathbf{F}} = \mu_{\mathrm{o}} \oiint \vec{\mathbf{H}} \left(\vec{\mathbf{H}} \cdot d\vec{\mathbf{S}} \right) - \frac{\mu_{\mathrm{o}}}{2} \oiint H^2 d\vec{\mathbf{S}} = -\frac{\mu_{\mathrm{o}}}{2} \oiint H^2 d\vec{\mathbf{S}} = \oiint \vec{\mathbf{F}}_S dS, \tag{7.34}$$

where:

$$\vec{\mathbf{F}}_S = -\frac{\mu_{\mathrm{o}} J^2 dV^2 \left(x^2 + y^2 \right)}{32\pi^2 r^6} \hat{\mathbf{a}}_r = -\frac{\mu_{\mathrm{o}} J^2 dV^2 \sin^2\theta}{32\pi^2 r^4} \hat{\mathbf{a}}_r, \tag{7.35}$$

$$F_{S_\rho} = -\frac{\mu_{\mathrm{o}} J^2 dV^2 \sin^3\theta}{32\pi^2 r^4}, \tag{7.36}$$

and

$$F_{S_z} = -\frac{\mu_{\mathrm{o}} J^2 dV^2 \sin^2\theta \cos\theta}{32\pi^2 r^4}. \tag{7.37}$$

Applying the variant of Stokes' Theorem using the method of Section 6.1 and solving

(6.19) for F_{ℓ_z} and then substituting F_{S_z} (7.37) yields:

$$\begin{aligned} F_{\ell_z} &= -\frac{1}{\sin\theta}\left(\int r\sin\theta F_{S_z}\,d\theta + K_z\right) \\ &= -\frac{1}{\sin\theta}\int r\sin\theta\left(-\frac{\mu_o J^2 dV^2\sin^2\theta\cos\theta}{32\pi^2 r^4}\right)d\theta - \frac{K_z}{\sin\theta} \\ &= \frac{\mu_o J^2 dV^2\sin^3\theta}{128\pi^2 r^3} - \frac{K_z}{\sin\theta}. \end{aligned} \tag{7.38}$$

The constant K_z is determined by setting the net force in the z direction on the differential ring equal to the net force on the surface bounded by the ring. The net force in the z direction on the differential ring is:

$$F_z = \int_0^{2\pi} F_{\ell_z} r\sin\theta\,d\phi = \frac{\mu_o J^2 dV^2\sin^4\theta}{64\pi r^2} - 2\pi r K_z, \tag{7.39}$$

and the net force in the z direction on the surface bounded by the ring is:

$$\begin{aligned} F_z &= \int_\theta^\pi\int_0^{2\pi} F_{S_z} r^2\sin\theta'\,d\phi\,d\theta' = -\frac{\mu_o J^2 dV^2}{16\pi r^2}\int_0^\pi \sin^3\theta'\cos\theta' d\theta' \\ &= \frac{\mu_o J^2 dV^2\sin^4\theta}{64\pi r^2}. \end{aligned} \tag{7.40}$$

Therefore, $K_z = 0$ and:

$$F_{\ell_z} = \frac{\mu_o J^2 dV^2\sin^3\theta}{128\pi^2 r^3}. \tag{7.41}$$

Continuing using the method of Section 6.1 and solving (6.20) for F_{ℓ_ρ} and then substituting F_{S_ρ} (7.36) yields:

$$\begin{aligned} F_{\ell_\rho} &= -\int\left(rF_{S_\rho} + F_{\ell_z}\right)d\theta + K_\rho \\ &= -\int\left[r\left(-\frac{\mu_o J^2 dV^2\sin^3\theta}{32\pi^2 r^4}\right) + \left(\frac{\mu_o J^2 dV^2\sin^3\theta}{128\pi^2 r^3}\right)\right]d\theta + K_\rho \\ &= -\frac{\mu_o J^2 dV^2\sin^2\theta\cos\theta}{128\pi^2 r^3} - \frac{\mu_o J^2 dV^2\cos\theta}{64\pi^2 r^3} + K_\rho, \end{aligned} \tag{7.42}$$

where the constant of integration K_ρ may be any function of r. Equations (7.41) and (7.42) are now used to solve for the $\vec{\mathbf{C}}$ of (6.17) that may be used to cancel Maxwell's stress equation for the spherical surface:

$$\begin{aligned}\vec{\mathbf{C}} =& \vec{\mathbf{F}}_\ell \times (-\hat{\mathbf{a}}_\phi) = -F_{\ell_z}\hat{\mathbf{a}}_\rho + F_{\ell_\rho}\hat{\mathbf{a}}_z \\ =& -\frac{\mu_\mathrm{o} J^2 dV^2 \sin^3\theta}{128\pi^2 r^3}\hat{\mathbf{a}}_\rho - \left(\frac{\mu_\mathrm{o} J^2 dV^2 \sin^2\theta\cos\theta}{128\pi^2 r^3} + \frac{\mu_\mathrm{o} J^2 dV^2 \cos\theta}{64\pi^2 r^3} - K_\rho\right)\hat{\mathbf{a}}_z \\ =& -\frac{\mu_\mathrm{o} J^2 dV^2 \sin^2\theta}{128\pi^2 r^3}\hat{\mathbf{a}}_r - \left(\frac{\mu_\mathrm{o} J^2 dV^2 \cos\theta}{64\pi^2 r^3} - K_\rho\right)\hat{\mathbf{a}}_z.\end{aligned} \tag{7.43}$$

In a similar manner, a $\vec{\mathbf{C}}$ may be derived such that when the variant of Stoke's theorem (5.12) is applied yields a spherical surface stress of:

$$\vec{\mathbf{F}}_{recast} = -\oiint \frac{\mathrm{f}(\theta)}{4\pi r^2}\hat{\mathbf{a}}_r \left(\hat{\mathbf{a}}_r \cdot d\vec{\mathbf{S}}\right), \tag{7.44}$$

where $\mathrm{f}(\theta)$ is an undetermined function of θ that is symmetric about the x–y plane (i.e., $\theta = \pi/2$ plane).

The magnetostatic Maxwell stress (per unit area) of (7.35) at concentric spherical surfaces (with radius r) away from the differential current element falls off as $1/r^4$. In contrast, the magnetostatic recast stress equation of (7.44) falls off as $1/r^2$. The recast stress equation of (7.44) depicts an inward surface tension only in the radial direction (referenced to the differential current element location) where the units of the function $\mathrm{f}(\theta)$ are N/sr. The choice of $\mathrm{f}(\theta)$ is made in the next chapter based on the interaction between two separated differential current elements.

7.4 Pinch Stress and QET

Maxwell's stress equation applied to a closed spherical surface external to an isolated, static differential current element has been recast using a variant of Stokes' Theorem. The recast stress equation (7.44) eliminates the stress aligned with the magnetic field and most of the stress normal to the magnetic field. The recast stress equation manifests an inward surface tension only in the radial direction (referenced to the differential current element location).

For the infinite line current of section 7.2, Maxwell's stress equation for a closed surface outside the line current has a net null result. However, Maxwell's stress equation may be used to determine the inward magnetostatic pressure [100] (N/m^2) on an infinite cylindrical shell with uniform surface current density, total current I and radius a:

$$\vec{\mathbf{p}}_a = -\frac{\mu_o}{2} H^2 \hat{\mathbf{a}}_\rho = -\frac{\mu_o I^2}{8\pi^2 a^2} \hat{\mathbf{a}}_\rho. \tag{7.45}$$

Similarly, the recast stress equation has some usefulness.

The recast stress equations (7.33) and (7.44) identifies the pinch stress associated with static current distributions. This pinch stress is external to the current distribution, directed inward. An external pinch stress may be modeled as an omnidirectional average rate of QET influx (W) in combination with an out-flux of an equal average rate of QETs. Since the average rate of influx and out-flux QETs are equal, there is no net gain or loss of energy in the current distribution. The average rate of QET influx and out-flux depict a mean valued sequence of energy carrier mediators. For instance, the energy carrier mediators (bosons) may be gravitons or photons [71, 35]. The impact force of QET influx and the

recoil force of QET out-flux accounts for the inward pressure (N/m^2).

Assume that the mean QET influx and out-flux is proportional to the equivalent magnetostatic mass of the current distribution. Chapter 4 described a net rate of QET absorptions, $\bar{P}_a$, and emissions, $\bar{P}_e$, both proportional to the mass, m, of a system: $\bar{P}_a = \bar{P}_e = \Gamma m$. The pinch stress is the sum of the impact force density of quantum energy absorptions and recoil force density of quantum energy emissions.

Equations (7.33) and (7.44) may be interpreted in light of Mach's principle. A given current distribution has an average rate of QET influx and out-flux interacting with the distant matter of the universe, proportional to the equivalent magnetostatic mass of the current distribution. The recast stress equation depicts an inward pressure (i.e., pinch stress) as a result of these QET interactions with the current distribution.

The pinch stress is the basis for the pinch phenomenon [102], pinch pressure [103], or pinch effect [100]. The pinch effect is traditionally viewed as a pressure internal to a current carrying conductor as a result of its own magnetic field and corresponding magnetostatic force on the conductor carrying the current [104]. The pinch effect has been attributed to the pinching off of current carrying liquids [102] and plasma [105], the propulsion of pencil shaped copper slugs in current carrying mercury [106, 107], the crumpling of hollow current carrying conductors and objects [108], as well as the explosion/mechanical fracturing of current carrying wires [109].

Similar to the Poincaré stress for charge distributions, the pinch stress is an external stress resulting from a mean valued, continual QETs between the current distribution and the distant matter of the universe. Maxwell emphasized: "It must be carefully remembered,

that the mechanical force which urges a conductor carrying a current ... acts, not on the electric current, but on the conductor which carries it" [110]. Therefore, the external pinch stress is a mechanical pressure on the solid or liquid conductor itself.

CHAPTER 8. A QET MODEL FOR THE NEUMANN AND PINCH STRESSES OF TWO SEPARATED, STATIC DIFFERENTIAL CURRENT ELEMENTS

The goal of this and the previous chapter is to establish a QET (boson interaction) model that provides a visualization of the stresses internal and external to constant current carrying solids. The internal and external magnetostatic stresses are derived from the recasting of Maxwell's stress equation and historical current force formulas known to be compatible with Maxwell's equations for closed circuits. Therefore, the magnetostatic QET model of this dissertation is mathematically consistent with Maxwell's equations.

Chapter 7 established a pinch stress by recasting Maxwell's stress equation for an infinite line current and an isolated, cylindrically symmetric static differential current element using a variant of Stokes' Theorem. The pinch stress is normal to the magnetic field and is directed inward toward the current distribution location. The pinch stress is modeled as an average rate of QET influx and an equivalent average rate of QET out-flux, the QETs exchanging bosons between the charge distribution and the distant matter of the universe. The inward pressure arises from the impact force of QET influx and the recoil force of QET out-flux. The pinch stress is proportional to the equivalent magnetostatic mass of the current distribution.

The principle aim of this chapter is to determine the QET magnetostatic stress equation for two separated, static differential current elements. The QET magnetostatic stress

only occurs at points aligned between the two differential current elements. The motivation to pursue this endeavor is to establish a mathematical basis for a Neumann stress[5] that only exists at each point on the straight path between the two differential current elements.

Two separated, static differential current elements are a key building block for magnetostatics. Any arbitrary current distribution may be assembled from a collection of interacting differential current elements. Therefore, differential current element results may be generalized for a circular loop or any other configuration of interest.

Equation (3.7) derived by Moon and Spencer, identifies an infinite number of formulas for the force between differential current elements only acting along the straight line between them. Repeated here, the differential force element on a first differential current element interacting with a second differential current element is:

$$d^2\vec{\mathbf{F}}_1 = -\frac{\mu_o}{4\pi d_{21}^2}\left\{\begin{array}{l} 3(1-k_1)\left[\left(\vec{\mathbf{J}}_1 dV_1\right)\cdot\hat{\mathbf{a}}_{21}\right]\left[\left(\vec{\mathbf{J}}_2 dV_2\right)\cdot\hat{\mathbf{a}}_{21}\right] \\ +(k_1-2)\left(\vec{\mathbf{J}}_1 dV_1\right)\cdot\left(\vec{\mathbf{J}}_2 dV_2\right) \\ +k_3\left[\left(\vec{\mathbf{J}}_1 dV_1\right)\times\left(\vec{\mathbf{J}}_2 dV_2\right)\right]\cdot\hat{\mathbf{a}}_{21} \end{array}\right\}\hat{\mathbf{a}}_{21}, \tag{8.1}$$

where k_1 and k_3 are arbitrary constants.

The goal of this chapter is to identify which combination(s) of the arbitrary constants k_1 and k_3 of (8.1) are compatible with the QET model of this dissertation. Any combinations of k_1 and k_3 give the correct total force between two closed circuits. However, as established in section 6.2 for electrostatics, the force resulting from QET exchanges be-

---

[5]The term Neumann stress is assigned to the line stress (developed in Section 8.1 from the historical current force formulas known to be compatible with Maxwell's equations for closed circuits) that only exists at each point on the straight path between two separated, differential current elements.

tween two ‘elements’ is related to the trapped energy between these ‘elements’. Therefore, the approach taken in this chapter is to determine if there are any constraints on k_1 and k_3 related to the trapped energy between differential current elements.

Section 8.1 identifies the constraints on the arbitrary constants k_1 and k_3 of (8.1) by analyzing the trapped energy associated with two different closed circuits. The end result is that only the Neumann formula (3.4) is compatible with the trapped energy for any two closed circuits.

Section 8.2 expounds on the Neumann stress identified in the magnetostatic stress equation. For two differential current elements in opposite directions, the Neumann stress is modeled as photon exchanges continually occurring between the two differential current elements. The amount of trapped energy associated with this continual photon exchange is shown to be equivalent to the magnetostatic potential energy of the two separated differential current elements.

Section 8.3 describes how two differential current elements in opposite directions and two differential current elements in the same direction may be modeled with energy carrier mediators associated with the Neumann stress and the pinch stress.

8.1 Determination of the QET Magnetostatic Stress Equation for the Interaction Between Two Isolated Differential Current Elements

Maxwell’s stress equation for magnetostatics (7.3) cannot be recast to determine the stress between two differential current elements because it is only valid when one of the differential elements is part of a set integrated around a closed circuit. Therefore, a different

approach is necessary for determining the magnetostatic stress between two differential current elements that is compatible with the QET model of this dissertation. The approach taken in this section is equating the trapped or missing energy corresponding to the force between all differential current elements of two separate closed circuits to the magnetostatic potential energy of the two separate closed circuits [111].

Equation (8.1) identifies an infinite number of formulas for the force between differential current elements only acting along the straight line between them, where k_1 and k_3 are arbitrary constants. Constraints on the arbitrary constants k_1 and k_3 may be determined by analyzing the trapped energy associated with two separated closed circuits.

Great precaution must be taken when analyzing differential current elements for magnetostatics because physically they do not independently exist. Maxwell's equation for magnetostatics based on the Biot-Savart Law and Lorentz's force equation "has meaning only as one element of a sum over a continuous set ... of a current loop or circuit" [101]. From the conservation of charge standpoint (i.e., continuity equation for charge), a static differential current element may be part of a circuit (i.e., closed path) or part of a finite wire where there is a buildup of positive and negative charges at the wire ends [112]. An isolated static differential current element is purely fictitious.

Differential current elements for magnetostatics must be part of a closed path, otherwise there would be a buildup of charge resulting from a dynamic electric field and thus a dynamic magnetic field. That is the case for the differential current elements analyzed in this chapter, they are always part of a closed circuit (even if not specifically mentioned on every occasion).

Section 6.2 and section 6.3 established a relationship for electrostatics between the Coulomb stress/force and the trapped (or missing) energy between two charge distributions. It was shown that for two like-charge distributions, the Coulomb force is a result of a mean rate of energy absorbed $\bar{P}_a$ (W) and emitted $\bar{P}_e$ (W) to and from each charge distribution. The repulsive Coulomb force on each charge distribution is the sum of the impact force from the mean energy absorbed and the recoil force from the mean energy emitted:

$$F = \frac{q_1 q_2}{4\pi\varepsilon_o d^2} = \frac{\bar{P}_a + \bar{P}_e}{c}. \tag{8.2}$$

The photon exchanges back and forth between the two charge distributions may be regarded as trapped energy along the path between them (i.e., the Coulomb stress) and is equivalent to the electrostatic potential energy of the two charge distribution system:

$$U_{trapped} = \left(\bar{P}_a + \bar{P}_e\right) t_{12} = \left(\bar{P}_a + \bar{P}_e\right) \frac{d}{c} = \frac{q_1 q_2}{4\pi\varepsilon_o d} = Fd = U_e. \tag{8.3}$$

This same relationship $U_{trapped} = Fd$, equivalent to the electrostatic potential energy may be used for magnetostatics as well. The magnitude (positive for repulsion, negative for attraction) of the differential force element of (8.1) multiplied by d may be viewed as the differential amount of trapped (or missing) energy between two differential current elements. For the QET model of this dissertation, the net trapped energy obtained by integrating the differential amount of trapped (or missing) energy around two closed circuits is equivalent to the magnetostatic energy of the two closed circuit system.

Neumann's mutual inductance formula for two closed filament current loops in free space contains a similar expression to the Neumann's formula for the differential force

between two differential current elements of (3.4) [16, 17]:

$$M_{12} = -\frac{\mu_o}{4\pi}\oint_1\oint_2 \frac{d\vec{\boldsymbol{\ell}}_1 \cdot d\vec{\boldsymbol{\ell}}_2}{d_{21}}, \tag{8.4}$$

where $d\vec{\boldsymbol{\ell}}_1$ and $d\vec{\boldsymbol{\ell}}_2$ are in the directions of the currents in loop 1 and loop 2 respectively.

The magnetostatic potential energy associated with the two filament current loops carrying currents I_1 and I_2 respectively is:

$$U_m = \frac{1}{2}M_{12}I_1I_2 = -\frac{\mu_o I_1 I_2}{8\pi}\oint_1\oint_2 \frac{d\vec{\boldsymbol{\ell}}_1 \cdot d\vec{\boldsymbol{\ell}}_2}{d_{21}}, \tag{8.5}$$

where the $\frac{1}{2}$ factor is so that the differential energy associated with a given differential current element of loop 1 and loop 2 isn't counted twice when integrating around both loops.

The magnetostatic potential energy corresponding to the Moon and Spencer formula (8.1) is therefore:

$$U_m = \frac{\mu_o I_1 I_2}{8\pi}\oint_1\oint_2 \left\{ 3(1-k_1)\frac{\left(d\vec{\boldsymbol{\ell}}_1\cdot\hat{\mathbf{a}}_{21}\right)\left(d\vec{\boldsymbol{\ell}}_2\cdot\hat{\mathbf{a}}_{21}\right)}{d_{21}} + (k_1-2)\frac{d\vec{\boldsymbol{\ell}}_1\cdot d\vec{\boldsymbol{\ell}}_2}{d_{21}} + k_3\frac{\left(d\vec{\boldsymbol{\ell}}_1\times d\vec{\boldsymbol{\ell}}_2\right)}{d_{21}} \right\}, \tag{8.6}$$

where the term with the (k_1-2) coefficient is the negative of the Neumann mutual inductance energy (8.5).

Determining if there are any constraints on k_1 requires a two circuit system such that $d\vec{\boldsymbol{\ell}}_1 \times d\vec{\boldsymbol{\ell}}_2 = 0$ and there is no contribution form the k_3 term. This is the case for two infinite parallel cylindrical shell surface currents carrying equal and opposite total currents I with cylindrical radius a separated by a distance d as shown in Figure 8.1.

The inductance per unit length (H/m) of this two conductor system is easily derived by calculating the magnetic flux density between the two conductors (assuming $d \gg a$)

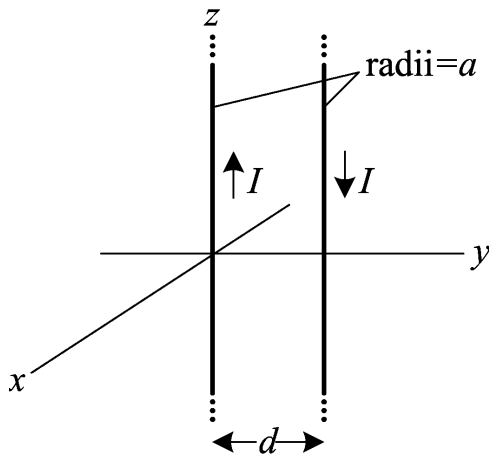

Figure 8.1: Two infinite cylindrical shell surface currents.

[113]:

$$\ell = \frac{\mu_{\rm o}}{2\pi} \ln\left(\frac{d^2}{a^2}\right). \tag{8.7}$$

Therefore, the magnetostatic potential energy per unit length (J/m) is:

$$u_m = \frac{1}{2}\ell I^2 = \frac{\mu_{\rm o} I^2}{4\pi} \ln\left(\frac{d^2}{a^2}\right). \tag{8.8}$$

The trapped/missing energy per unit length corresponding to the term with the $(k_1 - 2)$ coefficient in (8.6) is obtained by integrating the energy associated with the cylindrical shell elements in the x–y plane. By symmetry, the energy corresponding to each cylindrical shell element are equal. Therefore, the total energy per unit length will be twice that obtained for one of the cylindrical shell elements. In addition, the self interaction of a current filament element on the cylindrical shell surface about the z axis, interacting with the rest of the cylindrical shell surface is equivalent to the interaction as if all the current is contained in a current filament on the z axis. Therefore, the trapped energy per unit length corresponding

to the term with the (k_1-2) coefficient in (8.6) is (again, assuming $d \gg a$):

$$\begin{aligned} u_{\textit{trapped}:(k_1-2)} &= 2\left\{\frac{\mu_o I\left(\frac{I}{2\pi a}\right)}{8\pi}\int_0^{2\pi}\int_{-\infty}^{\infty}\left(\frac{1}{\sqrt{d^2+z^2}}+\frac{-1}{\sqrt{a^2+z^2}}\right)dz\,ad\phi\right\} \\ &= -\frac{\mu_o I^2}{4\pi}\ln\left(\frac{d^2}{a^2}\right). \end{aligned} \tag{8.9}$$

As expected, the energy per unit length of (8.9) is the negative of the Neumann mutual inductance energy (8.5). The trapped/missing energy per unit length corresponding to the term with the $3\,(1-k_1)$ coefficient in (8.6) is (assuming $d \gg a$):

$$\begin{aligned} u_{\textit{trapped}:3(1-k_1)} &= 2\left\{\frac{\mu_o I\left(\frac{I}{2\pi a}\right)}{8\pi}\int_0^{2\pi}\int_{-\infty}^{\infty}\left(\frac{-z^2}{\left(d^2+z^2\right)^{3/2}}+\frac{z^2}{\left(a^2+z^2\right)^{3/2}}\right)dz\,ad\phi\right\} \\ &= \frac{\mu_o I^2}{4\pi}\ln\left(\frac{d^2}{a^2}\right). \end{aligned} \tag{8.10}$$

In order for the net trapped energy to be equivalent to the magnetostatic potential energy:

$$3\,(1-k_1)\,u_{\textit{trapped}:3(1-k_1)} + (k_1-2)\,u_{\textit{trapped}:(k_1-2)} = u_m. \tag{8.11}$$

Therefore, combining (8.8), (8.9), (8.10), and (8.11) yields:

$$3\,(1-k_1) - (k_1-2) = 1, \tag{8.12}$$

or $k_1 = 1$.

Determining if there are any constraints on k_3 of (8.6) requires a two circuit system such that there is a contribution for $d\vec{\boldsymbol{\ell}}_1 \times d\vec{\boldsymbol{\ell}}_2$. Circular filament current loops provide a straight forward approach to achieve this. Consider two coaxial circular filament current loops with radii a separated by a distance d as shown in Figure 8.2.

The mutual inductance between these two coaxial circular current loops involving elliptic integrals is [114]:

$$M = \mu_o a\,\mathrm{h}\left(2\sqrt{\frac{a^2}{d^2+4a^2}}\right), \tag{8.13}$$

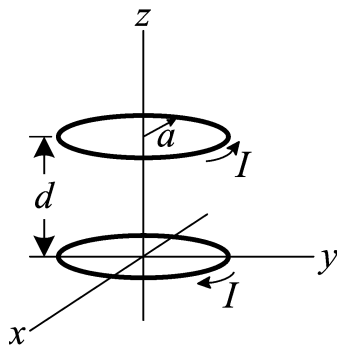

Figure 8.2: Two coaxial circular filament current loops.

where:

$$\mathrm{h}(k) = \left(\frac{2}{k} - k\right)\mathrm{K}(k) - \frac{2}{k}\mathrm{E}(k)\,, \tag{8.14}$$

$$\mathrm{K}(k) = \int_0^{\pi/2} \frac{1}{\sqrt{1 - k^2 \sin^2 \phi}} d\phi, \tag{8.15}$$

and:

$$\mathrm{E}(k) = \int_0^{\pi/2} \sqrt{1 - k^2 \sin^2 \phi}\, d\phi. \tag{8.16}$$

The magnetostatic potential energy for these two coaxial circular current loops is:

$$U_m = \frac{1}{2} M I^2 = \frac{\mu_\mathrm{o} a I^2}{2}\, \mathrm{h}\left(2\sqrt{\frac{a^2}{d^2 + 4a^2}}\right). \tag{8.17}$$

The trapped energy for the two coaxial circular current loops corresponding to the term with the k_3 coefficient in (8.6) is determined numerically using Mathcad as shown in Figure 8.3. This energy is null, therefore no constraint is found for this case.

Since the energy associated with the k_3 coefficient term is null, this two coaxial circular current loop example can also be used to numerically determine that $k_1 = 1$.

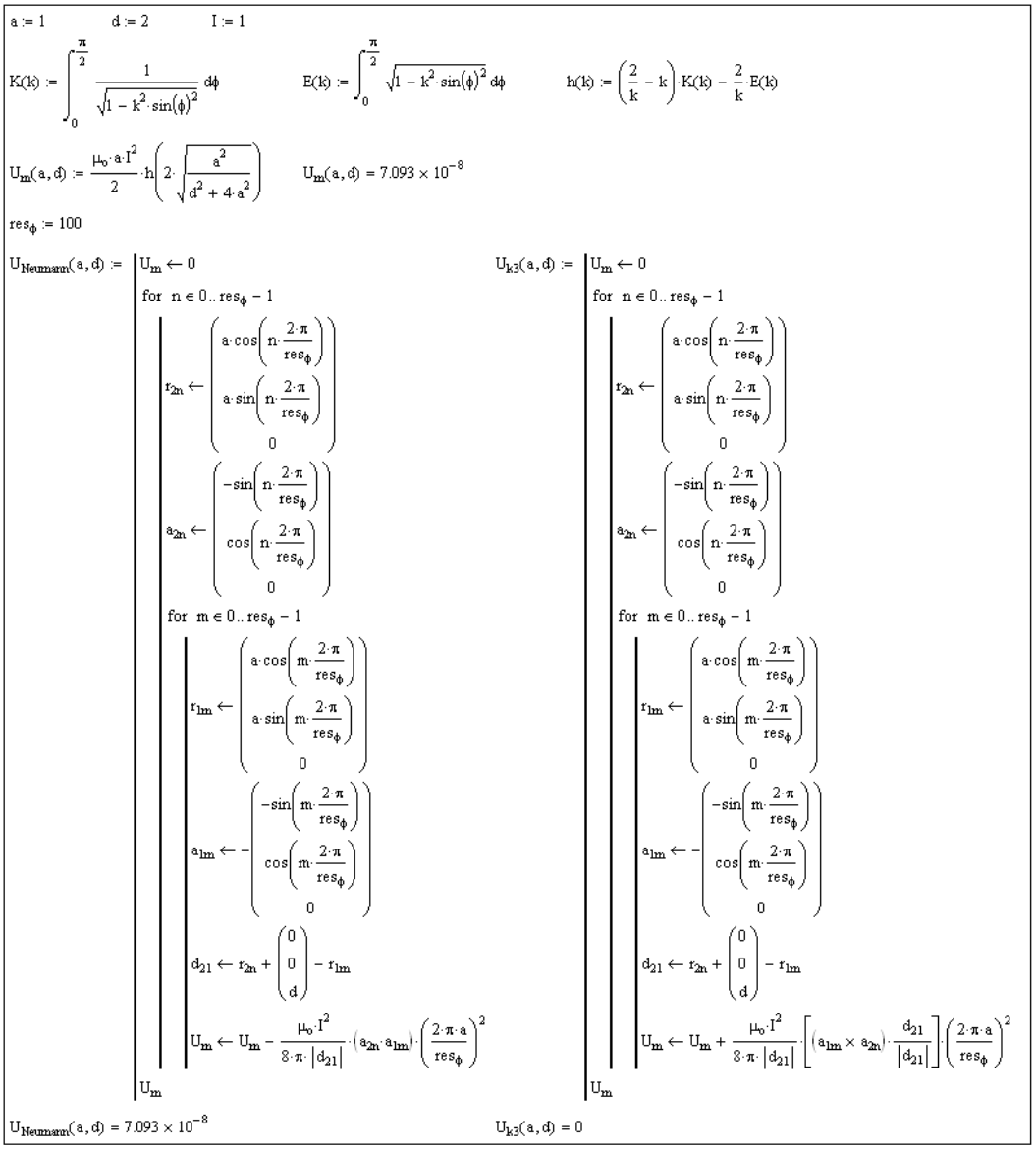

Figure 8.3: Numerical analysis (Mathcad) for two coaxial circular filament current loops.

Next, consider two circular filament current loops normal to each other with radii a separated by a distance d as shown in Figure 8.4. Because the loops are normal to each other, the mutual inductance is null.

The trapped energy for the two circular current loops corresponding to the term with

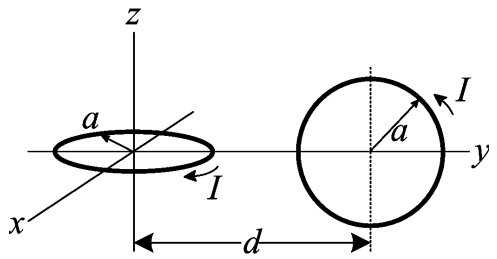

Figure 8.4: Two circular filament current loops normal to each other.

the k_3 coefficient in (8.6) is determined numerically using Mathcad as shown in Figure 8.5. Since this energy is nonzero for the two current loops normal to each other, the constant k_3 of (8.6) must be equal to 0.

As a side note, Mathcad was also used to verify numerically that the general force equation of (3.6) gave the same resulting force between a differential current element and a circular filament current loop covering all combinations of possible angles between the differential current element and current loop as well as possible combinations for k_1 and k_2. In addition, Mathcad was used to verify numerically that the Moon and Spencer force equation of (3.7) gave the same resulting force between two circular filament current loops covering all combinations of possible angles between the two loops as well as possible combinations for k_1 and k_3.

The two infinite parallel cylindrical shell surface currents carrying equal and opposite total currents and the two circular filament current loops normal to each other have been used to determine the constraints: $k_1 = 1$ and $k_3 = 0$ of (8.6). Therefore, the trapped energy (i.e., magnetostatic potential energy) for two filament current closed circuits of (8.6) having infinite possibilities reduces to the magnetostatic potential energy based on Neumann's

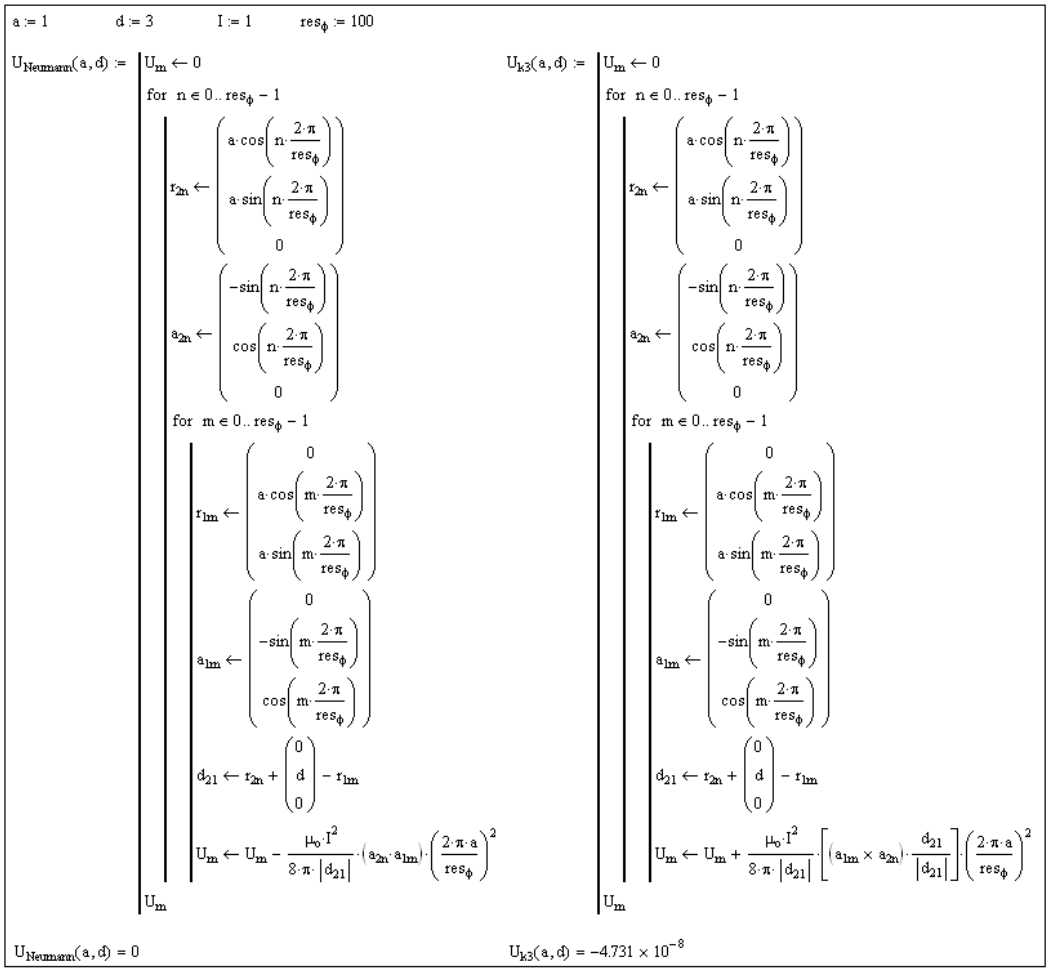

Figure 8.5: Numerical analysis (Mathcad) for two circular filament current loops normal to each other.

mutual inductance formula for two filament current closed circuits of (8.5).

And finally, the force formula for the interaction between two differential current elements of (8.1) having infinite possibilities reduces to the Neumann force formula of (3.4). Repeated here, the differential element of force on a first differential current element

interacting with a second differential current element is:

$$d^2\vec{\mathbf{F}}_1 = \frac{\mu_o}{4\pi}\frac{\left(\vec{\mathbf{J}}_1 dV_1\right)\cdot\left(\vec{\mathbf{J}}_2 dV_2\right)}{d_{21}^2}\hat{\mathbf{a}}_{21}. \tag{8.18}$$

When integrated around two closed circuits, this force is equivalent to the classical magnetostatic force [115, 116]. The differential amount of trapped (or missing) energy (i.e., magnetostatic potential energy) associated with the differential force of (8.18) is:

$$d^2U_{21} = -\frac{\mu_o}{4\pi}\frac{\left(\vec{\mathbf{J}}_1 dV_1\right)\cdot\left(\vec{\mathbf{J}}_2 dV_2\right)}{d_{21}}. \tag{8.19}$$

Similar to electrostatics, the force between two anti-parallel differential current elements for magnetostatics is a result of a mean rate of QETs absorbed and emitted by each differential current element consisting of a continual exchange of photons back and forth between the current elements. The continual exchange of energy carrier bosons along the straight line between the two differential current elements may be viewed as a line stress. The term Neumann stress is assigned to the line stress that only exists at each point on the straight path between two separated, differential current elements. The Neumann stress in magnetostatics is analogous to the Coulomb stress in electrostatics.

As an aside, a similar method may be used for analyzing the magnetostatic potential energy of the general force equation between two differential current elements of (3.6). Appendix F determines the constraints on this general force equation. The end result is that the Ampère force formula (3.3) between current elements is invalid because it does not give the correct magnetostatic potential energy between two closed circuits. The only commonly referenced formula agreeing with Ampère's original experimental conclusions and giving the correct magnetostatic potential energy for circuital currents is shown to be

the Grassmann force formula (3.5).

Ampère's force formula between current elements is based on his original experiments. Maxwell gave preference to Ampère's force formula as "...undoubtedly the best, since it is the only one which makes the forces on the two elements not only equal and opposite but in the straight line which joins them" [117]. Although Ampère's force formula has been preferred by many scientist and physicist, it is invalid because it does not produce the proper magnetostatic potential energy between two closed circuits.

Both the Grassmann and Neumann current element force formulas give the correct magnetostatic potential energy between two closed circuits. Therefore, any magnetostatic models or conclusions about the forces between closed circuits must be based on one of these two formulas to be valid. The Grassmann (Biot-Savart/Lorentz) force formula (applicable for closed circuits) provides the foundation for the static magnetic field $\vec{\mathbf{B}}$ of Maxwell's equation.

The Neumann current element force formula is the only force formula that corresponds to the appropriate magnetostatic potential energy as a result of removing Ampère's original constraint that a current element can't have a tangential force component (when interacting with a closed circuit), while maintaining Ampère's constraint that current element forces only act along the straight line between them. Therefore, the Neumann force formula also "makes the forces on the two elements not only equal and opposite but in the straight line which joins them".

8.2 Neumann Stress and QET

The Neumann force formula of (8.18) is the only force formula compatible with the QET model of this dissertation. The force between two differential current elements in the opposite directions is a result of photon exchanges continually occurring between the two differential current elements. The differential amount of trapped energy associated with this continual photon exchange is equivalent to the magnetostatic potential energy of the two separated differential current elements of (8.19).

The Neumann stress only exists at each point on the line between the two separated, differential current elements. In general, a Neumann stress equation may be defined for an arbitrary surface and arbitrary locations for two separated, differential current elements:

$$\vec{\mathbf{F}}_{Neumann} = \frac{\mu_o \left(\vec{\mathbf{J}}_1 dV_1\right) \cdot \left(\vec{\mathbf{J}}_2 dV_2\right)}{4\pi d_{21}^2} \oiint \delta^2(1+\hat{\mathbf{a}}_{r_1}\cdot\hat{\mathbf{a}}_{r_2}) \operatorname{sgn}(\hat{\mathbf{a}}_{r_1}\cdot\hat{\mathbf{a}}_n)\hat{\mathbf{a}}_{r_1} dS, \tag{8.20}$$

where $\left(\vec{\mathbf{J}}_1 dV_1\right)$ and $\left(\vec{\mathbf{J}}_2 dV_2\right)$ are the two differential current elements, d_{21} is the distance between the centers of the two current elements, $\delta^2()$ is the two dimensional or surface Dirac delta function [86], $\hat{\mathbf{a}}_{r_1}$ and $\hat{\mathbf{a}}_{r_2}$ are the directional unit vectors away from the first and second differential current elements respectively, sgn $()$ is the function defined in (6.12), and $\hat{\mathbf{a}}_n$ is the directional unit vector outward normal from the surface S.

The essence of (8.20) is a differential surface force element (equivalent to the Neumann force) for every non-tangential intersection of the arbitrary surface S with the straight line between the two differential current elements. Equation (8.20) may have the appearance of merely stating the point to point, action-at-a-distance property of Neumann's force formula. However, the analysis of the previous section shows that the Neumann stress

equation is mathematically compatible with Maxwell's equation for two closed current circuits.

If both differential current elements are generally in the opposite direction (i.e., the dot product of the two current elements is negative), then the Neumann stress may be modeled as an average rate of QETs (i.e., photons) exchanging back and forth between the two current elements. The line stress is modeled as the straight path of the photons. The impact force (of photons absorbed by the differential current elements) and recoil force (of photons emitted from the current elements) constitute the Neumann force on the differential current elements.

The photon exchanges back and forth between the two differential current elements may be regarded as trapped energy along the path between them (i.e., the Neumann stress). The amount of trapped energy is equivalent to the magnetostatic potential energy of (8.19) for two differential current elements generally in the opposite directions.

8.3 Pinch Stress, Neumann Stress and QET

The pinch stress related to the equivalent magnetostatic mass of each individual differential current element was ignored for the evaluation of Section 8.1. For an isolated differential current element, the pinch stress is normal to the magnetic field and is directed inward toward the differential current element. The recast stress equation of (7.44) identifies the pinch stress associated with a differential current element.

Based on the omnidirectional appearance of the Neumann force formula of (8.18), it

is presumed that the undetermined function of θ, f(θ) of (7.44) is a constant proportional to the equivalent magnetostatic mass of the current element. As such, the pinch stress associated with a differential element of current having a differential magnetostatic potential energy of u_m is:

$$\vec{\mathbf{F}}_{1_{pinch}} = -\oiint \frac{\Gamma u_m}{2\pi c^3 r_1^2} \hat{\mathbf{a}}_{r_1} \left(\hat{\mathbf{a}}_{r_1} \cdot d\vec{\mathbf{S}} \right). \tag{8.21}$$

The inward pressure arises from the impact force of QET influx and the recoil force of QET out-flux. The QET influx and out-flux has been modeled as energy carrier mediators (bosons) interacting between the current element and the distant matter of the universe. The pinch stress is proportional to the equivalent mass of the magnetostatic potential energy of the differential current element.

For two differential current elements generally in opposite directions (i.e., the dot product of the two current elements is negative) there is a pinch stress associated with each individual current element. In addition, there is a Neumann stress from QETs (i.e., photon exchanges) back and forth between the two current elements causing the current elements to be pushed apart.

The concentration of mean QET flux density (i.e., energy flux density magnitude) is modeled/depicted in Figure 8.6(a). The darker gray regions represent a higher concentration of QETs, while the lighter gray regions denote a lower concentration. The mean QET flux density associated with the pinch stress for each individual current element falls off as the inverse square of the distance from the current element. The mean QET flux density associated with the Neumann stress depicts the trapped energy from the photon exchanges back and forth between the two current elements in opposite directions. The actual direc-

tion of one of the current elements doesn't matter as long as the two current elements are in opposite directions.

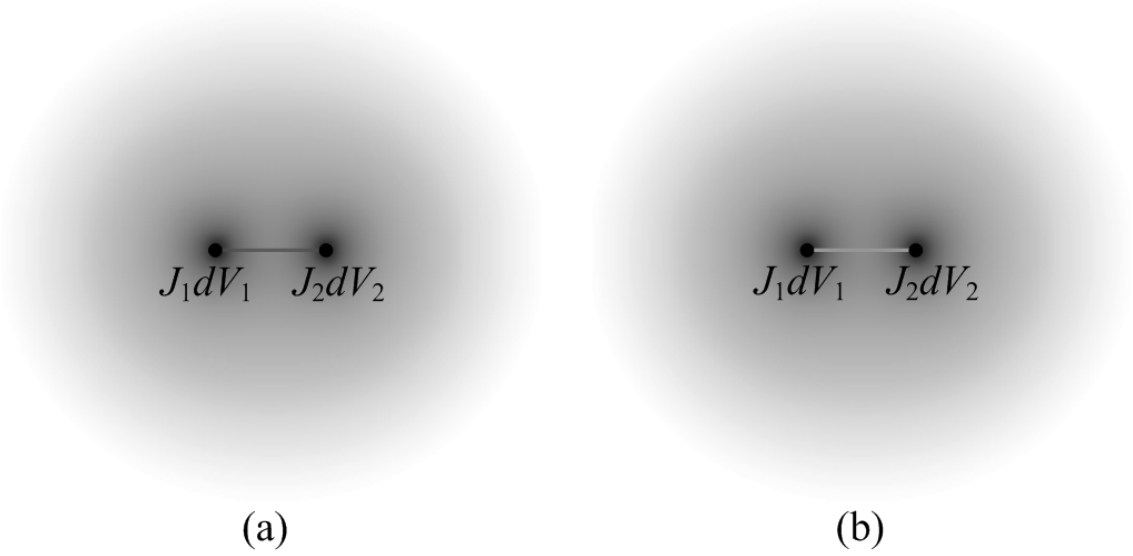

Figure 8.6: Illustration of pinch and Neumann stress for two differential current elements: (a) opposite directions, (b) same direction.

In addition to the pinch stress associated with the two individual current elements, for a static condition there is an additional pinch stress maintaining the two current elements at equilibrium. The net effect of this additional pinch stress is a force that counteracts the Neumann force associated with the photon exchange back and forth between the two current elements.

At a large distance away from the current elements (compared to the distance between the two current elements), this additional pinch stress is assumed to be omnidirectional inward proportional to the magnetostatic potential energy of the two current elements: $-\mu_o\left(\vec{\mathbf{J}}_1 dV_1\right)\cdot\left(\vec{\mathbf{J}}_2 dV_2\right)/(4\pi d_{21})$.

Two current elements in the same general direction (i.e., the dot product of the two current elements is positive) may be modeled in a similar, but slightly different manner. The two individual current elements have a pinch stress associated with them, omnidirectionally inward, proportional to the magnetostatic mass of each current element.

However, there is a missing amount of QETs back and forth between the two elements associated with the Neumann stress, causing the current elements to be pushed together. The concentration of mean QET flux density (i.e., energy flux density magnitude) is depicted in Figure 8.6(b).

The missing energy between the current elements is equivalent to the negative valued magnetostatic potential energy $U_{missing} = -\mu_o \left(\vec{\mathbf{J}}_1 dV_1\right) \cdot \left(\vec{\mathbf{J}}_2 dV_2\right) / \left(4\pi d_{21}\right)$ of the two current elements in the same direction. As a result of a decrease in the magnetostatic mass for the two current elements, there is a reduction in the overall pinch stress thus maintaining the two current elements in equilibrium (i.e., a net force equal and opposite to the Neumann force).

At a large distance away from the current elements (compared to the distance between the two current elements), the reduction in the pinch stress is assumed to be omnidirectional inward proportional to the magnetostatic potential energy (negative) of the two current elements in the same direction.

CHAPTER 9. COULOMB STRESS FOR TWO SEPARATED, SPHERICALLY SYMMETRIC CHARGE DISTRIBUTIONS BOTH MOVING WITH THE SAME CONSTANT VELOCITY

This chapter analyzes the Coulomb stress for two charge distributions moving with the same constant velocity by applying the Lorentz transformation. The Coulomb stress is found to be compatible with relativistic velocities. This chapter also provides a visual representation of the increase in energy and the relationship of forces associated with the Lorentz transformation.

Two extremely small charge configurations (i.e., point charges) are often referred to as a dumbbell [80, 81]. The movement with constant velocity of a like-charged dumbbell is easily analyzed with the Lorentz transformation [118].

Consider two reference frames as shown in Figure 9.1. The reference frame Σ is at rest. The reference frame Σ' is moving in the positive x direction with a constant velocity v.

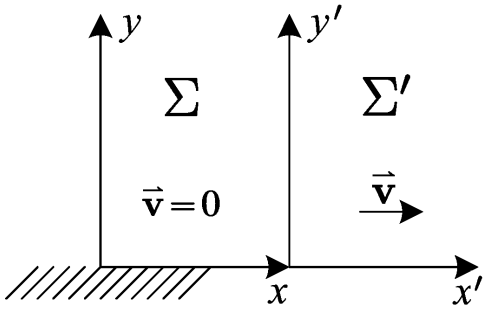

Figure 9.1: Reference frames for Lorentz transformation.

Two separate dumbbell configurations (a transverse configuration and a longitudinal configuration) are at rest in the moving reference frame Σ' as shown in Figure 9.2. For simplicity, the two differential charge elements are considered to have total charges q'_1 and q'_2.

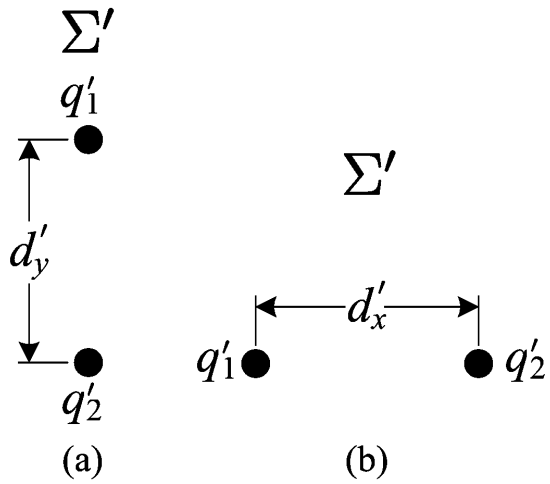

Figure 9.2: Charge dumbbells at rest in moving reference frame: (a) transverse, (b) longitudinal.

The following attributes are observed in the reference frame Σ at rest:

Time dilation [118]: $t = \gamma t'$, (9.1)

Length contraction [118]: $d_x = \dfrac{d'_x}{\gamma}$, (9.2)

Charge is invariant [119]: $q = q'$, (9.3)

Energy [120]: $U = \gamma U'$, (9.4)

where:

$$\gamma = \frac{1}{\sqrt{1-v^2/c^2}}. \tag{9.5}$$

The force and energy Lorentz transformation may be determined by analyzing the Lorentz transformation of the classical electric field and magnetic flux density. With the two charges at rest in Σ' (see Figure 9.2 (a)), the electric field from q_2' at q_1' only has a component in the positive y' direction: $E_y' = q_2'/\left(4\pi\varepsilon_o d_y'^2\right)$. Applying the Lorentz transformation for the electric field, an electric field in the y direction and a magnetic flux density in the positive z direction is calculated: $E_y = \gamma E_y'$ and $B_z = \gamma E_y' v/c^2$ [121]. The force on q_1 in the y direction is then calculated using Lorentz's force equation:

$$F_{transverse} = q_1\left(\gamma E_y' - \gamma E_y'\frac{v^2}{c^2}\right) = \frac{F'}{\gamma}. \tag{9.6}$$

For the longitudinal dumbbell at rest in Σ' (see Figure 9.2 (b)), the electric field from q_2' at q_1' only has a component in the negative x' direction: $E_x' = -q_2'/\left(4\pi\varepsilon_o d_x'^2\right)$. At this location, the x component of the electric field is unchanged in the Lorentz transformation and no magnetic flux density component is introduced: $E_x = E_x'$ [121]. Therefore, the force on q_1 in the negative x direction using Lorentz's force equation is:

$$F_{longitudinal} = q_1 E_x' = F'. \tag{9.7}$$

The sum of the energies for the transformed electric and magnetic fields agrees with the Lorentz transformation of the original electrostatic potential energy of the two charges at rest in Σ': $U = \gamma U'$. There are two invariants related to the relativistic Lorentz transformation of the electric field and magnetic flux density [122]. The first invariant is $\vec{\mathbf{E}} \cdot \vec{\mathbf{B}}$.

Since $\vec{\mathbf{B}}' = 0$ in Σ', $\vec{\mathbf{B}}$ will always be normal to $\vec{\mathbf{E}}$ in every other inertial reference frame. The second invariant is $\varepsilon_{\mathrm{o}}E^2 - B^2/\mu_{\mathrm{o}}$. Since $\vec{\mathbf{B}}' = 0$ in Σ', the electric field will always dominate in every other inertial reference frame.

The force and energy Lorentz transformation may also be determined by analyzing the electromagnetic model of this dissertation moving with relativistic velocities. The two separate dumbbell configurations (a transverse configuration and a longitudinal configuration) are at rest in Σ' as shown in Figure 9.3. The Coulomb stress between q'_1 and q'_2 is depicted as a line with an arrow from q'_1 to q'_2 and from q'_2 to q'_1. These lines/arrows represent a QET (i.e., emission [non-arrow end] and absorption [arrow end] of a photon from one charge to the other).

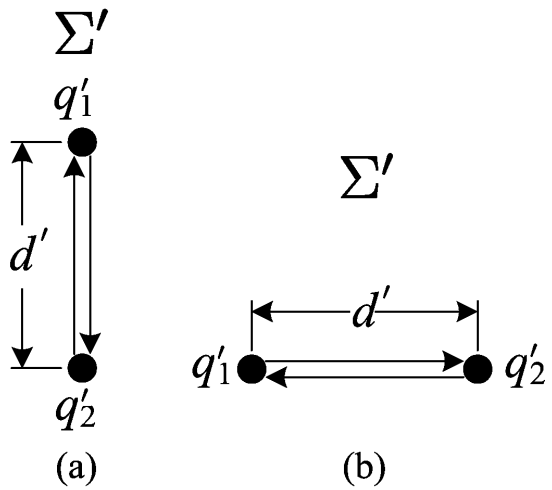

Figure 9.3: Charge dumbbells at rest in moving reference frame: (a) transverse, (b) longitudinal.

Assume the photons exchanging back and forth between the two charges q'_1 and q'_2 have a mean energy $\bar{U}'_{photon}$ (J) and a mean time repetition of photon exchanges $\bar{t}'_{rep}$ (s). Therefore, the mean rate of energy absorbed $\bar{P}'_a$ (W) and emitted $\bar{P}'_e$ (W) to and from each

charge is:

$$\bar{P}'_a = \bar{P}'_e = \frac{\bar{U}'_{photon}}{\bar{t}'_{rep}}. \tag{9.8}$$

The repulsive force between the two charges is:

$$F' = \frac{\bar{P}'_a + \bar{P}'_e}{c} = \frac{q'_1 q'_2}{4\pi\varepsilon_o d'^2}. \tag{9.9}$$

And, the trapped energy (from QETs) between the two charges (i.e., the electrostatic potential energy) is:

$$U'_{trapped} = \left(\bar{P}'_a + \bar{P}'_e\right) t'_{12} = \left(\bar{P}'_a + \bar{P}'_e\right) \frac{d'}{c} = \frac{q'_1 q'_2}{4\pi\varepsilon_o d'}. \tag{9.10}$$

The Lorentz transformation for both the transverse and longitudinal dumbbell configurations is used: $q_1 = q'_1$, $q_2 = q'_2$ (i.e., charge is invariant) [119], $\bar{U}_{photon} = \gamma\bar{U}'_{photon}$ [120], and $\bar{t}_{rep} = \gamma\bar{t}'_{rep}$ (i.e., time dilation), where $\gamma = 1/\sqrt{1-v^2/c^2}$. Therefore, the mean rate of energy absorbed $\bar{P}_a$ (W) and emitted $\bar{P}_e$ (W) to and from each charge as observed in the reference frame at rest Σ is:

$$\bar{P}_a = \bar{P}_e = \frac{\bar{U}_{photon}}{\bar{t}_{rep}} = \frac{\gamma\bar{U}'_{photon}}{\gamma\bar{t}'_{rep}} = \bar{P}'_a = \bar{P}'_e. \tag{9.11}$$

For the transverse dumbbell configuration, the Lorentz transformation is used: $d_y = d'$ and $t_{12} = \gamma t'_{12} = \gamma d'/c$ (i.e., time dilation). The force between the two charges as observed in the reference frame at rest can be determined by referring to Figure 9.4. Figure 9.4 shows three positions of each charge. The gray dot represents the past location of the charge, the solid black dot represents the present location, and the dotted white dot represents the future location. The three dots (gray, black, and white) have a separation corresponding to

the time it takes a photon to transfer t_{12} from the past position of one of the charges to the present position of other (or the present position of one of the charges to the future position of the other) multiplied by the velocity v.

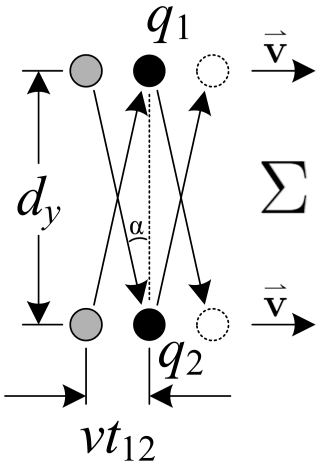

Figure 9.4: Transverse dumbbell as observed in reference frame at rest.

The repulsive force between the two charges is obtained by adding the components of force normal to the velocity of the charge ($\cos\alpha = d_y/(ct_{12})$) for the impact force from the mean rate of absorbed energy and the recoil force from the mean rate of emitted energy:

$$F_{transverse} = \frac{\bar{P}_a \dfrac{d_y}{ct_{12}} + \bar{P}_e \dfrac{d_y}{ct_{12}}}{c} = \frac{\bar{P}'_a \dfrac{d'}{c\left(\gamma \dfrac{d'}{c}\right)} + \bar{P}'_e \dfrac{d'}{c\left(\gamma \dfrac{d'}{c}\right)}}{c} = \frac{F'}{\gamma}. \tag{9.12}$$

And, the trapped energy (from QETs) between the two charges (i.e., the electrostatic potential energy) is:

$$U_{trapped} = \left(\bar{P}_a + \bar{P}_e\right) t_{12} = \left(\bar{P}'_a + \bar{P}'_e\right)\left(\gamma \frac{d'}{c}\right) = \gamma U'_{trapped}. \tag{9.13}$$

For the longitudinal dumbbell configuration, the Lorentz transformation is used: $d_x = d'/\gamma$ (i.e., length contraction), $t_{12} = \gamma\left(t'_{12} + vd'/c^2\right)$, and $t_{21} = \gamma\left(t'_{21} - vd'/c^2\right)$. The force between the two charges as observed in the reference frame at rest is:

$$F_{longitudinal} = \frac{\bar{P}_a}{c}\left(1 \pm \frac{v}{c}\right) + \frac{\bar{P}_e}{c}\left(1 \mp \frac{v}{c}\right) = \frac{\bar{P}_a + \bar{P}_e}{c} = \frac{\bar{P}'_a + \bar{P}'_e}{c} = F'. \tag{9.14}$$

And, the trapped energy (from QETs) between the two charges (i.e., the electrostatic potential energy) is:

$$\begin{aligned} U_{trapped} =& \bar{P}_a t_{12} + \bar{P}_e t_{21} = \bar{P}'_a\left[\gamma\left(t'_{12} + vd'/c^2\right)\right] + \bar{P}'_e\left[\gamma\left(t'_{21} - vd'/c^2\right)\right] \\ =& \gamma\left(\bar{P}'_a + \bar{P}'_e\right)t'_{12} = \gamma U'_{trapped}. \end{aligned} \tag{9.15}$$

Figure 9.5 shows three positions of each charge for the longitudinal configuration. The gray dot represents the past location of the charge, the solid black dot represents the present location, and the dotted white dot represents the future location. The three dots (gray, black, and white) have a separation corresponding to the average of the time it takes a photon to transfer from q_1 to q_2 and from q_2 to q_1: $\left(t_{12} + t_{21}\right)/2 = \gamma t'_{12}$ multiplied by the velocity v.

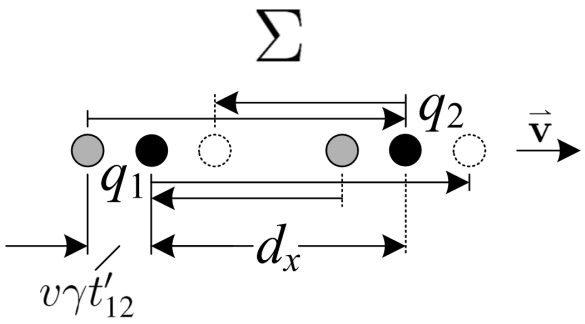

Figure 9.5: Longitudinal dumbbell as observed in reference frame at rest.

The relativistic changes in force and energy of the electromagnetic model of this dis-

sertation given in (9.12), (9.13), (9.14), and (9.15) are in agreement with those given early based on the classical electromagnetic field transformation of (9.6), (9.7), and (9.4). With the classical electromagnetic field approach, as the transverse dumbbell is moved with relativistic velocity, the electric field transforms into both an electric field and a magnetic flux density component (however, the electric field always dominated). For the electromagnetic model of this dissertation, the Coulomb stress is always exchanging between charges for observations made in any inertial reference frame (i.e., there is no transformation of the Coulomb stress into some kind of magnetic phenomena).

Figure 9.4 and Figure 9.5 provide a visual representation of the increase in energy and the relationship of forces associated with the Lorentz transformation.

The electrostatic model of this dissertation is not very static. Both figures also provide some visual insight into the causality of the QET model of this dissertation. With the charges moving, it is clear that the Coulomb force on one charge is dependent upon the past and future location of the other charge (and vise-versa).

Since the Neumann stress for magnetostatics also involves QET between differential current elements and the trapped QET corresponds to the magnetostatic potential energy, the results of this chapter are also applicable to magnetostatics [123]. The QET rate (W) associated with the Coulomb and Neumann stress is invariant (i.e., doesn't change relativistically).

CHAPTER 10. CONCLUSIONS

Four stress equations have been developed in this dissertation, two for electrostatics and two for magnetostatics. For electrostatics, the Poincaré stress was derived by recasting Maxwell's stress equation for electrostatics applied to an isolated spherically symmetric charge distribution:

$$\vec{\mathbf{F}}_{Poincaré} = -\oiint \frac{\Gamma U_e}{2\pi c^3 r^2} \hat{\mathbf{a}}_r \left(\hat{\mathbf{a}}_r \cdot d\vec{\mathbf{S}} \right). \tag{10.1}$$

The Poincaré stress is an omnidirectional inwardly directed stress proportional to the electrostatic potential energy of a charge distribution. The stress is a result of a mean rate of QET influx and out-flux to/from the charge distribution and the distant matter of the universe.

A Coulomb stress for electrostatics was also derived by recasting Maxwell's stress equation for electrostatics applied to two separated spherically symmetric charge distributions:

$$\vec{\mathbf{F}}_{Coulomb} = \frac{q_1 q_2}{4\pi\varepsilon_o d^2} \oiint \delta^2 (1 + \hat{\mathbf{a}}_{r_1} \cdot \hat{\mathbf{a}}_{r_2}) \operatorname{sgn}(\hat{\mathbf{a}}_{r_2} \cdot \hat{\mathbf{a}}_n) \hat{\mathbf{a}}_{r_1} dS. \tag{10.2}$$

The Coulomb stress is a line stress that exists between each pair of charge elements. The stress is a result of a mean rate of QETs back and forth between two like charges (or a missing amount of QETs between two opposite charges). The quantity of trapped or missing QETs between the two charges corresponds to the electrostatic potential energy of the two separated charges.

For magnetostatics, the pinch stress was derived by recasting Maxwell's stress equation for magnetostatics applied to an isolated differential current element:

$$\vec{\mathbf{F}}_{pinch} = -\oiint \frac{\Gamma U_m}{2\pi c^3 r^2} \hat{\mathbf{a}}_r \left(\hat{\mathbf{a}}_r \cdot d\vec{\mathbf{S}} \right). \tag{10.3}$$

The pinch stress is an omnidirectional inwardly directed stress proportional to the magnetostatic potential energy of a current element. The stress is a result of a mean rate of QET influx and out-flux to/from the current element and the distant matter of the universe.

A Neumann stress for magnetostatic was developed by analyzing the historical force formulas between two separated differential current elements:

$$\vec{\mathbf{F}}_{Neumann} = \frac{\mu_o \left(\vec{\mathbf{J}}_1 dV_1 \right) \cdot \left(\vec{\mathbf{J}}_2 dV_2 \right)}{4\pi d_{21}^2} \oiint \delta^2 (1 + \hat{\mathbf{a}}_{r_1} \cdot \hat{\mathbf{a}}_{r_2}) \operatorname{sgn} (\hat{\mathbf{a}}_{r_1} \cdot \hat{\mathbf{a}}_n) \hat{\mathbf{a}}_{r_1} dS. \tag{10.4}$$

The Neumann stress is a line stress that exists between each pair of current elements. The stress is a result of a mean rate of QETs back and forth between two current elements in opposite directions (or a missing amount of QETs between two current elements in the same direction). The quantity of trapped or missing QETs between the two current elements corresponds to the magnetostatic potential energy of the two separated current elements.

The four preceding static stress equations give the same result as Maxwell's stress equation for any arbitrary closed surfaces. They have been shown to be mathematically compatible with Maxwell's stress equation in the various chapters of this dissertation. The Neumann and pinch stress equations and Maxwell's stress equation for magnetostatics are only applicable to closed circuit paths.

APPENDIX A. DERIVATION OF Γ_e, THE CONSTANT OF QUANTUM ENERGY TRANSFER RATE TO MASS (W/kg)

Chapter 4 describes a net rate of quantum energy absorptions $\bar{P}_a$ and emissions $\bar{P}_e$ both proportional to the mass m of a system: $\bar{P}_a = \bar{P}_e = \Gamma m$ (W). This appendix provides a derivation of Γ_e (based on the electron), the constant of QET rate to mass (W/kg).

Given an electron model of spherical shell charge density σ with radius r_e and static charge e, the charge density is defined as:

$$\sigma = \frac{-e}{4\pi r_e^2} \quad \left(\text{C/m}^2\right). \tag{A.1}$$

The electric field for $r \geqslant r_e$ is:

$$\vec{\mathbf{E}}_e = \frac{-e}{4\pi\varepsilon_o r_e^2}\hat{\mathbf{a}}_r \quad (\text{V/m}). \tag{A.2}$$

The electrostatic potential energy of the electron is:

$$U_e = \frac{e^2}{8\pi\varepsilon_o r_e} \quad (\text{J}). \tag{A.3}$$

Assume the mass of the electron is entirely from the electrostatic potential energy:

$$m_e = \frac{U_e}{c^2} \quad (\text{kg}). \tag{A.4}$$

The radius of the electron (for this model of the electron and assumption) is solved for by combining (A.3) and (A.4):

$$r_e = \frac{e^2}{8\pi\varepsilon_o m_e c^2} \quad (\text{m}). \tag{A.5}$$

The Lorentz differential element of force on the spherical charge density shell of the electron is:

$$\begin{aligned} d\vec{\mathbf{F}}_e =& \sigma\vec{\mathbf{E}}_e dS = \left(\frac{-e}{4\pi r_e^2}\right)\left(\frac{-e}{4\pi r_e^2}\hat{\mathbf{a}}_r\right) r_e^2 \sin\theta d\theta d\phi \\ =& \frac{e^2}{16\pi^2\varepsilon_o r_e^2} d\Omega\hat{\mathbf{a}}_r \quad (\text{N/SR})\,. \end{aligned} \tag{A.6}$$

Combining (A.5) and (A.6), the Lorentz differential element of force on the spherical charge density shell of the electron is:

$$d\vec{\mathbf{F}}_e = \frac{4m_e^2\varepsilon_o c^4}{e^2} d\Omega\hat{\mathbf{a}}_r \quad (\text{N/SR})\,. \tag{A.7}$$

Jules Henri Poincaré concluded that the electron is in equilibrium between the outward force of charge wanting to push it apart and an inward normal stress [74]. Subsequently, the differential element of Poincaré stress may be defined as:

$$d\vec{\mathbf{F}}_P = -d\vec{\mathbf{F}}_e = -\frac{4m_e^2\varepsilon_o c^4}{e^2} d\Omega\hat{\mathbf{a}}_r \quad (\text{N/SR})\,. \tag{A.8}$$

Poincaré also hints of a relationship between this stress and gravity [75].

Assume that the Poincaré stress arises from the average boson emission and absorption QET rate, $\bar{P}_e$, and $\bar{P}_a$, where $\bar{P}_e = \bar{P}_a = \Gamma_e m$ (W):

$$d\vec{\mathbf{F}}_P = -\frac{\bar{P}_e + \bar{P}_a}{4\pi c} d\Omega\hat{\mathbf{a}}_r = -\frac{\Gamma_e m_e}{2\pi c} d\Omega\hat{\mathbf{a}}_r \quad (\text{N/SR})\,. \tag{A.9}$$

Finally, combining (A.8) and (A.9), yields the constant of QET rate to mass, Γ_e:

$$\Gamma_e = \frac{8\pi\varepsilon_o m_e c^5}{e^2} = 1.913 \times 10^{40} \quad (\text{W/kg})\,. \tag{A.10}$$

APPENDIX B. DERIVATION OF MAXWELL'S STRESS EQUATION FOR ELECTROSTATICS IN FREE SPACE

The following summarizes a derivation of Maxwell's Stress Equation for electrostatics in free space by O. D. Jefimenko [61]. Begin with the vector identity:

$$\frac{1}{2}\oiint A^2 d\vec{\mathbf{S}} - \oiint \vec{\mathbf{A}}\left(\vec{\mathbf{A}}\cdot d\vec{\mathbf{S}}\right) = \iiint \left[\vec{\mathbf{A}}\times\left(\nabla\times\vec{\mathbf{A}}\right) - \vec{\mathbf{A}}\left(\nabla\cdot\vec{\mathbf{A}}\right)\right] dV. \tag{B.1}$$

Applying Maxwell's equation (Faraday's Law) for electrostatics, $\nabla\times\vec{\mathbf{E}} = 0$, to (B.1) yields:

$$\varepsilon_{\mathrm{o}}\iiint\left(\nabla\cdot\vec{\mathbf{E}}\right)\vec{\mathbf{E}}dV = \varepsilon_{\mathrm{o}}\oiint\vec{\mathbf{E}}\left(\vec{\mathbf{E}}\cdot d\vec{\mathbf{S}}\right) - \frac{\varepsilon_{\mathrm{o}}}{2}\oiint E^2 d\vec{\mathbf{S}}. \tag{B.2}$$

Combining Lorentz's force equation, $\vec{\mathbf{F}} = q\vec{\mathbf{E}}$, and Maxwell's equation (Gauss' Law for electricity) for free space, $\nabla\cdot\left(\varepsilon_{\mathrm{o}}\vec{\mathbf{E}}\right) = \nabla\cdot\vec{\mathbf{D}} = \rho$, to the left side of (B.2) yields:

$$\varepsilon_{\mathrm{o}}\iiint\left(\nabla\cdot\vec{\mathbf{E}}\right)\vec{\mathbf{E}}dV = \iiint\rho\vec{\mathbf{E}}dV = \vec{\mathbf{F}}. \tag{B.3}$$

Combining (B.2) and (B.3) yields the Maxwell's Stress Equation:

$$\vec{\mathbf{F}} = \varepsilon_{\mathrm{o}}\oiint\vec{\mathbf{E}}\left(\vec{\mathbf{E}}\cdot d\vec{\mathbf{S}}\right) - \frac{\varepsilon_{\mathrm{o}}}{2}\oiint E^2 d\vec{\mathbf{S}}. \tag{B.4}$$

APPENDIX C. VARIANT OF STOKES' THEOREM

The following is based on a derivation by X. Chen [124] starting with Stokes' Theorem:

$$\iint \left(\nabla \times \vec{\mathbf{A}}\right) \cdot d\vec{\mathbf{S}} = \oint \vec{\mathbf{A}} \cdot d\vec{\boldsymbol{\ell}}. \tag{C.1}$$

Let $\vec{\mathbf{A}} = \vec{\mathbf{C}} \times \vec{\mathbf{B}}$ and let $\vec{\mathbf{B}}$ be a non-zero constant vector. Evaluating the integrand in the right side of (C.1) and applying vector identity (D.1) yields:

$$\vec{\mathbf{A}} \cdot d\vec{\boldsymbol{\ell}} = \left(\vec{\mathbf{C}} \times \vec{\mathbf{B}}\right) \cdot d\vec{\boldsymbol{\ell}} = \left(d\vec{\boldsymbol{\ell}} \times \vec{\mathbf{C}}\right) \cdot \vec{\mathbf{B}} = -\left(\vec{\mathbf{C}} \times d\vec{\boldsymbol{\ell}}\right) \cdot \vec{\mathbf{B}}. \tag{C.2}$$

Evaluating the integrand in the left side of (C.1) and applying vector identity (D.2) yields:

$$\begin{aligned} \left(\nabla \times \vec{\mathbf{A}}\right) \cdot d\vec{\mathbf{S}} &= \left[\nabla \times \left(\vec{\mathbf{C}} \times \vec{\mathbf{B}}\right)\right] \cdot d\vec{\mathbf{S}} \\ &= \left[\left(\vec{\mathbf{B}} \cdot \nabla\right)\vec{\mathbf{C}} + \vec{\mathbf{C}}\left(\nabla \cdot \vec{\mathbf{B}}\right) - \left(\vec{\mathbf{C}} \cdot \nabla\right)\vec{\mathbf{B}} - \vec{\mathbf{B}}\left(\nabla \cdot \vec{\mathbf{C}}\right)\right] \cdot d\vec{\mathbf{S}}. \end{aligned} \tag{C.3}$$

Since $\vec{\mathbf{B}}$ is constant, $\nabla \cdot \vec{\mathbf{B}} = 0$ and $\left(\vec{\mathbf{C}} \cdot \nabla\right)\vec{\mathbf{B}} = 0$, thus (C.3) reduces to:

$$\left(\nabla \times \vec{\mathbf{A}}\right) \cdot d\vec{\mathbf{S}} = -\left(\nabla \cdot \vec{\mathbf{C}}\right) d\vec{\mathbf{S}} \cdot \vec{\mathbf{B}} + \left[\left(\vec{\mathbf{B}} \cdot \nabla\right)\vec{\mathbf{C}}\right] \cdot d\vec{\mathbf{S}}. \tag{C.4}$$

Expanding in Cartesian coordinates using vector identity (D.3) and applying vector

identity (D.4), the last term on the right in equation (C.4) becomes:

$$\begin{aligned}\left[\left(\vec{\mathbf{B}}\cdot\nabla\right)\vec{\mathbf{C}}\right]\cdot d\vec{\mathbf{S}} &= \begin{bmatrix} B_x\dfrac{\partial C_x}{\partial x}+B_y\dfrac{\partial C_x}{\partial y}+B_z\dfrac{\partial C_x}{\partial z} \\ B_x\dfrac{\partial C_y}{\partial x}+B_y\dfrac{\partial C_y}{\partial y}+B_z\dfrac{\partial C_y}{\partial z} \\ B_x\dfrac{\partial C_z}{\partial x}+B_y\dfrac{\partial C_z}{\partial y}+B_z\dfrac{\partial C_z}{\partial z} \end{bmatrix}\cdot d\vec{\mathbf{S}} \\ &= \begin{bmatrix} dS_x\dfrac{\partial C_x}{\partial x}+dS_y\dfrac{\partial C_y}{\partial x}+dS_z\dfrac{\partial C_z}{\partial x} \\ dS_x\dfrac{\partial C_x}{\partial y}+dS_y\dfrac{\partial C_y}{\partial y}+dS_z\dfrac{\partial C_z}{\partial y} \\ dS_x\dfrac{\partial C_x}{\partial z}+dS_y\dfrac{\partial C_y}{\partial z}+dS_z\dfrac{\partial C_z}{\partial z} \end{bmatrix}\cdot\vec{\mathbf{B}} \\ &= \left[\left(\nabla\vec{\mathbf{C}}\right)\cdot d\vec{\mathbf{S}}\right]\cdot\vec{\mathbf{B}} = \nabla_{\mathrm{C}}\left(\vec{\mathbf{C}}\cdot d\vec{\mathbf{S}}\right)\cdot\vec{\mathbf{B}},\end{aligned} \tag{C.5}$$

where the C subscript of the del operator indicates that partial derivatives are only applied to the vector field $\vec{\mathbf{C}}$.

Combining equations (C.1), (C.2), (C.4), (C.5), and removing $\cdot\vec{\mathbf{B}}$ from each term yields the variant of Stokes' Theorem (see corollary of Stokes' Theorem [125] for an alternate form):

$$\oint\vec{\mathbf{C}}\times d\vec{\boldsymbol{\ell}} = \iint\left[\left(\nabla\cdot\vec{\mathbf{C}}\right)d\vec{\mathbf{S}} - \nabla_{\mathrm{C}}\left(\vec{\mathbf{C}}\cdot d\vec{\mathbf{S}}\right)\right]. \tag{C.6}$$

APPENDIX D. VECTOR IDENTITIES

Useful vector identities [126]:

$$\vec{\mathbf{A}} \cdot \left(\vec{\mathbf{B}} \times \vec{\mathbf{C}}\right) = \vec{\mathbf{B}} \cdot \left(\vec{\mathbf{C}} \times \vec{\mathbf{A}}\right), \tag{D.1}$$

$$\nabla \times \left(\vec{\mathbf{A}} \times \vec{\mathbf{B}}\right) = \left(\vec{\mathbf{B}} \cdot \nabla\right) \vec{\mathbf{A}} + \vec{\mathbf{A}} \left(\nabla \cdot \vec{\mathbf{B}}\right) - \left(\vec{\mathbf{A}} \cdot \nabla\right) \vec{\mathbf{B}} - \vec{\mathbf{B}} \left(\nabla \cdot \vec{\mathbf{A}}\right), \tag{D.2}$$

where

$$\left(\vec{\mathbf{A}} \cdot \nabla\right) \vec{\mathbf{B}} = \begin{bmatrix} \left(\vec{\mathbf{A}} \cdot \nabla\right) B_x \\ \left(\vec{\mathbf{A}} \cdot \nabla\right) B_y \\ \left(\vec{\mathbf{A}} \cdot \nabla\right) B_z \end{bmatrix} = \begin{bmatrix} A_x \dfrac{\partial B_x}{\partial x} + A_y \dfrac{\partial B_x}{\partial y} + A_z \dfrac{\partial B_x}{\partial z} \\ A_x \dfrac{\partial B_y}{\partial x} + A_y \dfrac{\partial B_y}{\partial y} + A_z \dfrac{\partial B_y}{\partial z} \\ A_x \dfrac{\partial B_z}{\partial x} + A_y \dfrac{\partial B_z}{\partial y} + A_z \dfrac{\partial B_z}{\partial z} \end{bmatrix}. \tag{D.3}$$

Gradient of a vector [66]:

$$\nabla_{\mathrm{A}} \left(\vec{\mathbf{A}} \cdot \vec{\mathbf{B}}\right) = \left(\nabla \vec{\mathbf{A}}\right) \cdot \vec{\mathbf{B}} = \begin{bmatrix} \dfrac{\partial A_x}{\partial x} & \dfrac{\partial A_y}{\partial x} & \dfrac{\partial A_z}{\partial x} \\ \dfrac{\partial A_x}{\partial y} & \dfrac{\partial A_y}{\partial y} & \dfrac{\partial A_z}{\partial y} \\ \dfrac{\partial A_x}{\partial z} & \dfrac{\partial A_y}{\partial z} & \dfrac{\partial A_z}{\partial z} \end{bmatrix} \cdot \vec{\mathbf{B}} \tag{D.4}$$

APPENDIX E. DERIVATION OF MAXWELL'S STRESS EQUATION FOR MAGNETOSTATICS IN FREE SPACE

The following summarizes a derivation of Maxwell's Stress Equation for magnetostatics in free space by O. D. Jefimenko [127]. Begin with the vector identity:

$$\frac{1}{2}\oiint A^2 d\vec{\mathbf{S}} - \oiint \vec{\mathbf{A}}\left(\vec{\mathbf{A}}\cdot d\vec{\mathbf{S}}\right) = \iiint \left[\vec{\mathbf{A}}\times\left(\nabla\times\vec{\mathbf{A}}\right) - \vec{\mathbf{A}}\left(\nabla\cdot\vec{\mathbf{A}}\right)\right] dV. \tag{E.1}$$

Applying Maxwell's equation (Gauss's Law for magnetism), $\nabla\cdot\vec{\mathbf{B}} = 0$, to (E.1) yields:

$$\mu_{\mathrm{o}}\iiint\left(\nabla\times\vec{\mathbf{H}}\right)\times\vec{\mathbf{H}}dV = \mu_{\mathrm{o}}\oiint\vec{\mathbf{H}}\left(\vec{\mathbf{H}}\cdot d\vec{\mathbf{S}}\right) - \frac{\mu_{\mathrm{o}}}{2}\oiint H^2 d\vec{\mathbf{S}}. \tag{E.2}$$

Combining Lorentz's force equation, $\vec{\mathbf{F}} = q\left(\vec{\mathbf{v}}\times\vec{\mathbf{B}}\right)$, and Maxwell's equation (Ampère's Law) for magnetostatics and free space, $\nabla\times\vec{\mathbf{H}} = \vec{\mathbf{J}}$, to the left side of (E.2) yields:

$$\mu_{\mathrm{o}}\iiint\left(\nabla\times\vec{\mathbf{H}}\right)\times\vec{\mathbf{H}}dV = \iiint\left(\vec{\mathbf{J}}dV\right)\times\vec{\mathbf{B}} = \vec{\mathbf{F}}. \tag{E.3}$$

Combining (E.2) and (E.3) yields the Maxwell's Stress Equation:

$$\vec{\mathbf{F}} = \mu_{\mathrm{o}}\oiint\vec{\mathbf{H}}\left(\vec{\mathbf{H}}\cdot d\vec{\mathbf{S}}\right) - \frac{\mu_{\mathrm{o}}}{2}\oiint H^2 d\vec{\mathbf{S}}. \tag{E.4}$$

APPENDIX F. DETERMINATION OF CONSTRAINTS FOR THE GENERAL FORCE EQUATION BETWEEN TWO DIFFERENTIAL CURRENT ELEMENTS

There is much literature on the equivalence of the Ampère and Grassmann (Biot-Savart/Lorentz) current element force formulas [128, 129, 25, 130, 131]. However, this appendix reveals that the magnetostatic potential energy associated with the Ampère and Grassmann current element force formulas are nonequivalent. Thus, the validity of using the Ampère force formula comes into question.

Because an isolated differential current element does not physically exist, the actual force on a differential current element cannot be determined experimentally [24]. Despite this fact, there has been much literature through the years emphasizing the importance (or even absolute correctness) of Ampère's original force formula [132, 133, 134, 135, 136]. However, based on the results of this appendix, Ampère's force formulas is invalid because it does not produce the proper magnetostatic potential energy between two closed circuits.

The magnetostatic potential energy corresponding to the general formula (3.6) is:

$$U_m = \frac{\mu_o I_1 I_2}{8\pi} \oint_1 \oint_2 \left\{ \begin{array}{l} 3(1-k_1)\dfrac{\left(d\vec{\boldsymbol{\ell}}_1 \cdot \hat{\mathbf{a}}_{21}\right)\left(d\vec{\boldsymbol{\ell}}_2 \cdot \hat{\mathbf{a}}_{21}\right)}{d_{21}} \\ +(k_1-2)\dfrac{d\vec{\boldsymbol{\ell}}_1 \cdot d\vec{\boldsymbol{\ell}}_2}{d_{21}} \\ +k_1\dfrac{\left(d\vec{\boldsymbol{\ell}}_1 \cdot \hat{\mathbf{a}}_{21}\right)}{d_{21}} d\ell_2 + k_2\dfrac{\left(d\vec{\boldsymbol{\ell}}_2 \cdot \hat{\mathbf{a}}_{21}\right)}{d_{21}} d\ell_1 \end{array} \right\}, \tag{F.1}$$

where the term with the (k_1-2) coefficient is the negative of the Neumann mutual induc-

tance energy (8.5).

For the two infinite parallel cylindrical shell surface currents carrying equal and opposite total currents (see Figure 8.1 of Section 8.1), there is no contribution from the k_2 term. Therefore, the constraint of $k_1 = 1$ determined in Section 8.1 also applies to the general formula (3.6).

It is fairly straight forward to show numerically (i.e., with Matlab, Mathcad, ect.) that for two circular filament current loops the k_2 term of (3.6) and (F.1) yields a net zero force and net zero magnetostatic potential energy respectively. This is true for any two closed circuits [27]. Therefore, an argument could be made that further constraining k_2 is irrelevant since it has no net effect for two closed circuits. However, understanding the interactions of two current elements provide the building blocks for understanding and modeling any static current distribution.

If a constraint on k_2 exists, it will be determined by analyzing the force and magnetostatic potential energy of an isolated current element interacting with a separate closed loop. The obvious constraint is $k_2 = 0$ yielding the Grassmann formula (3.5). This is the basis for the Biot-Savart Law defining the magnetic field $\vec{\mathrm{B}}$ in Maxwell's equation. It must be kept in mind that the use of Maxwell's equation and the Lorentz force law involving static current elements (where there is no dynamic electric field) is only applicable for two closed circuits.

For example, analysis of the force between a current element $(J_1 dV_1)$ and a filament current loop with current I_2 as shown in Figure F.1 has atypical results.

The force on $(J_1 dV_1)$ exerted by the filament current loop can be calculated using the

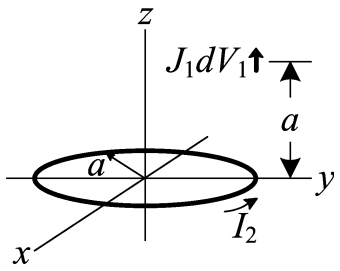

Figure F.1: Interaction between a current element and a filament current loop.

Grassmann formula (3.5), integrating around the closed filament current loop:

$$\begin{aligned}\vec{\mathbf{F}}_1 =& \frac{\mu_o}{4\pi} \oint \frac{1}{d_{12}^2} \left\{ \begin{array}{l} \left[\left(\vec{\mathbf{J}}_1 dV_1 \right) \cdot \hat{\mathbf{a}}_{12} \right] \left(\vec{\mathbf{J}}_2 dV_2 \right) \\ - \left(\vec{\mathbf{J}}_1 dV_1 \right) \cdot \left(\vec{\mathbf{J}}_2 dV_2 \right) \hat{\mathbf{a}}_{12} \end{array} \right\} \\ =& \frac{\mu_o}{4\pi} \int_0^{2\pi} \frac{(J_1 dV_1)}{\sqrt{3–2\sin\phi}} I_2 \begin{bmatrix} -\sin\phi \\ \cos\phi \\ 0 \end{bmatrix} \frac{}{a^2 \left(3–2\sin\phi\right)} a d\phi, \end{aligned} \tag{F.2}$$

where the force in the x direction is:

$$\begin{aligned}\vec{\mathbf{F}}_{1x} =& -\frac{\mu_o \left(J_1 dV_1\right) I_2}{4\pi a} \int_0^{2\pi} \frac{\sin\phi}{\left(3–2\sin\phi\right)^{3/2}} d\phi \\ =& –1.143 \frac{\mu_o \left(J_1 dV_1\right) I_2}{4\pi a}, \end{aligned} \tag{F.3}$$

and the force in the y direction is:

$$\vec{\mathbf{F}}_{1y} = \frac{\mu_o \left(J_1 dV_1\right) I_2}{4\pi a} \int_0^{2\pi} \frac{\cos\phi}{\left(3–2\sin\phi\right)^{3/2}} d\phi = 0. \tag{F.4}$$

However, the force on the filament current loop exerted by the current element is

zero:

$$\begin{aligned}\vec{\mathbf{F}}_2 =& \frac{\mu_o}{4\pi}\oint\frac{1}{d_{21}^2}\left\{\begin{array}{l}\left[\left(\vec{\mathbf{J}}_2 dV_2\right)\cdot\hat{\mathbf{a}}_{21}\right]\left(\vec{\mathbf{J}}_1 dV_1\right)\\ -\left(\vec{\mathbf{J}}_2 dV_2\right)\cdot\left(\vec{\mathbf{J}}_1 dV_1\right)\hat{\mathbf{a}}_{21}\end{array}\right\}\\ =& \frac{\mu_o}{4\pi}\int_0^{2\pi}\frac{\frac{-I_2\cos\phi}{\sqrt{3-2\sin\phi}}\left(\vec{\mathbf{J}}_1 dV_1\right)}{a^2\left(3-2\sin\phi\right)}ad\phi\\ =& -\frac{\mu_o\left(\vec{\mathbf{J}}_1 dV_1\right)I_2}{4\pi a}\int_0^{2\pi}\frac{\cos\phi}{\left(3-2\sin\phi\right)^{3/2}}d\phi = 0.\end{aligned} \tag{F.5}$$

The calculated forces for (F.3) and (F.5) are not equal and opposite. This result supports the reality that isolated current elements are fictitious. Maxwell's equations for magnetostatics based on the Biot-Savart Law and Lorentz's force law (where there is no dynamic electric field) are only applicable for analyzing two or more closed circuits.

Another viable constraint for k_2 is: $k_2 = k_1 = 1$. This results in equal and opposite forces between two current elements or between one current element and a separate closed circuit. However, this constraint cannot be fit into the magnetic field concept and Maxwell's equation. In addition, since the resulting force is not necessarily acting along the straight line between the current elements, its usefulness in any electromagnetic model is questionable.

The primary result of this appendix is that Ampère's current element force formula (3.3) does not yield the correct magnetostatic potential energy between two closed circuits. Therefore, it's use to explain any phenomena is invalid. Secondly, constraints for k_2 are undetermined. However, the constraint $k_2 = 0$ yielding the Grassmann formula (3.5) is extremely useful (i.e., the basis for the magnetic field concept of Maxwell's equations). Although the constraint $k_2 = k_1 = 1$ is viable, it's usefulness is unknown.

APPENDIX G. QET AND ELECTRODYNAMICS

Dominique Francois Jean Arago discovered[6] that rotating a copper disc below a compass needle caused the needle to revolve in the same direction as the copper disc. He was led to this discovery by observing the dampening of an oscillating compass needle when placed over a copper plate [137].

Michael Faraday conducted an experiment[7] with an iron ring which had two coils wound on it. One of the coils was connected to a battery through a contact. The second coil was connected to a galvanometer (used to measure low currents). Faraday observed that whenever the contact was either closed or opened, the needle of the galvanometer would be momentarily disturbed and then return to it's original position [138, 139]. Michael Faraday made a second major discovery[8]. He constructed a helix coil connected to a galvanometer. Faraday observed that whenever a cylindrical bar magnet is pushed in or pulled out of the coil, the needle of the galvanometer would be deflected for as long as the magnet was moving [140, 141].

Chapter 3 provided additional background for electrodynamics including Lienard-

---

[6]November, 1824

[7]August, 1831

[8]October, 1831

Wiechert potentials, retarded potentials, and the force equations of Ritz and Weber for moving charge elements. For the electromagnetic model of this dissertation, electrodynamic forces may also be modeled as QETs between moving current and/or charge elements. The details are not addressed in this work, but are left for a future endeavor.

It is assumed that an additional line stress (similar to the Coulomb stress or Neumann stress) models the force between moving current and/or charge elements. This line stress may later be coined the term Faraday stress, Weber stress, Ritz stress or even Helmholtz [142, 143] stress. The actual name is dependent on which force formula(s) are compatible with the QET model.

For an isolated charge or current distribution the total QET rate (W) corresponding to the Poincaré stress and pinch stress is invariant. The only thing that changes for the Poincaré stress and pinch stress (under relativistic transformation) is the QET power density at a given angle. It is assumed that the QET power density under relativistic Lorentz transformation varies similar to the electric field [144] and is proportional to $\frac{\left(1-\frac{v^2}{c^2}\right)}{\left(1-\frac{v^2}{c^2}\sin^2\theta\right)^{3/2}}$.

As a charge is accelerated, it is assumed that the combination of the changing Poincaré stress density and the electrodynamic stress makes up the Larmor radiation formula for non-relativistic velocities as well as the generalized formula for relativistic velocities [145].

APPENDIX H. QET AND THE COSMOS

The QET model of this dissertation is applicable to more than just electrostatics and magnetostatics. Chapter 4 briefly touches on the QETs interacting with mass associated with gravity and inertia. The gravitational potential energy of two masses may be modeled as a missing amount of QETs between the two masses.

The term inertial stress is coined for the QETs between an isolated, uncharged mass at the origin and the distant mass of the universe. The inertial stress equation is:

$$\vec{\mathbf{F}}_{inertial} = -\oiint \frac{\Gamma m}{2\pi c r^2}\hat{\mathbf{a}}_r \left(\hat{\mathbf{a}}_r \cdot d\vec{\mathbf{S}}\right). \tag{H.1}$$

The term Newton stress is coined for the missing QETs between two masses. The Newton stress equation is:

$$\vec{\mathbf{F}}_{Newton} = G\frac{m_1 m_2}{d_{21}^2} \oiint \delta^2(1+\hat{\mathbf{a}}_{r_1}\cdot\hat{\mathbf{a}}_{r_2}) \operatorname{sgn}(\hat{\mathbf{a}}_{r_1}\cdot\hat{\mathbf{a}}_n)\hat{\mathbf{a}}_{r_1} dS, \tag{H.2}$$

where m_1 and m_2 are the two masses, d_{21} is the distance between the centers of the two masses, $\delta^2()$ is the two dimensional or surface Dirac delta function [86], $\hat{\mathbf{a}}_{r_1}$ and $\hat{\mathbf{a}}_{r_2}$ are the directional unit vectors away from the first and second mass respectively, $\operatorname{sgn}()$ is the function defined in (6.12), and $\hat{\mathbf{a}}_n$ is the directional unit vector outward normal from the surface S.

The QET model is also applicable to the cosmos since the Poincaré stress, pinch stress, and inertial stress is a QET interaction with the distant matter of the universe. This appendix describes a cosmos model that is compatible with the QET model of this disser-

tation. In addition, this appendix briefly describes the QET interaction between molecular regions.

A valid cosmos model is one with an origin to the universe, a location in space considered at rest where all galaxies are moving away from. The origin can be viewed as the center of mass/energy for the universe. For any spherical closed surface with center at the origin of the universe, the mean rate of mass (with equivalent energy $U = mc^2$) and QETs outwardly crossing the spherical boundary (W) is equal to the mean rate of QETs inwardly crossing the boundary (W).

New galaxies are created at the center of the universe [146]. An accumulation of energy at the origin from QETs directed inwardly, eventually births a new galaxy which is pushed away from the origin. When masses approach the fringe of the universe (no mass exists beyond the fringe), all of the corresponding energy of the mass is transfered back (i.e., via QETs) inward toward the origin. The death of a galaxy occurs when it nears this fringe boundary. Since QETs only occur between masses, QETs do not exist outwardly beyond the fringe (i.e., where no mass exists).

The physics of our world applies between two spherical boundaries with centers at the origin of the universe. The inner boundary is somewhere away form the origin of the universe, the outer boundary is somewhere inside the fringe. Galaxies in this region move at a fairly constant velocity away from the origin. The Milky Way galaxy is well within these two boundaries.

For galaxies within these two boundaries, this cosmos model contains an abundance of mass at vast distances in all directions that is interacting with localized mass systems

by means of QETs. The omnidirectional aspect of the Poincaré stress, pinch stress, and inertial stress is a result of a homogeneous density of the distant matter of the universe in all directions.

Galaxies approaching the fringe have an increasing acceleration away from the origin of the universe. The acceleration increases because the majority of QETs are inward toward the origin since there is less mass outward toward the fringe. Molecular regions approach instability as a mass is accelerated toward and approaches the fringe. In this cosmos model, old galaxies are constantly dying off (as they approach the fringe) and new galaxies are constantly being born (at the origin of the universe).

Two molecular regions have distances where the corresponding masses are being pushed together and other distances where the masses are being pushed apart [147]. This concept is similar to Boscovich's theory of 'point forces' having repulsion at very close distances (infinitely increases as the distance approaches zero), attraction at far distances (according to Newton's gravitation law), and many equilibrium points in between (two 'point forces' tend to stay at a distance of one of the equilibrium points) [148].

The molecular regions in a solid are at an equilibrium condition between being pushed together and pushed apart (1st equilibrium condition). The molecular regions in a liquid are at the 2nd equilibrium condition between being pushed together and pushed apart. The molecular regions of gases are typically not at equilibrium conditions, however there may be 3rd, 4th, etc. equilibrium conditions that exist momentarily until they are disturbed by the movement of other molecular regions in close proximity.

Two molecular regions pushing apart with a maximum force (somewhere between

two equilibrium conditions) is a result of isochronous QETs between the molecular regions. Two molecular regions being pushed together with a maximum force (somewhere between two equilibrium conditions) is a result of missing QETs (i.e., anti-isochronous) between the molecular regions.

Bibliography

[1] Michael Faraday. *Experimental Researches in Electricity, Volume III*, pages 2–3, 410, 418, 443–441. In [149], 2005. Unabridged facsimile of the edition published in 1855 by Richard Taylor and William Francis, London.

[2] James Clerk Maxwell. *A Treatise on Electricity and Magnetism*, pages 270–285. Volume 2 of [150], 1954. Republication of the third edition, 1891.

[3] Richard Phillips Feynman. *QED: the Strange Theory of Light and Matter*, pages 91–123. Princeton University Press, Princeton, NJ, 1988.

[4] Isaac Newton. *Newton's Principia: The Mathematical Principles Of Natural Philosophy (1687) [English translation by A. Motte]*. Daniel Adee, New York, NY, 1846.

[5] Charles Augustin de Coulomb. Premier & Second mémoire sur l'électricité et le magnétisme. *Mémoires de l'Académie Royale des Sciences*, 88:569–611, 1785. English translation extracts: First & Second Memoirs on Electricity and Magnetism [151].

[6] Stephen S. Attwood. *Electric and Magnetic Fields*, page 217. John Whiley & Sons, New York, 1949.

[7] Alessandro Volta. On the electricity excited by the mere contact of conducting substances of different kinds. *Philosophical Transactions of the Royal Society of London*, 90:403–431, 1800. English translation by B. Dibner [152].

[8] Paul Mottelay. *Bibliographical History of Electricity & Magnetism: Chronologically Arranged*, pages 453–454. In [153], 1922.

[9] Hans Christian Oersted. Experiments on the effect of a current of electricity on the magnetic needle. *Annals of Philosophy*, 16:273–276, 1820.

[10] Herbert W. Meyer. *A History of Electricity and Magnetism*, page 48. In [154], 1872.

[11] Herbert W. Meyer. *A History of Electricity and Magnetism*, pages 50–51. In [154], 1872.

[12] André-Marie Ampère. Memoir on the mathematical theory of electrodynamic phenomena, experimentally deduced. *Mémoires de l'Académie Royale des Sciences*, 6:175–388, 1823. English translation by O. Blunn [155].

[13] R. A. R. Tricker. *Early Electrodynamics: The First Law of Circulation*, page 56. In [156], 1965.

[14] Franz Ernst Neumann. Die mathematischen gesetze der inducirten elektrischen ströme. *Akademie der Wissenschaften, Berlin*, 1845.

[15] Franz Ernst Neumann. Uber ein allgemeines prinoip der mathematischen theorie inducirter elektrischer ströme. *Akademie der Wissenschaften, Berlin*, 1847.

[16] Gaylord P. Harnwell. *Principles of Electricity and Electromagnetism*, page 322. McGraw-Hill Book Company, Inc., New York, 1949.

[17] Frederick W. Grover. *Inductance Calculations*, page 8. Dover Publications, Inc., Mineola, NY, 1973.

[18] Michael Faraday. *On the Physical Character of the Lines of Magnetic Force*, page 410. In [149], June 1852. Unabridged facsimile of the edition published in 1855 by Richard Taylor and William Francis, London.

[19] Michael Faraday. *On the Lines of Magnetic Force*, page 405. In [149], January 1852. Unabridged facsimile of the edition published in 1855 by Richard Taylor and William Francis, London.

[20] Michael Faraday. *On the Lines of Magnetic Force*, pages 408–409. In [149], January 1852. Unabridged facsimile of the edition published in 1855 by Richard Taylor and William Francis, London.

[21] James Clerk Maxwell. On action at a distance. In *The Scientific Papers of James Clerk Maxwell*, volume 2, chapter 54, pages 311–323. Cambridge University Press, London, 1890. From the Proceedings of the Royal Institution of Great Britain, Vol. 7, 1875, pp. 44–54.

[22] Jean-Baptiste Biot and Félix Savart. Note on the magnetism of Volta's battery. *Annales de Chimie et de Physique*, 15:222–223, 1820. English translation by O. Blunn [157].

[23] Hermann Günther Grassmann. A new theory of electrodynamics. *Annalen der Physik und Chemie*, 64:1–18, 1845. English translation by O. Blunn [158].

[24] C. Christodoulides. Comparison of the Ampère and Biot-Sarvart magnetostatic force laws in their line-current-element forms. *American Journal of Physics*, 56(4):357–362, April 1988.

[25] A. K. T. Assis and Marcelo A. Bueno. Equivalence between Ampère and Grassmann's forces. *IEEE Transactions on Magnetics*, 32(2):431–436, March 1996.

[26] E. T. Whittaker. *A History of the Theories of Aether and Electricity: From the Age of Descartes to the Close of the Nineteenth Century*, pages 89–92. In [159], 1910.

[27] A. O'Rahilly. *Electromagnetic Theory, a Critical Examination of Fundamentals*, pages 102–113. Volume 1 of [160], 1965.

[28] J. Strnad. Stefan's equations of electrodynamics. *European Journal of Physics*, 10(4):276–280, 1989.

[29] Parry Moon and Domina Eberle Spencer. Interpretation of the Ampère experiments. *Journal of the Franklin Institute*, 257(3):203–220, March 1954.

[30] Hendrik Antoon Lorentz. *Attempt at a Theory of Electrical and Optical Phenomena in Moving Bodies*. Leiden: E. J. Brill, Leiden, 1895. English translation available: http://de.wikisource.org/wiki/Versuch_einer_Theorie_der_electrischen_und_optischen_Erscheinungen_in_bewegten_K%C3%B6rpern.

[31] John David Jackson. *Classical Electrodynamics*, page 260. In [161], 1999.

[32] Max Mason and Warren Weaver. *The Electromagnetic Field*, page 273. In [162], 1929.

[33] John Henry Poynting. On the transfer of energy in the electromagnetic field. *Philosophical Transactions of the Royal Society of London*, 175:343–361, 1884.

[34] Oliver Heaviside. *Electromagnetic Theory*, pages 605–606. Volume 3 of [163], 1971. First published in 1912: The Electrician printing and publishing company, limited, London.

[35] David J. Griffiths. *Introduction to Elementary Particles*, pages 17–18, 49, 59. Wiley-VCH, Weinheim, Germany, 2009.

[36] J. Al-Khalili. *Quantum, a Guide for the Perplexed*, pages 174–175. Weidenfeld & Nicolson, London, 2004.

[37] H. J. Josephs. *Some Unpublished Notes of Oliver Heaviside*, pages 632–634. In [163], 1971.

[38] Georges-Louis Le Sage. Lucrèce newtonien. *Nouveaux Mémoires de l' Académie Royale des Sciences et Belles-Lettres, Année 1782*, pages 404–427, 1784. Translated to English by C. G. Abbot and S. P. Langley [164].

[39] Richard Phillips Feynman. *The Character of Physical Law*, pages 38–39. The MIT Press, Cambridge, MA, 1970.

[40] Richard Phillips Feynman, F. B. Moringo, and W. G. Wagner. *Feynman Lectures on Gravitation*, pages 23–28. Addison-Wesley Publishing Company, Reading, MA, 1995.

[41] Eanst Mach. *The Science of Mechanics: a Critical and Historical Account of its Development*, page 296. The Open Court Publishing Company, LaSalle, IL, 1974. English translation first published in 1893.

[42] N. Graneau P. Graneau. *In the Grip of the Distant Universe, the Science of Inertia*, pages 1–2, 144. World Scientific Publishing Co., Singapore, 2006.

[43] Wilhelm Eduard Weber. Electrodynamische maassbestimmungen: Ueber ein allgemeines grundgesetz der elektrischen wirkung. In *Werke*, volume III, chapter Galvanismus und Electrodynamik, part 1, edited by H. Weber, pages 25–214. Julius Springer Verlag, Berlin, 1893. English translation by Susan P. Johnson, edited by Laurence Hecht and A. K. T. Assis, .pdf available: http://www.21stcenturysciencetech.com, 2007, p. 89.

[44] A. K. T. Assis. *Weber's Electrodyanmics*, page 56. In [165], 1994.

[45] A. K. T. Assis. *Weber's Electrodyanmics*, pages 84–87. In [165], 1994.

[46] Walter Ritz. Critical researches on general electrodynamics. *Annales de Chimie et de Physique*, 13:145–275, 1908. English translation: "Critical Researches on General Electrodynamics" by Jocyln Lucier, George Toth, Elizabeth Bull, edited by Robert Fritzius, Yefim Bakman, available: http://www.datasync.com/ rsf1/crit/1908a.htm, 2008, p. 64.

[47] A. O'Rahilly. *Electromagnetic Theory, a Critical Examination of Fundamentals*, page 520. Volume 2 of [160], 1965.

[48] A. K. T. Assis. *Weber's Electrodyanmics*, page 245. In [165], 1994.

[49] Georg Friedrich Bernhard Riemann. A contribution to electrodynamics. *Annalen der Physik*, 131:237–243, 1867. English translation by C. White [166].

[50] Ludvig Valentin Lorenz. On the identity of the vibrations of light with electrical currents. *The London, Edinburgh and Dublin philosophical magazine and journal of science (Series 4)*, 34:289, 291, 1867.

[51] Oleg D. Jefimenko. *Electromagnetic Retardation and Theory of Relativity*, pages 19, 34–35. In [167], 2004.

[52] John Archibald Wheeler and Richard Feynman. Interaction with the absorber as the mechanism of radiation. *Reviews of Modern Physics*, 17(1 & 2):157–181, 1945.

[53] Hugo Martin Tetrode. On the causal connection of the world, an extension of classical dynamics. *Zeitschrift fur Physik*, 10:317–328, 1922. English translation by M. Seevinck, available: http://www.phys.uu.nl/igg/seevinck/Translation_Tetrode.pdf, pp. 8-10.

[54] Timothy Michael Minteer. Electrostatic stress: Insightful analysis and manipulation of Maxwell's stress equation for electrostatics. Submitted to IEEE Transactions on Dielectrics and Electrical Insulation (Paper # 3840), November 2012.

[55] Timothy Michael Minteer. Recasting of Maxwell's stress equation for electrostatics part I: A boson interaction model for the Poincaré stress of an isolated, spherically

symmetric static charge distribution. Submitted to Foundations of Physics (FOOP-D-12-00214), August 2012.

[56] Alexander L. Kholmetskii. On "gauge renormalization" in classical electrodynamics. *Foundations of Physics*, 36(5):715–744, 2006.

[57] David J. Griffiths and Russell E. Owen. Mass renormalization in classical electrodynamics. *American Journal of Physics*, 51(12):1120–1126, December 1983.

[58] David J. Griffiths. Resource letter EM-1: Electromagnetic momentum. *American Journal of Physics*, 80(1):7–18, January 2012.

[59] John David Jackson. *Classical Electrodynamics*, page 261. In [161], 1999.

[60] Max Mason and Warren Weaver. *The Electromagnetic Field*, pages 272–274. In [162], 1929.

[61] Oleg D. Jefimenko. *Electricity and Magnetism*, pages 215–216. In [168], 1989.

[62] James Clerk Maxwell. *A Treatise on Electricity and Magnetism*, pages 157–165. Volume 1 of [150], 1954. Republication of the third edition, 1891.

[63] Oleg D. Jefimenko. *Electricity and Magnetism*, pages 191–195. In [168], 1989.

[64] David J. Griffiths. *Introduction to Electrodynamics*, pages 93–96. In [169], 1981.

[65] David J. Griffiths. *Introduction to Electrodynamics*, page 65. In [169], 1981.

[66] Joseph D. Romano and Richard H. Price. Why no shear in "div, grad, curl, and all that"? *American Journal of Physics*, 80(6):519–524, June 2012.

[67] Fritz Rohrlich. *Classical Charged Particles: Foundations of Their Theory*, pages 124–125. Addison-Wesley Publishing Company, Redwood City, CA, 1990.

[68] Julian Schwinger. Electromagnetic mass revisited. *Foundations of Physics*, 13(3):373–383, 1983.

[69] Fritz Rohrlich. Self-energy and stability of the classical electron. *American Journal of Physics*, 28(7):639–643, October 1960.

[70] H. M. Schwartz. Poincaré's Rendiconti paper on relativity. Part I. *American Journal of Physics*, 39(11):1287–1294, November 1971. English translation of J. H. Poincaré, "Sur la dynamique de l'électron," Rendiconti del Circolo Matematico di Palermo, 1906.

[71] Tony Rothman and Stephen Boughn. Can gravitons be detected? *Foundations of Physics*, 36(12):1801–1825, 2006.

[72] Hendrik Antoon Lorentz. *The Theory of the Electrons and its Applications to the Phenomena of Light and Radiant Heat*, pages 33–34. In [170], 1952. Unabridged reproduction of the second edition, 1915.

[73] Richard Phillips Feynman, Robert B. Leighton, and Matthew Sands. *The Feynman Lectures on Physics*, pages 8–2, 8–3. Volume 2 of [171], 1977.

[74] Hendrik Antoon Lorentz. *The Theory of the Electrons and its Applications to the Phenomena of Light and Radiant Heat*, pages 213–214. In [170], 1952. Unabridged reproduction of the second edition, 1915.

[75] H. M. Schwartz. Poincaré's Rendiconti paper on relativity. Part II. *American Journal of Physics*, 40(6):862–872, June 1972. English translation of J. H. Poincaré, "Sur la dynamique de l'électron," Rendiconti del Circolo Matematico di Palermo, 1906.

[76] Julian Barbour. The definition of mach's principle. *Foundations of Physics*, 40(9–10):1263–1284, 2010.

[77] Ronald Newburgh. Inertial forces, absolute space, and Mach's principle: The genesis of relativity. *American Journal of Physics*, 75(5):427–430, May 2007.

[78] R. H. Dicke. Cosmology, Mach's principle and relativity. *American Journal of Physics*, 31(7):500–509, July 1963.

[79] Timothy Michael Minteer. Recasting of Maxwell's stress equation for electrostatics part II: A boson interaction model for the Coulomb and Poincaré stresses of two separated, spherically symmetric static charge distributions. Submitted to Foundations of Physics (FOOP-D-12-00216), August 2012.

[80] J. A. E. Roa-Neri and J. L. Jimenez. An analysis of the radiation reaction in a charged dumbbell. *Foundations of Physics Letters*, 7(5):403–417, 1994.

[81] David J. Griffiths and Ellen W. Szeto. Dumbbell model for the classical radiation reaction. *American Journal of Physics*, 46(3):244–248, March 1978.

[82] S. M. Blinder. Delta functions in spherical coordinates and how to avoid losing

them: Fields of point charges and dipoles. *American Journal of Physics*, 71(8):816–818, August 2003.

[83] David J. Griffiths and Stephen Walborn. Dirac deltas and discontinuous functions. *American Journal of Physics*, 67(5):446–447, May 1999.

[84] A. E. Taylor. L'Hospital's rule. *The American Mathematical Monthly*, 59(1):20–24, January 1952.

[85] R. C. Hibbeler. *Mechanics of Materials*, pages 436–437, 462. Pearson Prentice Hall, Upper Saddle River, NJ, 2008.

[86] Ronald Newbold Bracewell. *The Fourier Transform and Its Applications*, pages 84–85. McGraw-Hill, Inc., New York, 1978.

[87] Domingo J. Louis-Martinez. Relativistic action at a distance and fields. *Foundations of Physics*, 42(2):215–223, 2012.

[88] José M. Sánchez-Ron. Actions at a distance, four-dimensionality, and the problem of "where is the energy?". *American Journal of Physics*, 50(8):739–742, August 1982.

[89] Krzysztof Rebilas. A way to discover Maxwell's equations theoretically. *Foundations of Physics*, 19(4):337–351, 2006.

[90] Peter Heering. On Coulomb's inverse square law. *American Journal of Physics*, 60(11):988–994, November 1992.

[91] Charis Anastopoulos. Classical versus quantum probability in sequential measurements. *Foundations of Physics*, 36(11):1601–1661, 2006.

[92] Daniel T. Gillespie. A theorem for physicists in the theory of random variables. *American Journal of Physics*, 51(6):520–533, June 1983.

[93] W. B. Joyce. Radiation force and the classical mechanics of photons and phonons. *American Journal of Physics*, 43(3):245–255, March 1975.

[94] Karl Svozil. Conventions in relativity theory and quantum mechanics. *Foundations of Physics*, 32(4):479–502, 2002.

[95] Kenneth S. Mendelson. The story of c. *American Journal of Physics*, 74(11):995–997, November 2006.

[96] Richard Phillips Feynman, Robert B. Leighton, and Matthew Sands. *The Feynman Lectures on Physics*, pages 8–1. Volume 2 of [171], 1977.

[97] Timothy H. Boyer. Electrostatic potential energy leading to a gravitational mass change for a system of two point charges. *American Journal of Physics*, 47(2):129–131, February 1979.

[98] Timothy Michael Minteer. Recasting of Maxwell's stress equation for magnetostatics: A boson interaction model for the pinch and Neumann stresses of two separated, differential current elements. Submitted to Foundations of Physics (FOOP-S-12-00633), November 2012.

[99] Timothy Michael Minteer. Magnetostatic stress: Insightful analysis and manipulation of maxwell's stress equation for magnetostatics. Submitted to IEEE Transactions on Magnetics (Paper # TMAG-12-11-0746), November 2012.

[100] Oleg D. Jefimenko. *Electricity and Magnetism*, pages 448–449. In [168], 1989.

[101] John David Jackson. *Classical Electrodynamics*, page 175. In [161], 1999.

[102] Carl Hering. The stretching of a conductor by its current. *Journal of the Franklin Institute*, 171:73–85, 1911.

[103] Jan Nasilowski. Unduloids and striated disintegration of wires. *Exploding Wires*, 3:295–313, 1964.

[104] Edwin F. Northrup. Some newly observed manifestations of forces in the interior of an electric conductor. *Physical Review*, 24(6):474–497, 1907.

[105] S. Lee. Energy balance and the radius of electromagnetically pinched plasma columns. *Plasma Physics*, 25(5):571–576, 1983.

[106] James Paul Wesley. Ampere repulsion drives the Graneau-Hering submarine and Hering's pump. In *Progress in Space-Time Physics*, pages 187–192. Benjamin Wesley, Blumberg, West Germany, 1987.

[107] A. M. Hillas. Electromagnetic jet propulsion: Non-Lorentzian forces on currents? *Nature*, 302:271, March 1983.

[108] Brian James. The discovery of the pinch effect. *Australian Physics*, 44(1):9, 2007.

[109] Harold Aspden. The exploding wire phenomenon. *Physics Letters A*, 107A(5):238–240, February 1985.

[110] James Clerk Maxwell. *A Treatise on Electricity and Magnetism*, page 157. Volume 2 of [150], 1954. Republication of the third edition, 1891.

[111] Timothy Michael Minteer. Nonequivalence of the magnetostatic potential energy corresponding to the Ampère and Grassmann current element force formulas. Accepted and provisionally scheduled for publication in European Journal of Physics (Manuscript # 455416), March 2013.

[112] J. L. Jiménez, I. Campos, and N. Aquino. Exact electromagnetic fields produced by a finite wire with constant current. *European Journal of Physics*, 29(1):163–175, 2008.

[113] Clayton R. Paul. *Introduction to Electromagnetic Compatibility*, pages 192–193. John Whiley & Sons Ltd, New York, 2006.

[114] Peter Peet Silvester. *Modern Electromagnetic Fields*, pages 155–157. Prentice-Hall, Englewood Cliffs, NJ, 1968.

[115] Oleg D. Jefimenko. *Electricity and Magnetism*, page 451. In [168], 1989.

[116] David J. Griffiths. *Introduction to Electrodynamics*, page 250. In [169], 1981.

[117] James Clerk Maxwell. *A Treatise on Electricity and Magnetism*, page 174. Volume 2 of [150], 1954. Republication of the third edition, 1891.

[118] Richard Phillips Feynman, Robert B. Leighton, and Matthew Sands. *The Feynman Lectures on Physics*, pages 15–2–15–8. Volume 1 of [171], 1977.

[119] Oleg D. Jefimenko. *Electromagnetic Retardation and Theory of Relativity*, page 182. In [167], 2004.

[120] Richard Phillips Feynman, Robert B. Leighton, and Matthew Sands. *The Feynman Lectures on Physics*, pages 15–10, 15–11. Volume 1 of [171], 1977.

[121] Oleg D. Jefimenko. *Electromagnetic Retardation and Theory of Relativity*, page 150. In [167], 2004.

[122] L. D. Landau and E. M. Lifshitz. *The Classical Theory of Fields*, pages 63–64. Pergamon Press, Reading, MA, 1971.

[123] Timothy Michael Minteer. Instructive insights into static current distributions moving at relativistic velocities. Submitted to European Journal of Physics (Manuscript # 459690), January 2013.

[124] Xiao-Bo Chen. Middle-field formulation for the computation of wave-drift loads. *Journal of Engineering Mathematics*, 59(1):61–82, September 2007.

[125] Earle B. Mullen. A new vector identity and physical application. *American Journal of Physics*, 20(7):453–454, October 1952.

[126] Ralph J. Gagnon. Distribution theory of vector fields. *American Journal of Physics*, 38(7):879–891, July 1970.

[127] Oleg D. Jefimenko. *Electricity and Magnetism*, pages 446–447. In [168], 1989.

[128] R. C. Lyness. The equivalence of Ampère's electrodynamic law and that of Biot and Savart. *Contemporary Physics*, 4:453–455, 1963.

[129] J. G. Ternan. Equivalence of the Lorentz and Ampere force laws in magnetostatics. *Journal of Applied Physics*, 57(5):1743–1745, March 1985.

[130] D. C. Jolly. Identity of the Ampere and Biot-Savart electromagnetic force laws. *Physics letters A*, 107(5):231–234, February 1985.

[131] T. A. Weber and D. J. Macomb. On the equivalence of the laws of Biot-Sarvart and Ampere. *American Journal of Physics*, 57(1):57–59, January 1989.

[132] Carl Hering. Electromagnetic forces; a search for more rational fundamentals; a proposed revision of the laws. *Transactions of the American Institute of Electrical Engineers*, 42:311–340, 1923.

[133] Peter Graneau. Ampere tension in electric conductors. *Magnetics, IEEE Transactions on*, 20(2):444–455, 1984.

[134] T. E. Phipps Jr. Ampere tension and newton's laws. *Apeiron*, 17:1–5, October 1993.

[135] Peter Graneau, T. Phipps Jr, and D. Roscoe. An experimental confirmation of longitudinal electrodynamic forces. *The European Physical Journal D*, 15(1):87–97, 2001.

[136] James Paul Wesley. Proposed motors driven solely by ampère repulsion. *Europhysics Letters*, 63(2):214–219, July 2003.

[137] Paul Mottelay. *Bibliographical History of Electricity & Magnetism: Chronologically Arranged*, pages 478–479. In [153], 1922.

[138] Percy Dunsheath. *A History of Electrical Power Engineering*, page 95. In [172], 1962.

[139] Jill Jonnes. *Empires of Light*, pages 39–40. In [173], 2003.

[140] Percy Dunsheath. *A History of Electrical Power Engineering*, page 96. In [172], 1962.

[141] Jill Jonnes. *Empires of Light*, pages 40–41. In [173], 2003.

[142] E. T. Whittaker. *A History of the Theories of Aether and Electricity: From the Age of Descartes to the Close of the Nineteenth Century*, page 261. In [159], 1910.

[143] A. O'Rahilly. *Electromagnetic Theory, a Critical Examination of Fundamentals*, page 115. Volume 1 of [160], 1965.

[144] Oleg D. Jefimenko. *Electromagnetic Retardation and Theory of Relativity*, page 68. In [167], 2004.

[145] John David Jackson. *Classical Electrodynamics*, pages 665–671. In [161], 1999.

[146] F. Hoyle. A new model for the expanding universe. *Monthly Notices of the Royal Astronomical Society*, 108:372–382, 1948.

[147] O. F. Mossotti. On forces which regulate the internal constitution of bodies. *Scientific Memoirs*, 1:448–469, 1966. Johnson Reprint Corporation, New York.

[148] Roger Joseph Boscovich. *A Theory of Natural Philosophy*, pages 39–45. Open Court Publishing Company, Chicago, IL, 1922. From the text of the first venetian edition published under the personal superintendence of the author in 1763.

[149] Michael Faraday. *Experimental Researches in Electricity, Volume III*. Adamant Media Corporation, Chestnut Hill, MA, 2005. Unabridged facsimile of the edition published in 1855 by Richard Taylor and William Francis, London.

[150] James Clerk Maxwell. *A Treatise on Electricity and Magnetism*. Dover Publications, Inc., New York, 1954. Republication of the third edition, 1891.

[151] Morris H. Shamos. *Great Experiments in Physics: Firsthand Accounts from Galileo to Einstein*, pages 61–73. Dover Publications Inc., New York, 1987.

[152] Bern Dibner. *Alessandro Volta and the Electric Battery*, pages 111–131. Franklin Watts, Inc, New York, 1964.

[153] Paul Mottelay. *Bibliographical History of Electricity & Magnetism: Chronologically Arranged*. Charles Griffin & Company Limited, London, 1922.

[154] Herbert W. Meyer. *A History of Electricity and Magnetism*. The Massachusetts Institute of Technology, 1872.

[155] R. A. R. Tricker. *Early Electrodynamics: The First Law of Circulation*, pages 172, 181. In [156], 1965.

[156] R. A. R. Tricker. *Early Electrodynamics: The First Law of Circulation*. Pergamon Press, Oxford, 1965.

[157] R. A. R. Tricker. *Early Electrodynamics: The First Law of Circulation*, pages 118–119. In [156], 1965.

[158] R. A. R. Tricker. *Early Electrodynamics: The First Law of Circulation*, pages 201–214. In [156], 1965.

[159] E. T. Whittaker. *A History of the Theories of Aether and Electricity: From the Age of Descartes to the Close of the Nineteenth Century*. Logmans, Green, and Co., London, 1910.

[160] A. O'Rahilly. *Electromagnetic Theory, a Critical Examination of Fundamentals*. Dover Publications, Inc., New York, 1965.

[161] John David Jackson. *Classical Electrodynamics*. John Wiley & Sons, Inc., New York, 1999.

[162] Max Mason and Warren Weaver. *The Electromagnetic Field*. Dover Publications, Inc., New York, 1929.

[163] Oliver Heaviside. *Electromagnetic Theory*. Chelsea Publishing Company, New York, 1971. First published in 1912: The Electrician printing and publishing company, limited, London.

[164] C. G. Abbot and S. P. Langley. The Le Sage theory of gravitation. *Annual Report*

of the Board of Regents of the Smithsonian Institution for the Year Ending June 30, pages 139–160, June 1898.

[165] A. K. T. Assis. *Weber's Electrodyanmics*. Kluwer Academic Publishers, Dordrecht, The Netherlands, 1994.

[166] C. White. *Energy Potentials: Towards a New Electromagnetic Field Theory*, pages 295–297. Campaigner Publications, Inc., New York, 1977.

[167] Oleg D. Jefimenko. *Electromagnetic Retardation and Theory of Relativity*. Electret Scientific Company, Star City, WV, 2004.

[168] Oleg D. Jefimenko. *Electricity and Magnetism*. Electret Scientific Company, Star City, WV, 1989.

[169] David J. Griffiths. *Introduction to Electrodynamics*. Prentice-Hall, Englewood Cliffs, NJ, 1981.

[170] Hendrik Antoon Lorentz. *The Theory of the Electrons and its Applications to the Phenomena of Light and Radiant Heat*. Dover Publications, Inc., New York, 1952. Unabridged reproduction of the second edition, 1915.

[171] Richard Phillips Feynman, Robert B. Leighton, and Matthew Sands. *The Feynman Lectures on Physics*. Addison-Wesley Publishing Company, Reading, MA, 1977.

[172] Percy Dunsheath. *A History of Electrical Power Engineering*. The M.I.T Press, Cambridge, MA, 1962.

[173] Jill Jonnes. *Empires of Light*. Random House, New York, 2003.